Beam Instrumentation & Diagnostics Part 2

CAS Introduction to Accelerator Physics

Constanţa, 27th of September 2018

Peter Forck

Gesellschaft für Schwerionenforschnung (GSI)

2nd part of this lecture covers:

- **Transverse profile techniques**
- **Emittance determination and transfer lines**
- **Diagnostics for bunch length and momentum spread**

The beam width can be changed by focusing via quadruples.
Transverse matching between ascending accelerators is done by focusing.
→ Profiles have to be controlled at many locations.

Synchrotrons: Lattice functions ***β (s)*** and ***D(s)*** are fixed ⇒ width ***σ*** and emittance ***ε*** are:

$$\sigma_x^2(s) = \varepsilon_x \beta_x(s) + \left(D(s) \frac{\Delta p}{p} \right)^2 \quad \text{and} \quad \sigma_y^2(s) = \varepsilon_y \beta_y(s) \quad \text{(no vertical bend)}$$

Transfer lines: Lattice functions are 'smoothly' defined due to variable input emittance.

Typical beam sizes:

e⁻-beam: typically Ø 0.1 to 3 mm, **protons:** typically Ø 1 to 30 mm

A great variety of devices are used:

- ***Optical techniques**:* Scintillating screens (all beams), synchrotron light monitors (e−), optical transition radiation (e−, high energetic p), ionization profile monitors (protons)
- ***Electronics techniques:*** Secondary electron emission SEM grids, wire scanners (all)

Particle's energy loss in matter produces light

→ the most direct way of profile observation as used from the early days on!

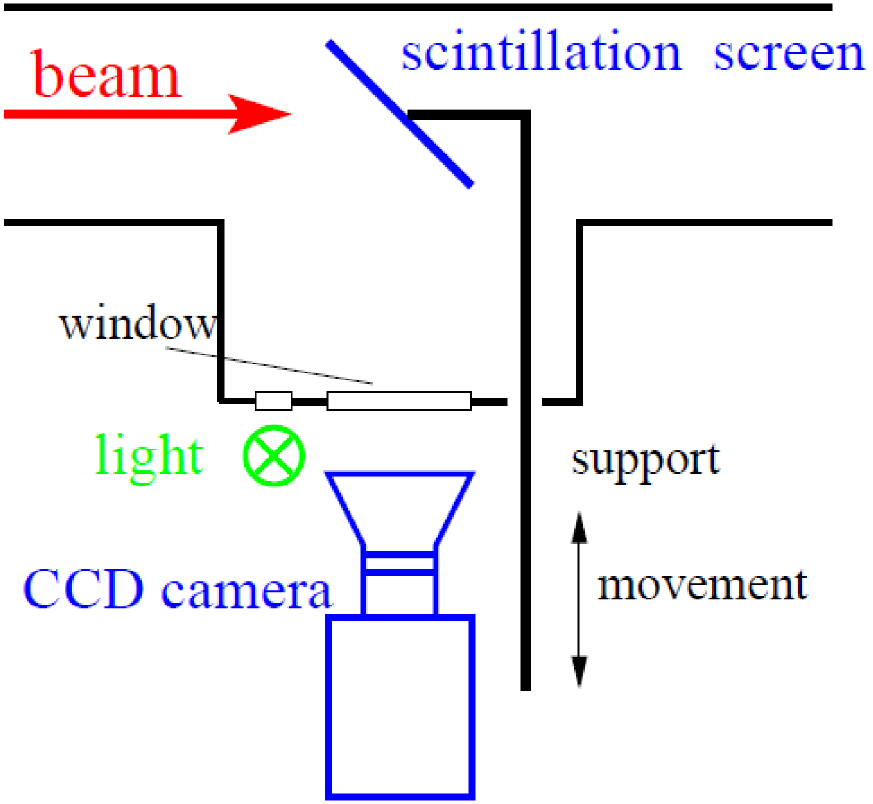

Pneumatic feed-through with Ø70 mm screen:

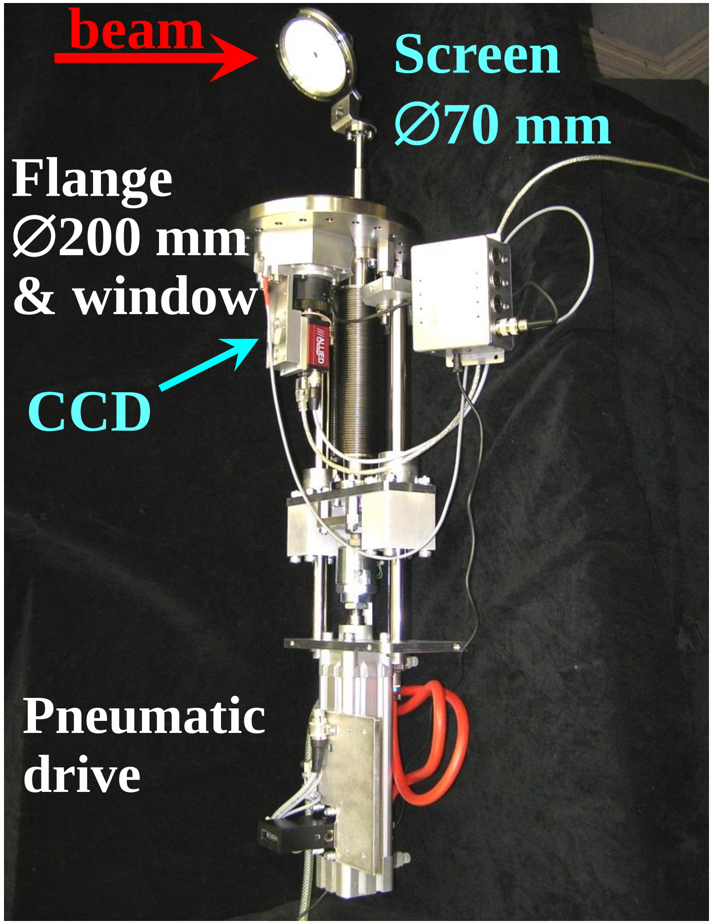

Example of Screen based Beam Profile Measurement

Example: GSI LINAC, 4 MeV/u, low current, YAG:Ce screen

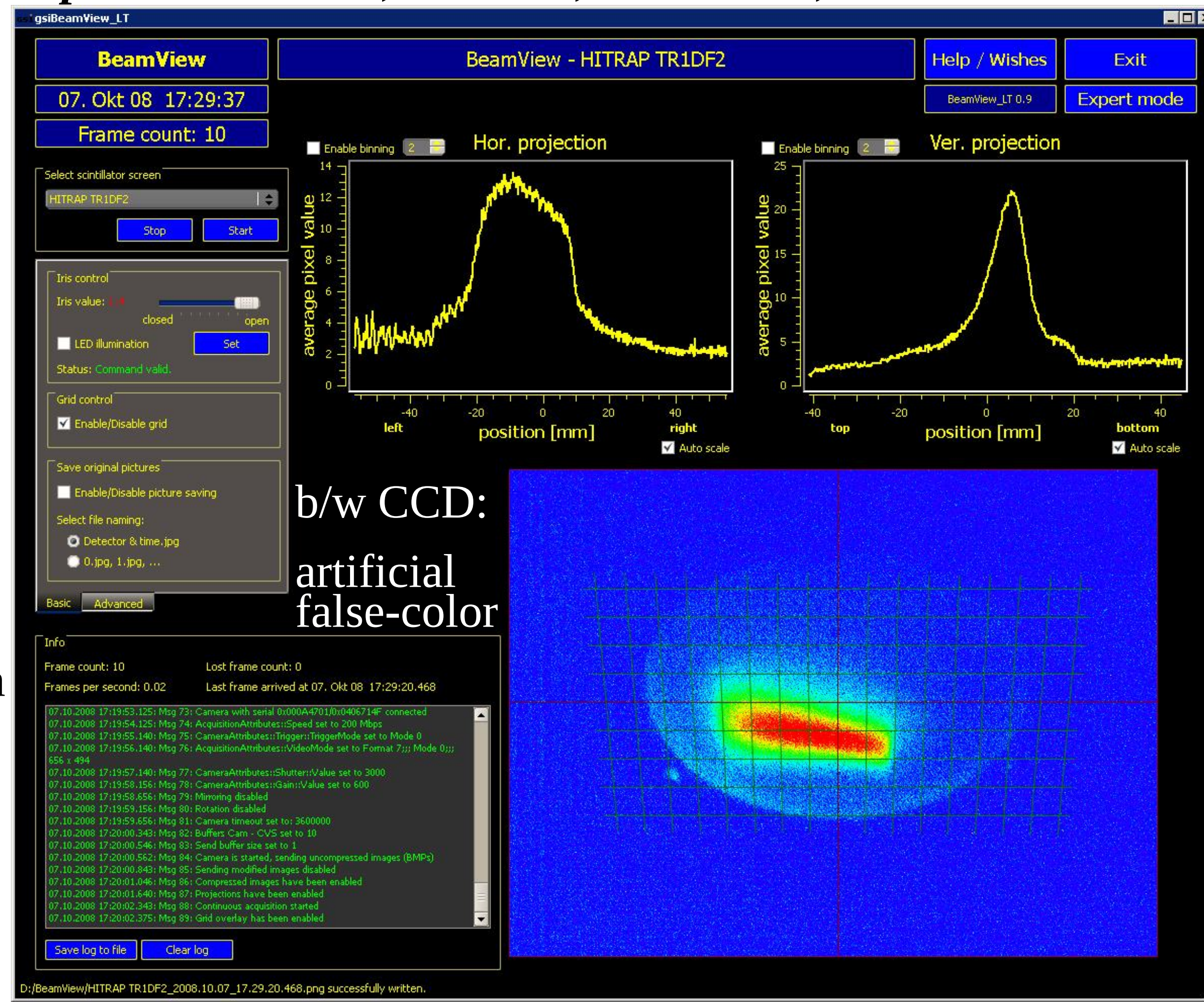

b/w CCD:

artificial false-color

Advantage of screens:

- ➢Direct 2-dim measurement
- ➢High spatial resolution
- ➢Cheap realization

⇒ widely used at transfer lines

Disadvantage of screens:

- ➢Intercepting device
- ➢ Some material might brittle
- ➢ Low dynamic range
- ➢Might be destroyed by the beam

Observation with

a CCD, CMOS or video camera

Scintillation Screen (beam stopped)

Light output from various Scintillating Screens

Example: Color CCD camera: Images at different particle intensities determined for U at 300 MeV/u

Al_2O_3

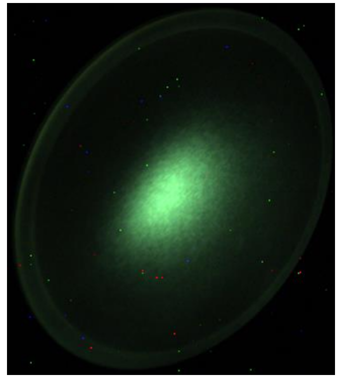

CsI:Tl

Al_2O_3:Cr

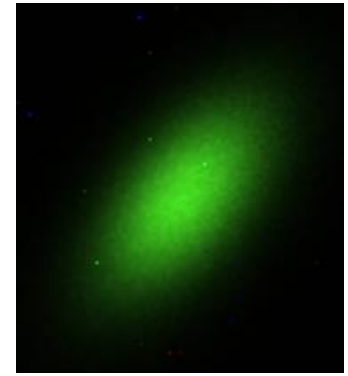

P43

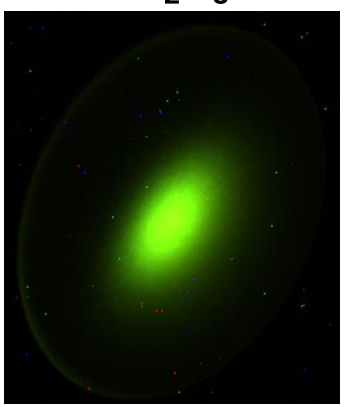

YAG:Ce

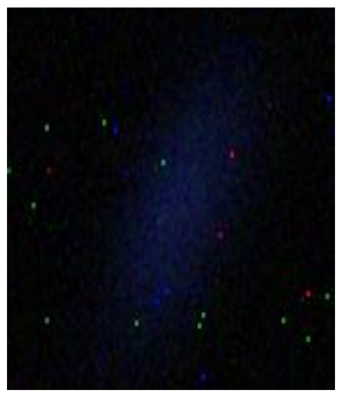

Quartz

Quartz:Ce

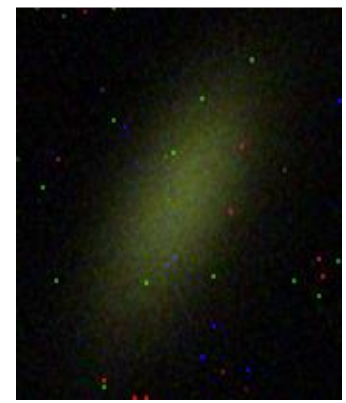

ZrO_2:Mg

- Very different light yield i.e. photons per ion‘s energy loss
- Different wavelength of emitted light

Material Properties for Scintillating Screens

Some materials and their basic properties:

Name	Type	Material	Activ.	Max. λ	Decay
Chromox	Cera-mics	Al_2O_3	Cr	700 nm	≈ 10 ms
Alumina		Al_2O_3	Non	380 nm	≈ 10 ns
YAG:Ce	Crystal	$Y_3Al_5O_{12}$	Ce	550 nm	200 ns
P43	Powder	Gd_2O_3S	Tb	545 nm	1 ms
P46		$Y_3Al_5O_{12}$	Ce	530 nm	300 ns
P47		$Y_3Si_5O_{12}$	Ce&Tb	400 nm	100 ns

Properties of a good scintillator:

- Large light output at optical wavelength
  → standard CCD camera can be used
- Large dynamic range → usable for different ions
- Short decay time → observation of variations
- Radiation hardness → long lifetime
- Good mechanical properties → typ. size up to Ø 10 cm

(Phosphor Pxx grains of Ø ≈ 10 μm on glass or metal).

Standard drive with P43 screen

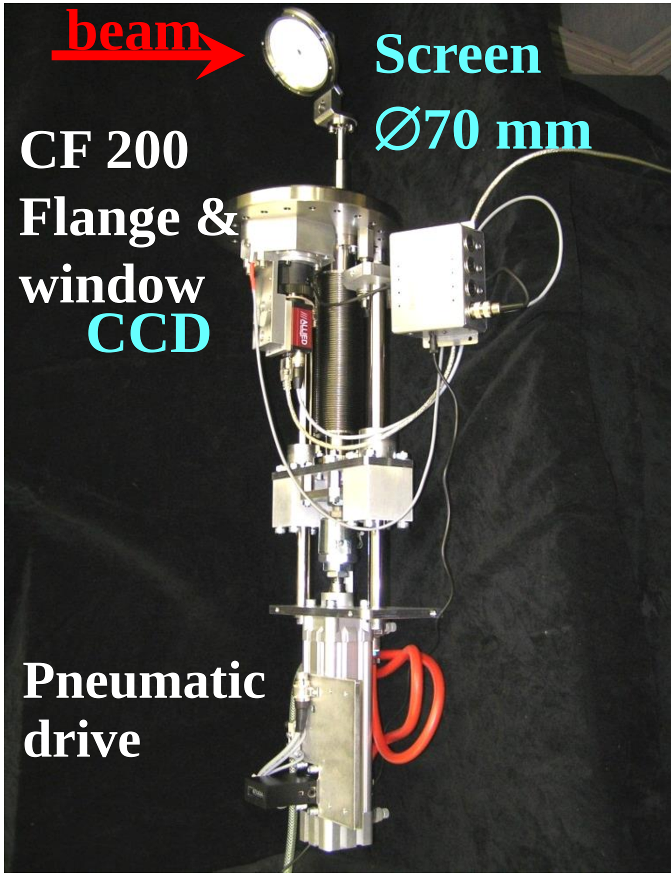

Outline:

- Scintillation screens:
  emission of light, universal usage, limited dynamic range
- **SEM-Grid:** emission of electrons, workhorse, limited resolution
- Wire scanner
- Ionization Profile Monitor
- Optical Transition Radiation
- Synchrotron Light Monitors
- Summary

Secondary Electron Emission by Ion Impact

Energy loss of ions in metals close to a surface:

Closed collision with large energy transfer: → fast e⁻ with E_{kin} >> 100 eV

Distant collision with low energy transfer → slow e⁻ with $E_{kin} \lesssim$ 10 eV

→ 'diffusion' & scattering with other e⁻: scattering length $L_s \approx$ 1 - 10 nm

→ at surface ≈ 90 % probability for escape

Secondary **electron yield** and energy distribution comparable for all metals!

⇒ $Y = const. * dE/dx$ (Sternglass formula)

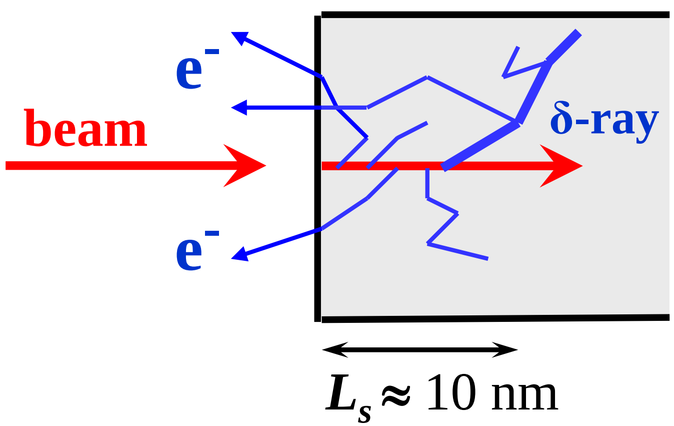

Different targets:

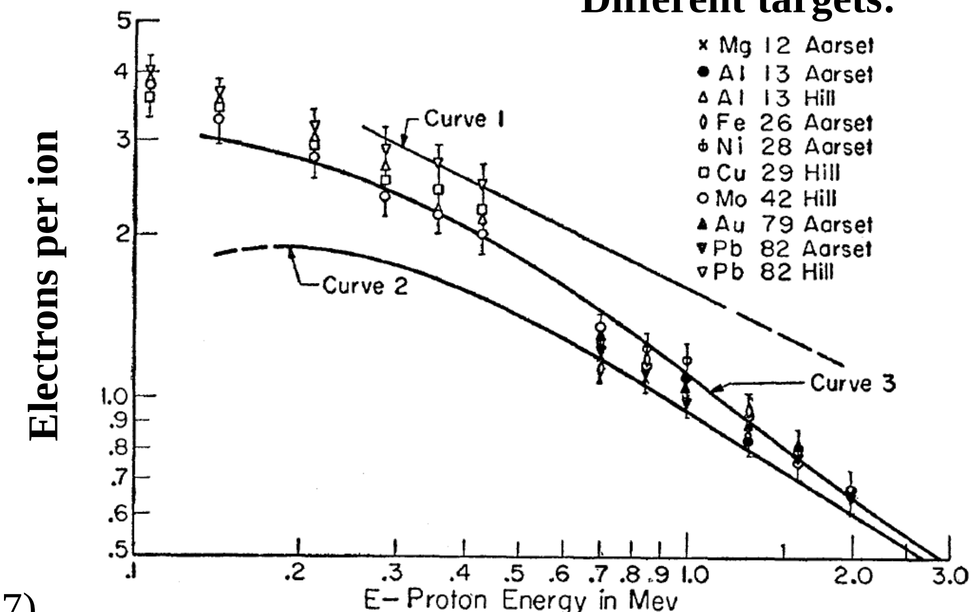

From E.J. Sternglass, Phys. Rev. 108, 1 (1957)

Secondary Electron Emission Grids = SEM-Grid

Beam surface interaction: e⁻ emission → measurement of current.

Example: 15 wire spaced by 1.5 mm:

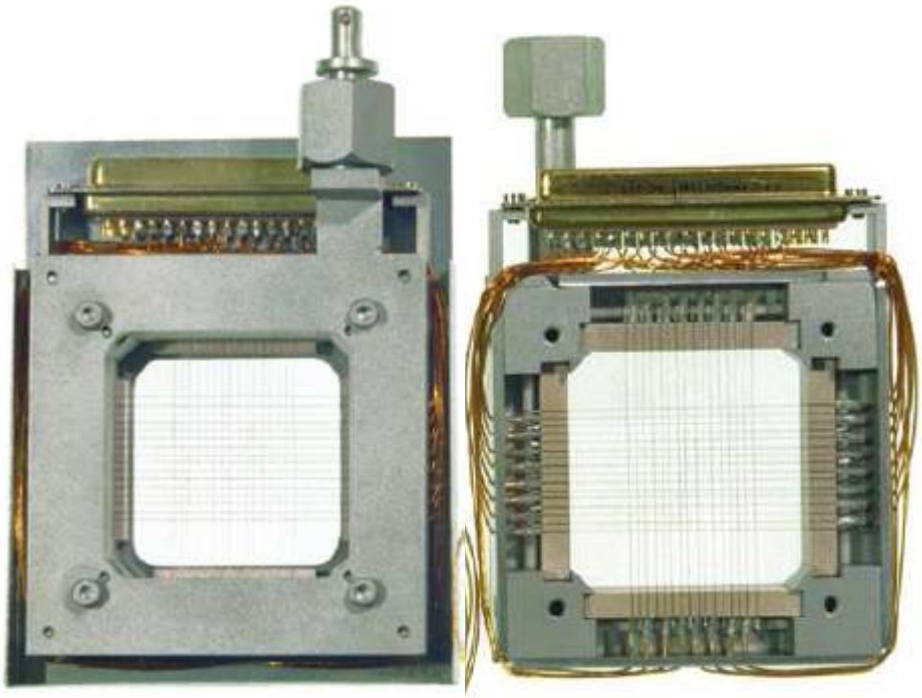

SEM-Grid feed-through on CF200:

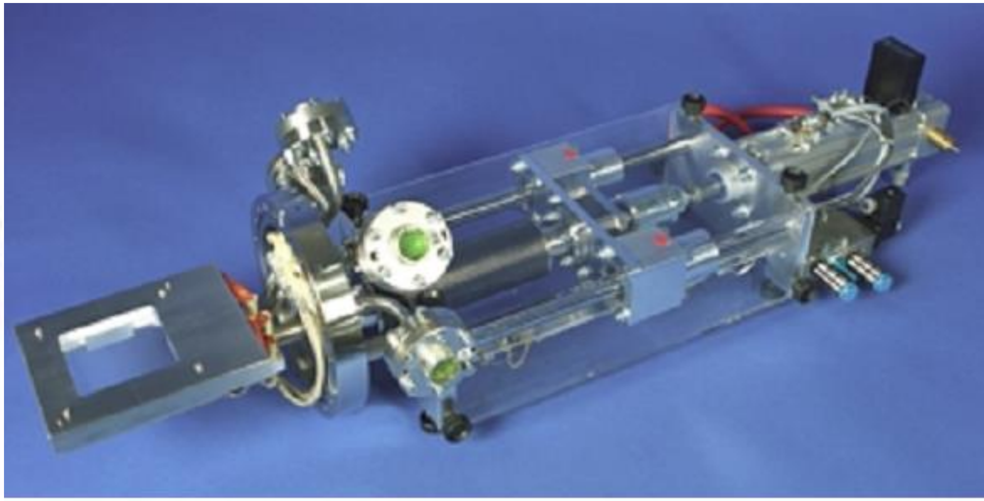

Beam surface interaction: e^- emission → measurement of current.

Example: 15 wire spaced by 1.5 mm:

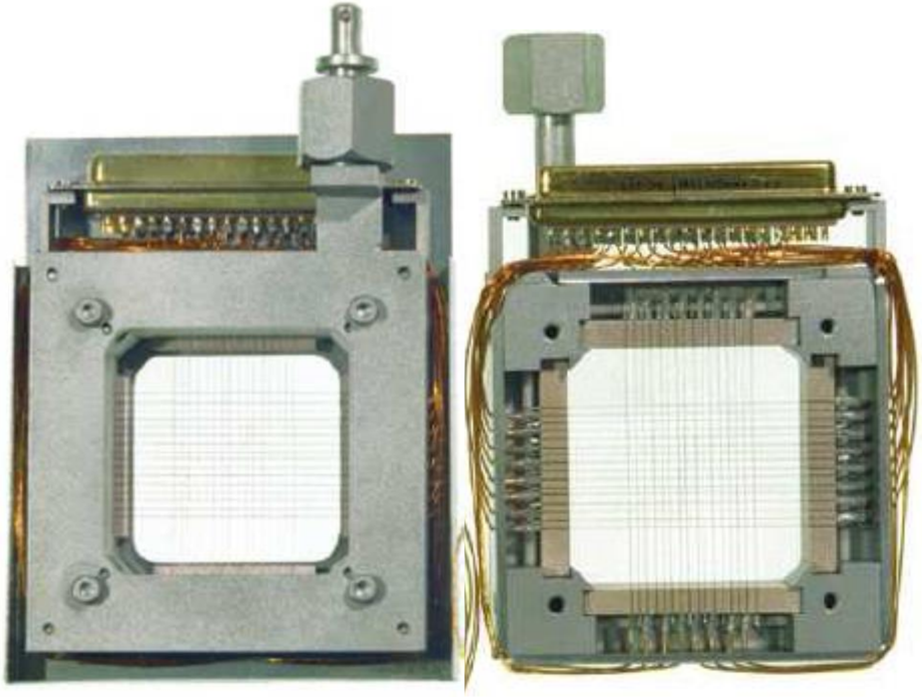

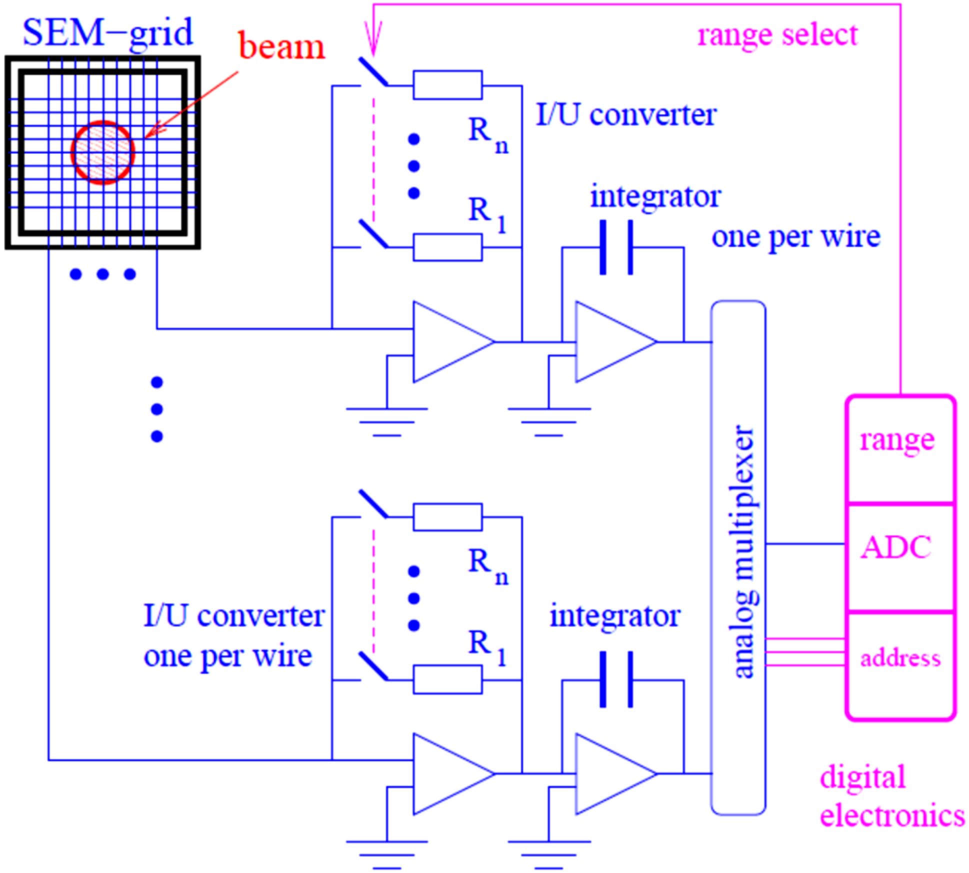

Each wire is equipped with one I/U converter
different ranges settings by R_i
→ very large dynamic range up to 10^6.

Even for low energies, several SEM-Grid can be used due to the ≈80 % transmission
⇒ frequently used instrument beam optimization: setting of quadrupoles, energy….

Example: C^{6+} beam of 11.4 MeV/u at different locations at GSI-LINAC

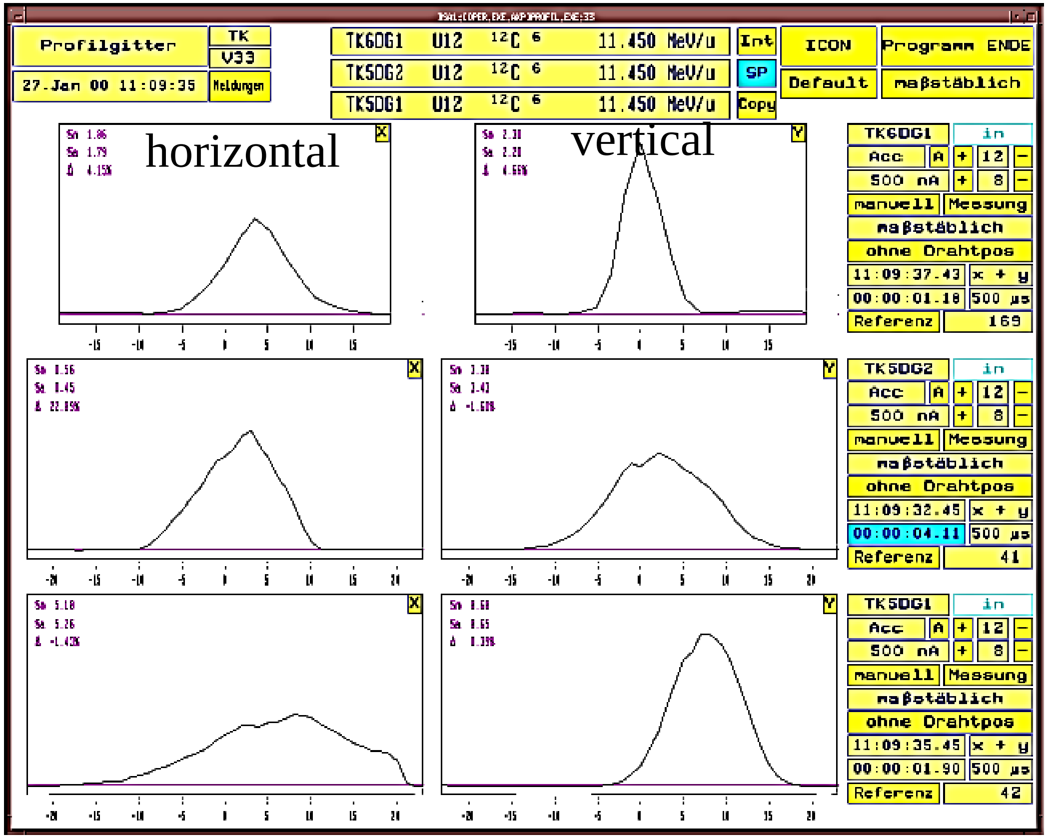

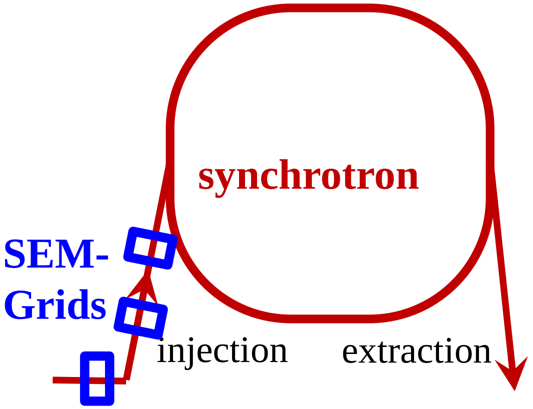

The Artist view of a SEM-Grid = Harp

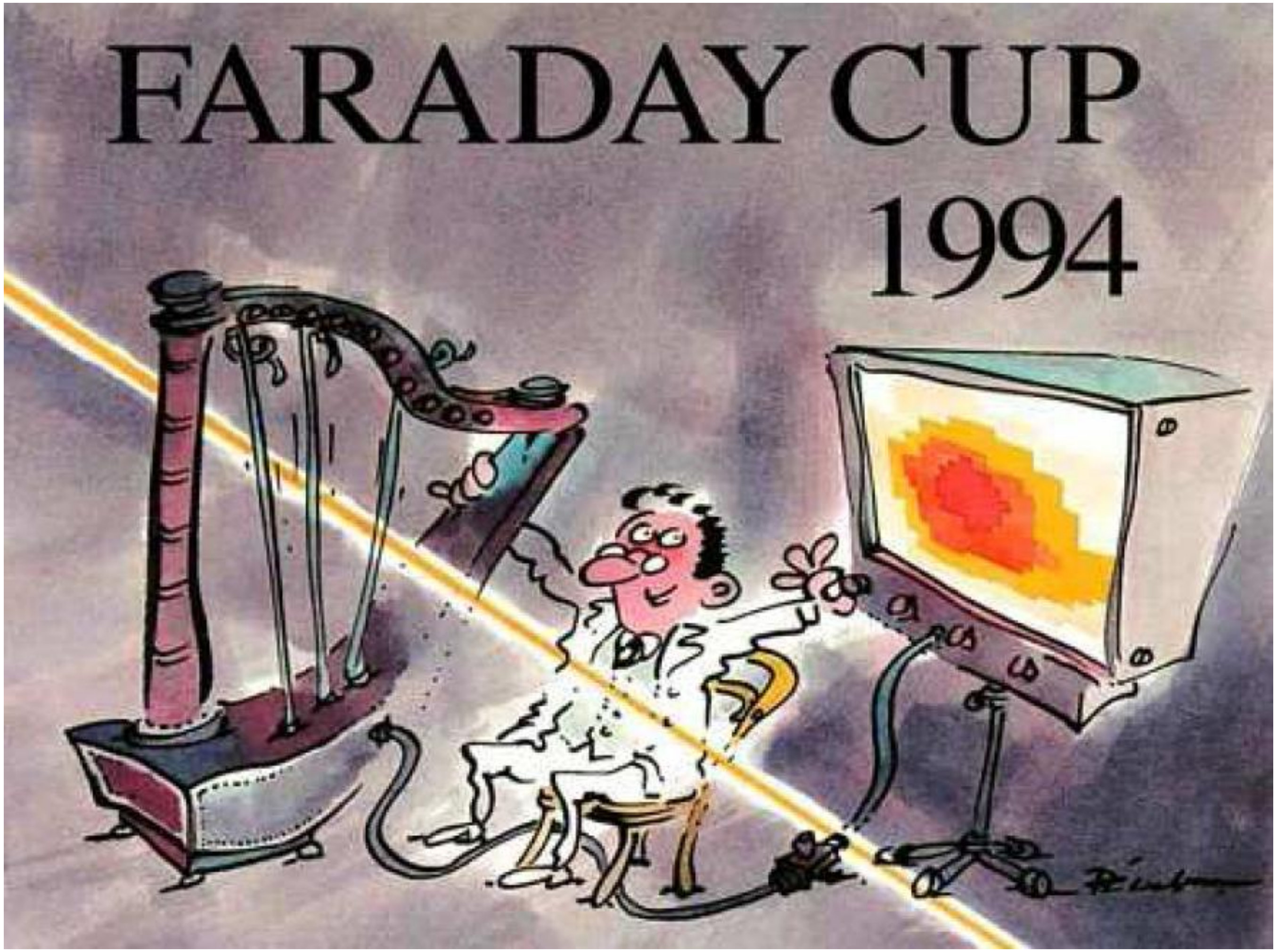

Outline:

- Scintillation screens:
  emission of light, universal usage, limited dynamic range
- SEM-Grid: emission of electrons, workhorse, limited resolution
- **Wire scanner:** emission of electrons, workhorse, scanning method
- Ionization Profile Monitor
- Optical Transition Radiation
- Synchrotron Light Monitors
- Summary

Idea: One wire is scanned through the beam!

Slow, linear scanner are used for:

- low energy protons
- high resolution measurements e.g. usable at e^+-e^- colliders by de-convolution $\sigma^2_{beam} = \sigma^2_{meas} - d^2_{wire}$
  $\Rightarrow$ resolution down to 10 µm range can be reached
- detection of beam halo.

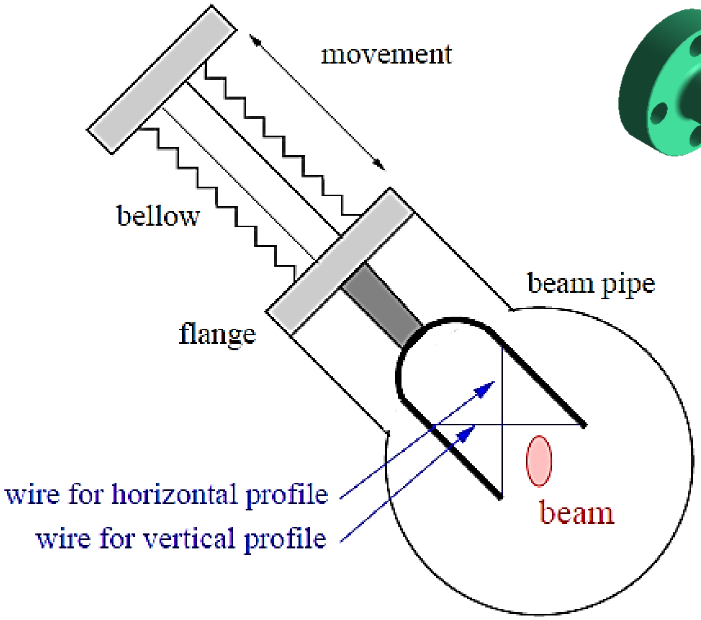

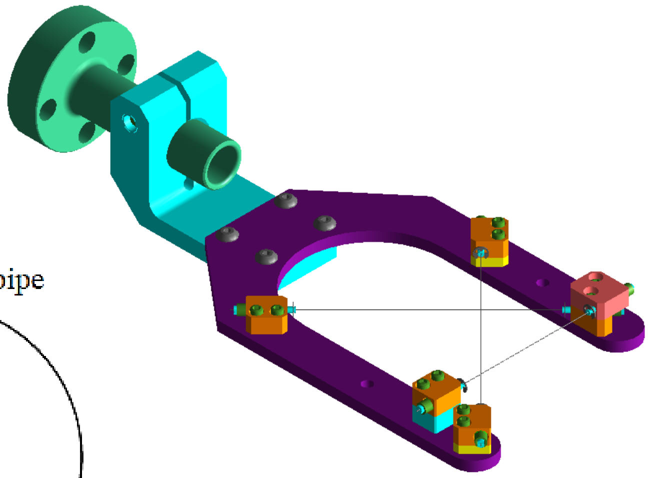

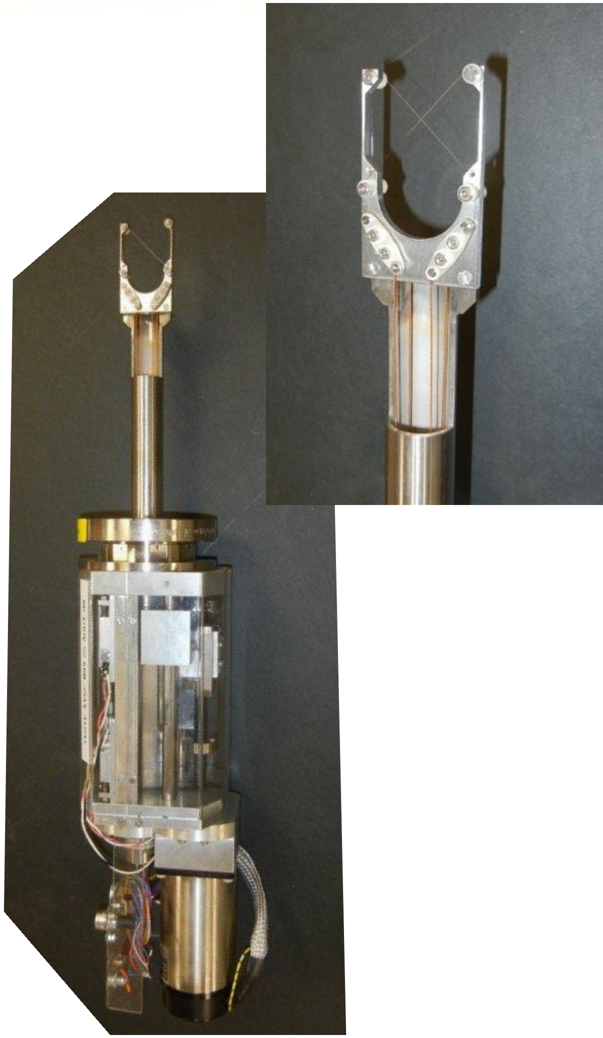

The Artist view of a Beam Scraper or Scanner

Fast, Flying Wire Scanner

In a synchrotron ***one*** wire is scanned though the beam as fast as possible.

Fast pendulum scanner for synchrotrons; sometimes it is called ***'flying wire'***:

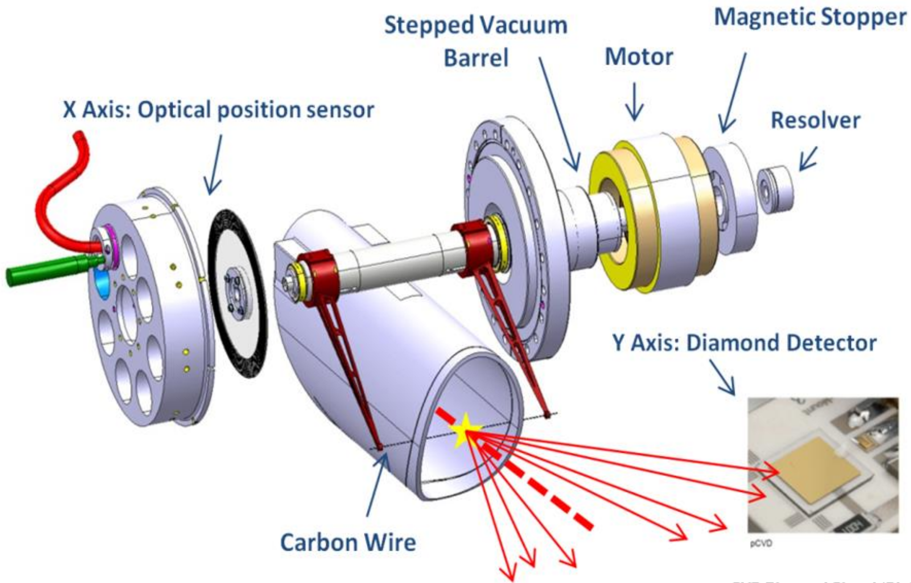

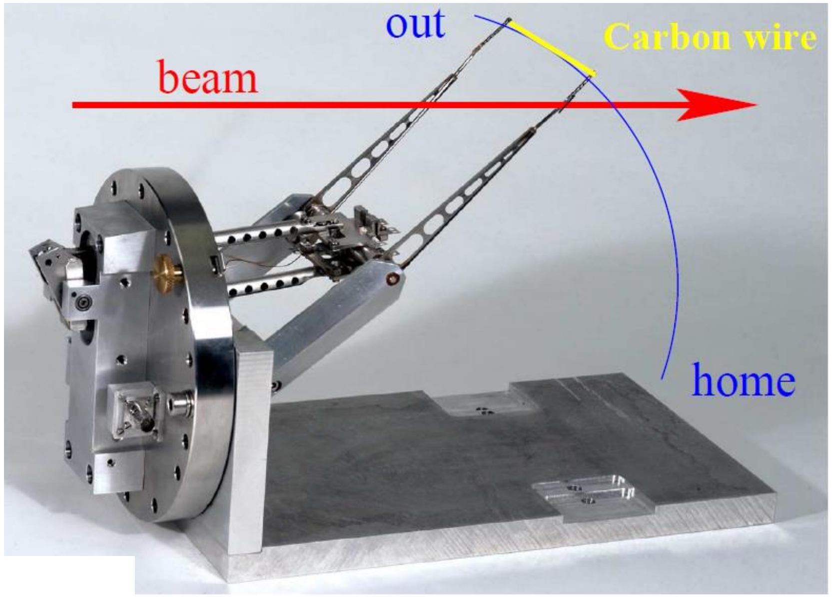

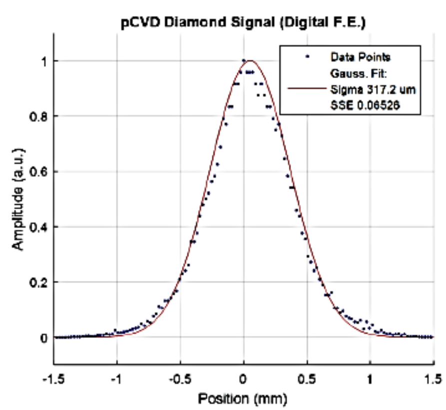

From https://twiki.cern.ch/twiki/bin/viewauth/BWSUpgrade/

Material: carbon or SiC → low Z-material for low energy loss and high temperature.

Thickness: down to 10 μm → high resolution.

Detection: Either the **secondary current** (like SEM-grid) or
high energy **secondary particles** (like beam loss monitor)
flying wire: only sec. particle detection due to induced current by movement.

Secondary particles:

Proton beam → hadrons shower (π, n, p...)

Electron beam → Bremsstrahlung photons.

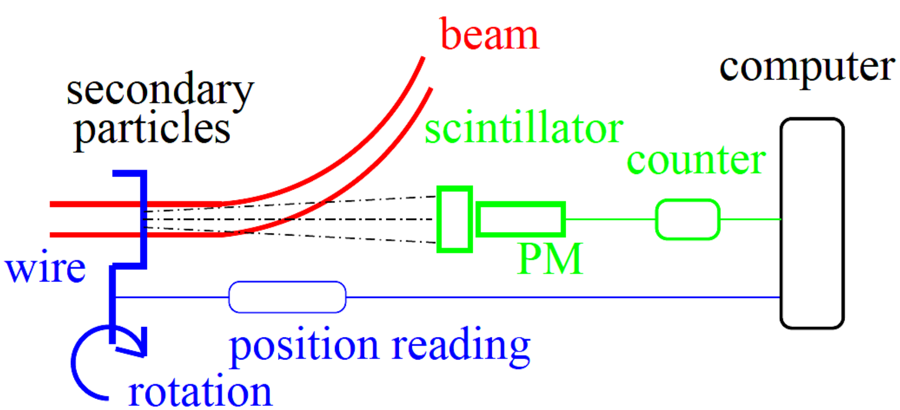

Proton impact on scanner at CERN-PS Booster:

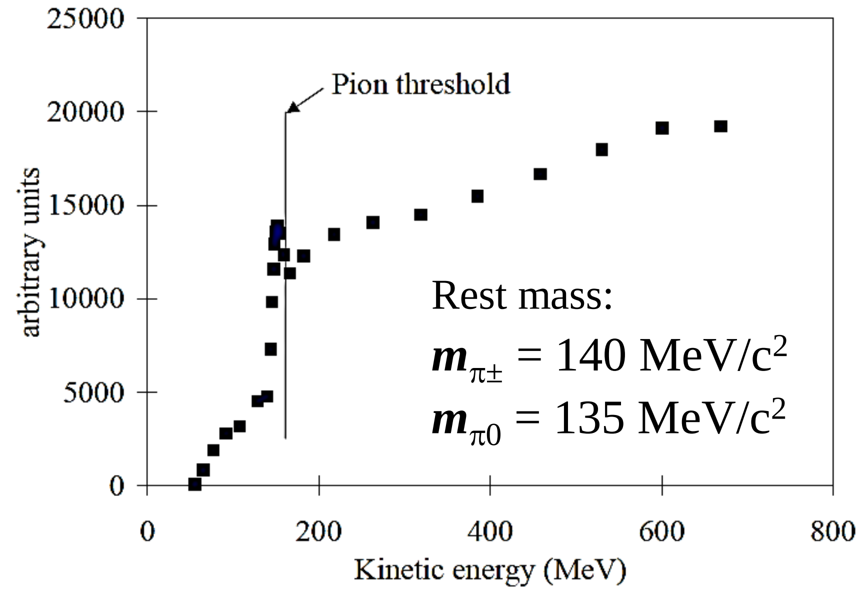

U. Raich et al., DIPAC 2005

Kinematics of flying wire:

Velocity during passage typically 10 m/s = 36 km/h and
typical beam size ∅ 10 mm ⇒ time for traversing the beam $t \approx 1$ ms

Challenges: Wire stability for fast movement with high acceleration

The Artist View of a Wire Scanner

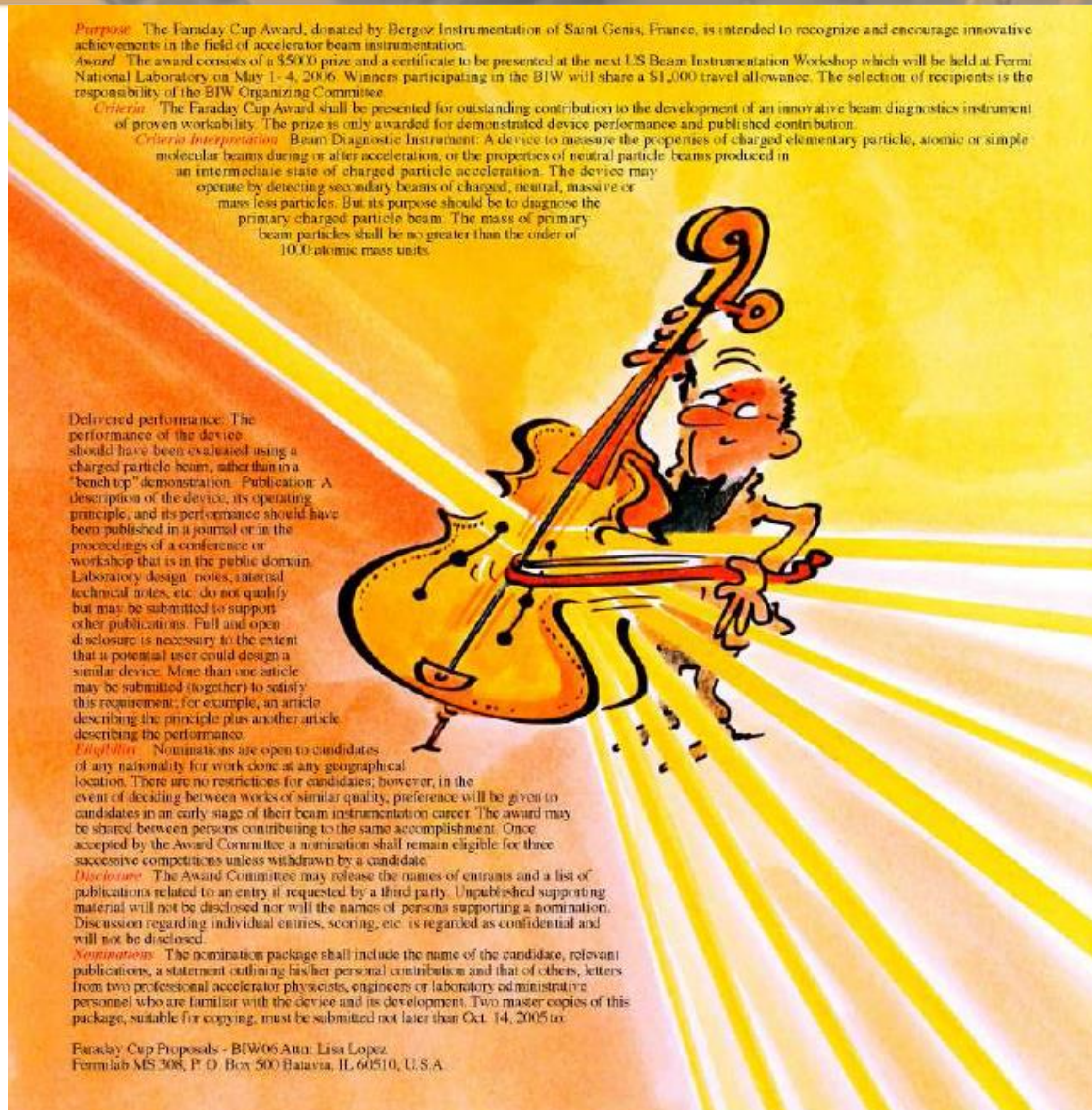

Purpose The Faraday Cup Award, donated by Bergoz Instrumentation of Saint Genis, France, is intended to recognize and encourage innovative achievements in the field of accelerator beam instrumentation.

Award The award consists of a $5000 prize and a certificate to be presented at the next US Beam Instrumentation Workshop which will be held at Fermi National Laboratory on May 1 - 4, 2006. Winners participating in the BIW will share a $1,000 travel allowance. The selection of recipients is the responsibility of the BIW Organizing Committee.

Criteria The Faraday Cup Award shall be presented for outstanding contribution to the development of an innovative beam diagnostics instrument of proven workability. The prize is only awarded for demonstrated device performance and published contribution.

Criteria Interpretation Beam Diagnostic Instrument: A device to measure the properties of charged elementary particle, atomic or simple molecular beams during or after acceleration, or the properties of neutral particle beams produced in an intermediate state of charged particle acceleration. The device may operate by detecting secondary beams of charged, neutral, massive or mass less particles. But its purpose should be to diagnose the primary charged particle beam. The mass of primary beam particles shall be no greater than the order of 100 atomic mass units.

Delivered performance: The performance of the device should have been evaluated using a charged particle beam, rather than in a "bench top" demonstration. Publication: A description of the device, its operating principle, and its performance should have been published in a journal or in the proceedings of a conference or workshop that is in the public domain. Laboratory design notes, internal technical notes, etc. do not qualify but may be submitted to support other publications. Full and open disclosure is necessary to the extent that a potential user could design a similar device. More than one article may be submitted (together) to satisfy this requirement; for example, an article describing the principle plus another article describing the performance.

Eligibility Nominations are open to candidates of any nationality for work done at any geographical location. There are no restrictions for candidates; however, in the event of deciding between works of similar quality, preference will be given to candidates in an early stage of their beam instrumentation career. The award may be shared between persons contributing to the same accomplishment. Once accepted by the Award Committee a nomination shall remain eligible for three successive competitions unless withdrawn by a candidate.

Disclosure The Award Committee may release the names of entrants and a list of publications related to an entry if requested by a third party. Unpublished supporting material will not be disclosed nor will the names of persons supporting a nomination. Discussion regarding individual entries, scoring, etc. is regarded as confidential and will not be disclosed.

Nominations The nomination package shall include the name of the candidate, relevant publications, a statement outlining his/her personal contribution and that of others, letters from two professional accelerator physicists, engineers or laboratory administrative personnel who are familiar with the device and its development. Two master copies of this package, suitable for copying, must be submitted not later than Oct. 14, 2005 to:

Faraday Cup Proposals - BIW06 Attn: Lisa Lopez
Fermilab MS 308, P. O. Box 500 Batavia, IL 60510, U.S.A.

Comparison between SEM-Grid and Wire Scanners

Grid: Measurement at a single moment in time

Scanner: Fast variations can not be monitored

→ for pulsed LINACs precise synchronization is needed

Grid: Not adequate at synchrotrons for stored beam parameters

Scanner: At high energy synchrotrons flying wire scanners are nearly non-destructive

---

Grid: Resolution of a grid is fixed by the wire distance (typically 1 mm)

Scanner: For slow scanners the resolution is about the wire thickness (down to 10 μm)

→ used for e^--beams having small sizes (down to 10 μm)

Grid: Needs one electronics channel per wire

→ expensive electronics and data acquisition

Scanner: Needs a precise movable feed-through → expensive mechanics.

Outline:

- Scintillation screens:
  emission of light, universal usage, limited dynamic range
- SEM-Grid: emission of electrons, workhorse, limited resolution
- Wire scanner: emission of electrons, workhorse, scanning method
- **Ionization Profile Monitor:**
  secondary particle detection from interaction beam-residual gas
- Optical Transition Radiation
- Synchrotron Light Monitors
- Summary

Ionization Profile Monitor at GSI Synchrotron

Non-destructive device for proton synchrotron:

- beam ionizes the residual gas by electronic stopping
- gas ions or e⁻ accelerated by E -field ≈1 kV/cm
- spatial resolved single particle detection

Realization at GSI synchrotron:

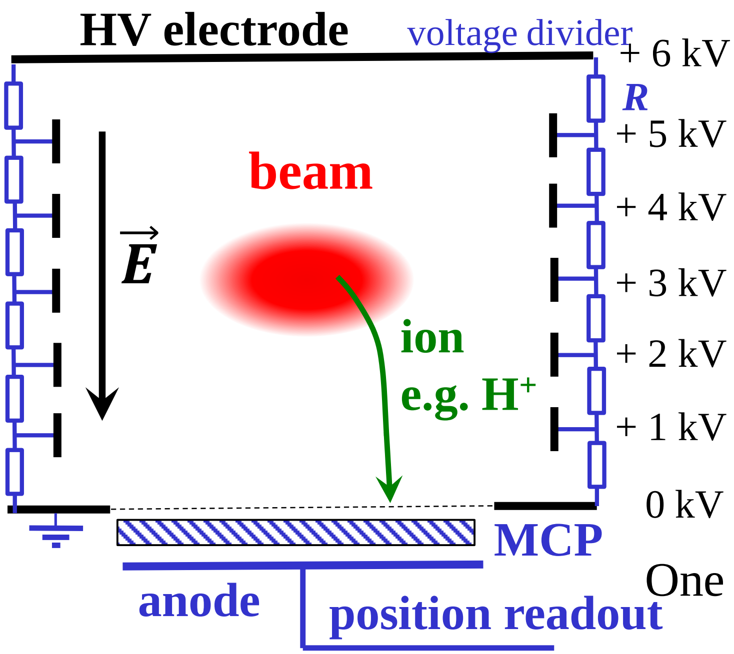

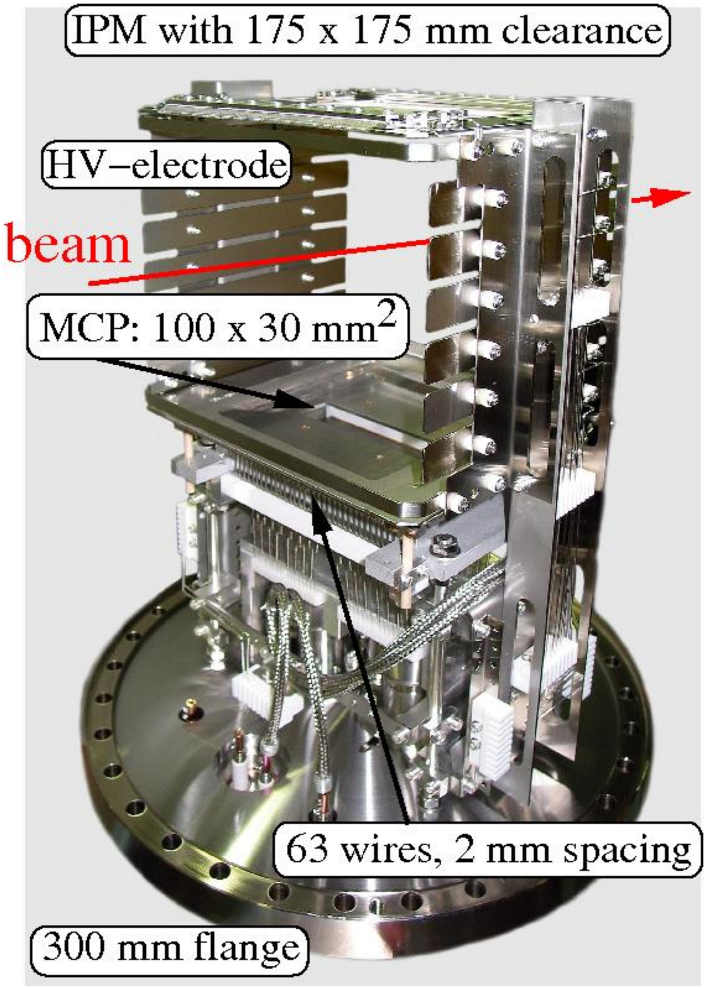

One device per plane

Typical vacuum pressure:

Transfer line: N_2 $10^{-8}...10^{-6}$ mbar $\cong 3\cdot10^{8}...3\cdot10^{10}$ cm^{-3}

Synchrotron: H_2 $10^{-11}...10^{-9}$ mbar $\cong 3\cdot10^{5}...3\cdot10^{7}$ cm^{-3}

Ionization Profile Monitor Realization

The realization for the heavy ion storage ring ESR at GSI:

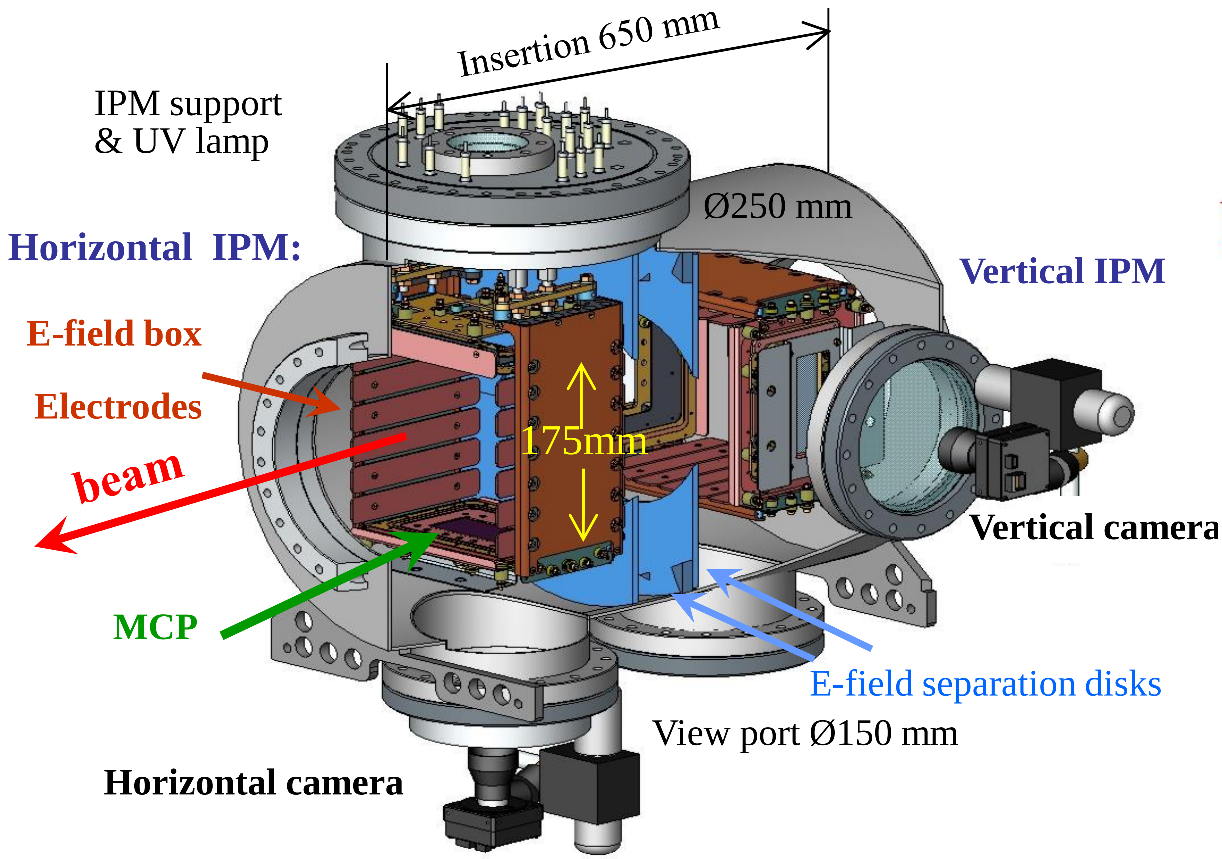

Realization at GSI synchrotron:

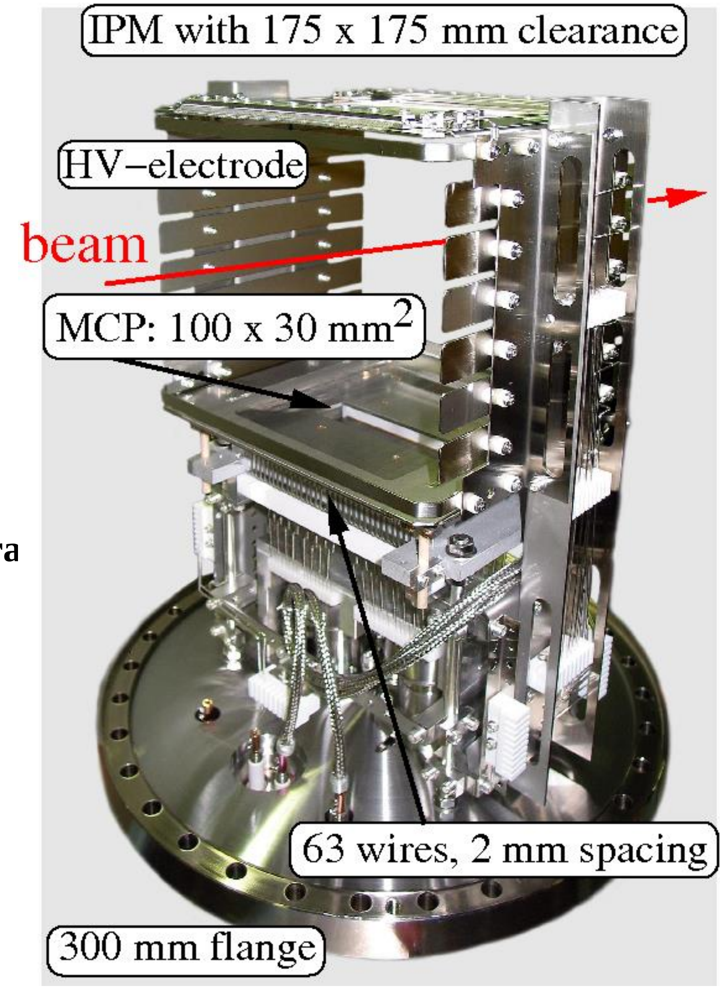

Ionization Profile Monitor Realization

The realization for the heavy ion storage ring ESR at GSI:

Realization at GSI synchrotron:

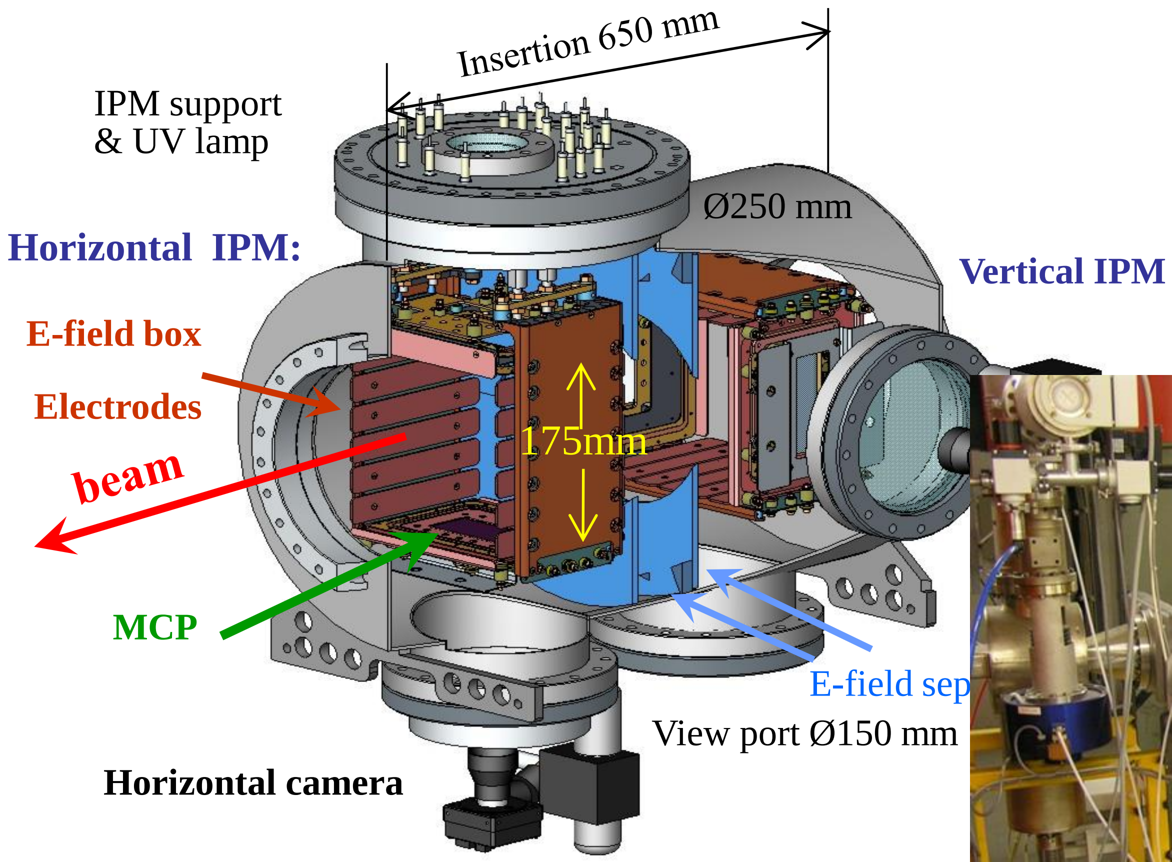

The emittance $\varepsilon = \int dxdx'$ is defined via the position deviation and angle in **lab-frame**

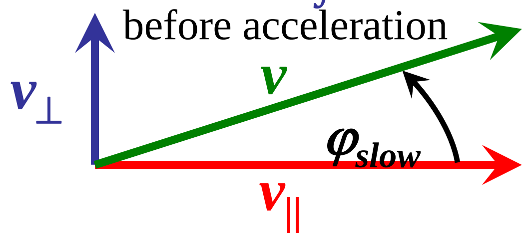

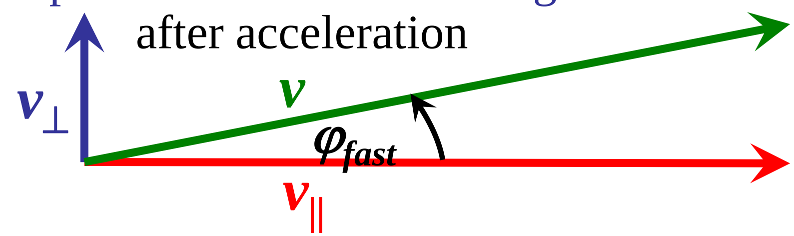

After acceleration the longitudinal velocity is increased $\Rightarrow$ angle φ is smaller

The angle is expressed in momenta: $x' = p_\perp / p_\parallel$ the emittance is $\langle xx' \rangle = 0$: $\varepsilon = x \cdot x' = x \cdot p_\perp / p_\parallel$

$\Rightarrow$ under ideal conditions the emittance can be normalized to the momentum $p_\parallel = \gamma \cdot m \cdot \beta c$

$\Rightarrow$ normalized emittance $\varepsilon_{norm} = \beta \gamma \cdot \varepsilon$ is preserved with the Lorentz factor γ and velocity $\beta = v/c$

Example: Acceleration in GSI-synchrotron for C^{6+} from 6.7 $\rightarrow$ 600 MeV/u (β = 12 $\rightarrow$ 79 %) observed by IPM

theoretical width: $\langle x \rangle_f = \sqrt{\dfrac{\beta_i \cdot \gamma_i}{\beta_f \cdot \gamma_f}} \cdot \langle x \rangle_i$

$= 0.33 \cdot \langle x \rangle_i$

measured width: $\langle x \rangle_f \approx 0.37 \cdot \langle x \rangle_i$

IPM is well suited
for long time observations
without beam disturbance
$\rightarrow$ mainly used at proton synchrotrons.

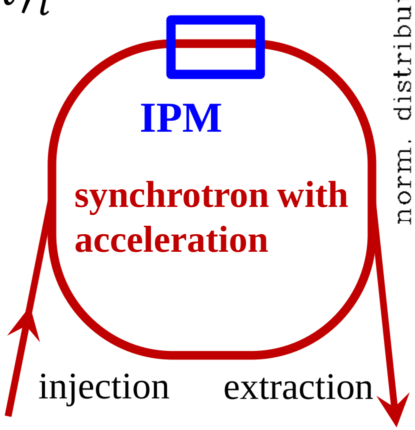

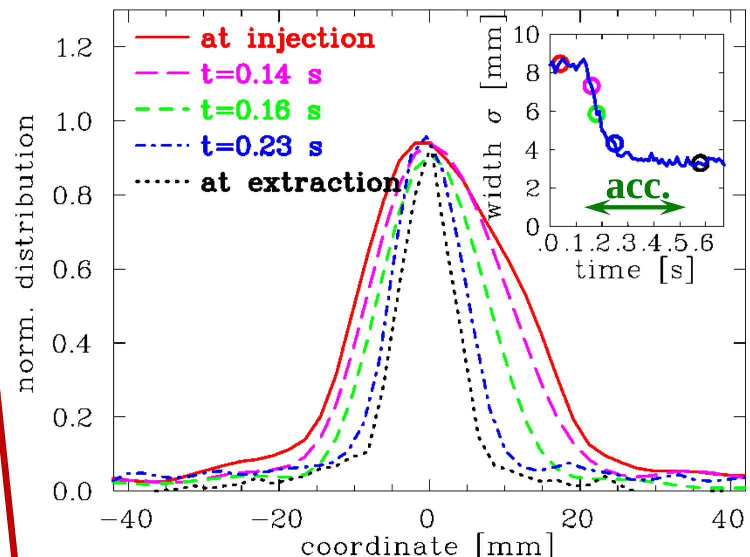

→ OTR

Ideal case of injection matching:

Orientation of injected beam matches phase space as given by synchrotron

Twiss parameters α, β, and γ i.e. 'machine emittance'

⇔ no change after each turn ⇔ stable storage

⇔ The beam ellipse $\boldsymbol{\sigma}_{beam}$ correspond to the machine ellipse at injection point for N=0 i.e.

$$\boldsymbol{\sigma}_{beam}(N=0) = \varepsilon_{beam}\begin{pmatrix}\beta_{synch} & -\alpha_{synch} \\ -\alpha_{synch} & \gamma_{synch}\end{pmatrix}$$

⇒ **only in this case stable storage** (math: $t \rightarrow \infty$)

$$\boldsymbol{\sigma}_{beam}(N=0) = \boldsymbol{\sigma}_{beam}(N \rightarrow \infty)$$

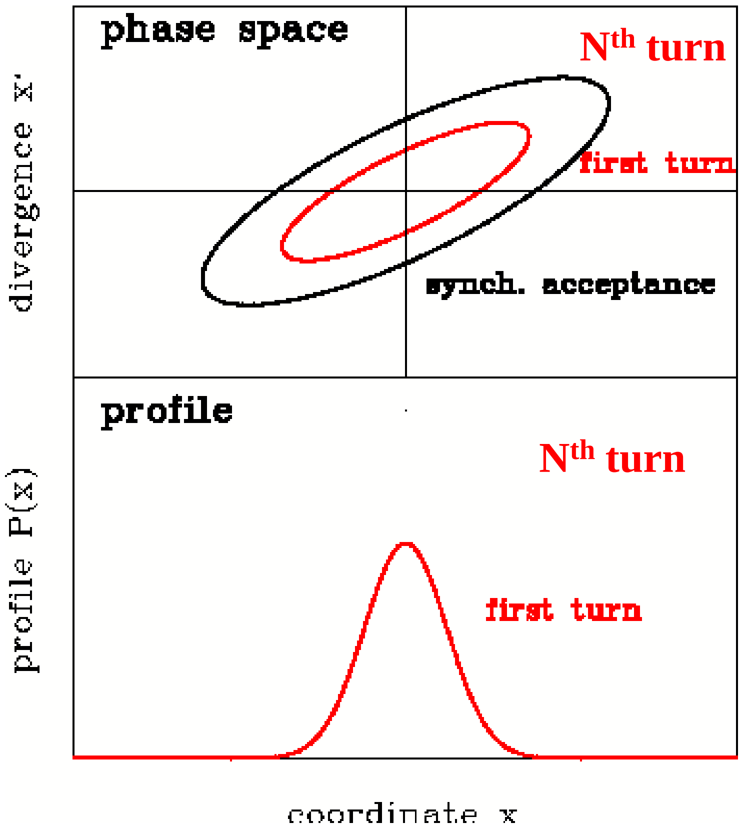

Injection Matching into a Synchrotron: Phase Space Mismatch

Ideal case of injection matching:

Orientation of injected beam matches phase space as given by synchrotron Twiss parameters α, β, and γ i.e. 'machine emittance' ⇔ no change after each turn ⇔ stable storage

Mismatched case:

- The beam ellipse $\boldsymbol{\sigma}_{beam}$ has different orientation as machine ellipse at injection point for N=0 i.e.
- Transformation after one turn

$$\boldsymbol{\sigma}_{beam}(N=1) = \mathbf{M}\boldsymbol{\sigma}_{beam}(N=0)\,\mathbf{M}^T \neq \boldsymbol{\sigma}_{beam}(N=0)$$

i.e. rotation in phase space by the tune

i.e. phase advance per turn

Depictive argument: A particle on both ellipses

Observable quantity: Beam profile oscillates

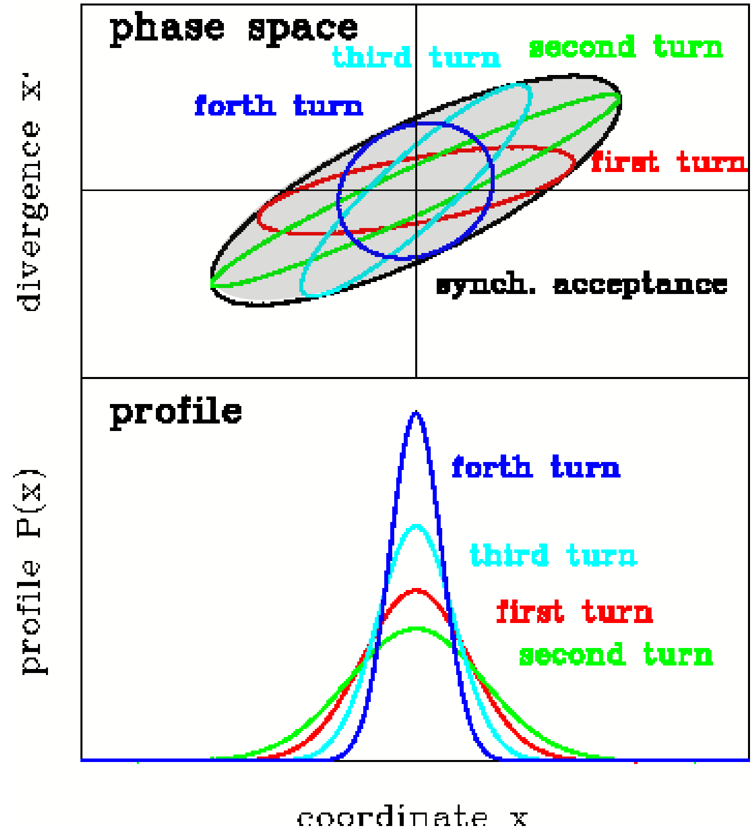

After many turns:

Particle have different tunes e.g. by longitudinal momentum deviation and chromaticity $\frac{\Delta Q}{Q_0} = \xi \cdot \frac{\Delta p}{p_0}$

or space charge ΔQ_{incoh} ⇒ Entire transverse phase space is filled i.e. beam with enlarged emittance

Mis-matched injection into a synchrotron:

Can be monitored by beam profile measurement:

Example: Injection of a 80 ns bunch of protons into CERN PS at 1.4 GeV/u (2.2 μs revolution time)
Profile measurement by SEM-Grid

- Turn-by-turn profile variation related to tune
- Used for improvement of injection parameters

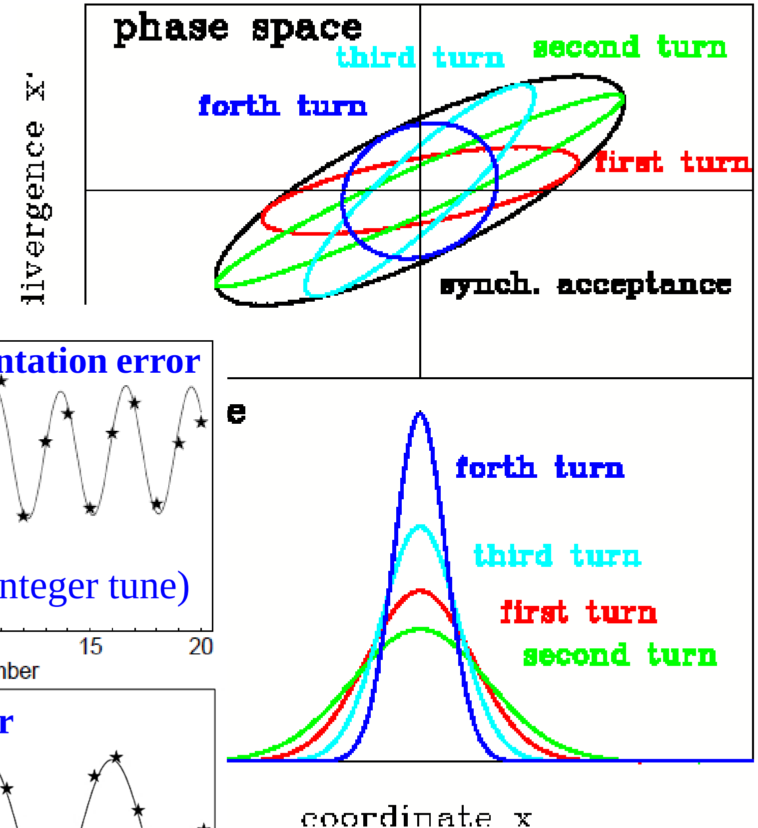

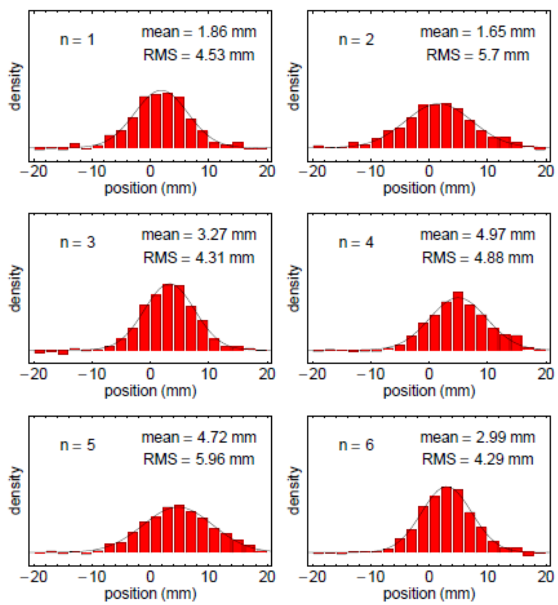

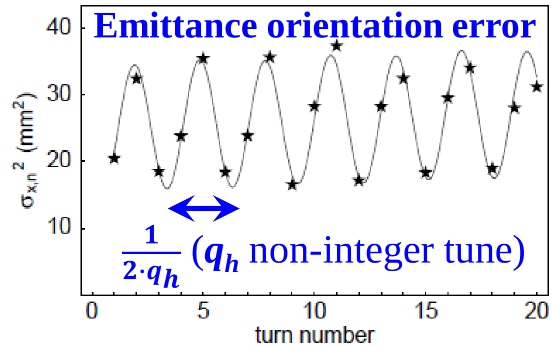

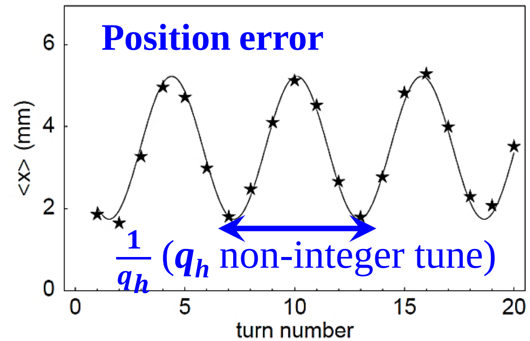

From M. Benedikt et al., DIPAC 2001

Outline:

- Scintillation screens:
  emission of light. universal usage, limited dynamic range
- SEM-Grid: emission of electrons, workhorse, limited resolution
- Wire scanner: emission of electrons, workhorse, scanning method
- Ionization Profile Monitor:
  secondary particle detection from interaction beam-residual gas
- Optical Transition Radiation:
  crossing material boundary, for relativistic beams only
- Synchrotron Light Monitors
- Summary

Optical Transition Radiation OTR for a single charge *e*:

Assuming a charge ***e*** approaches an ideal conducting boundary e.g. metal foil

- image charge is created by electric field
- dipole type field pattern
- field distribution depends on velocity β and Lorentz factor γ due to relativistic trans. field increase
- penetration of charge through surface within t < 10 fs: sudden change of source distribution
- emission of radiation with dipole characteristic

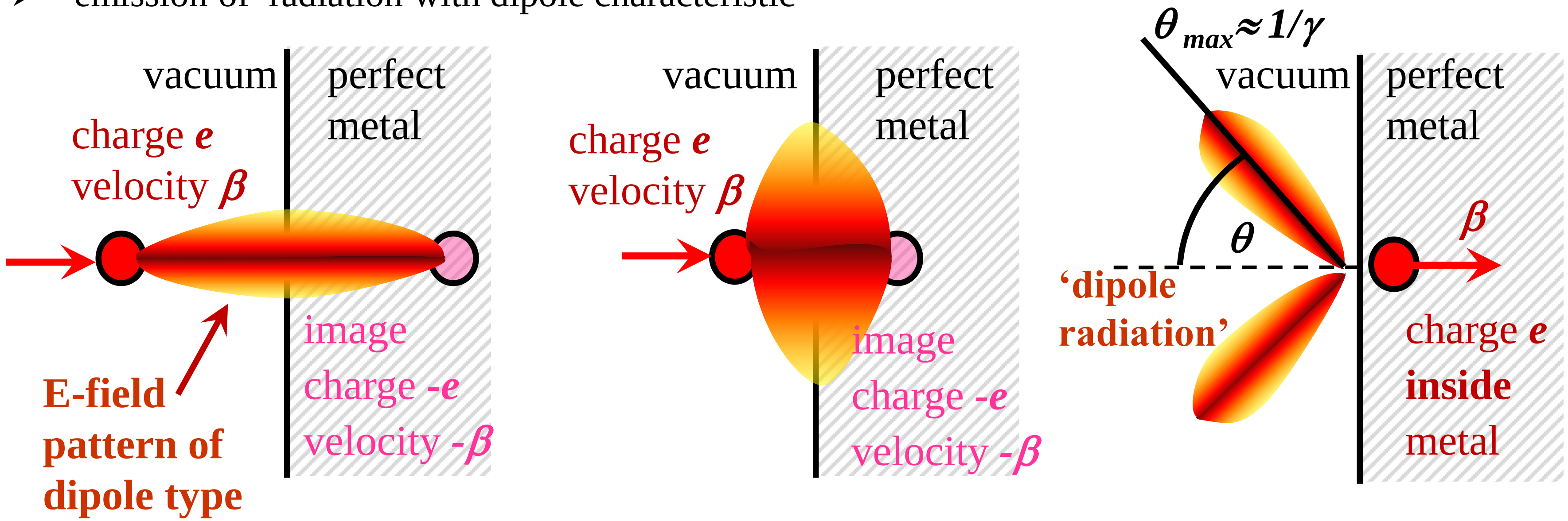

sudden change charge distribution
rearrangement of sources ⇔ radiation

Other physical interpretation: Impedance mismatch at boundary leads to radiation

Optical Transition Radiation OTR can be described in classical physics:

approximated formula for normal incidence & in-plane polarization:

$$\frac{d^2W}{d\theta\, d\omega} \approx \frac{2e^2\beta^2}{\pi c} \cdot \frac{\sin^2\theta \cdot \cos^2\theta}{\left(1-\beta^2\cos^2\theta\right)^2}$$

W: radiated energy

ω: frequency of wave

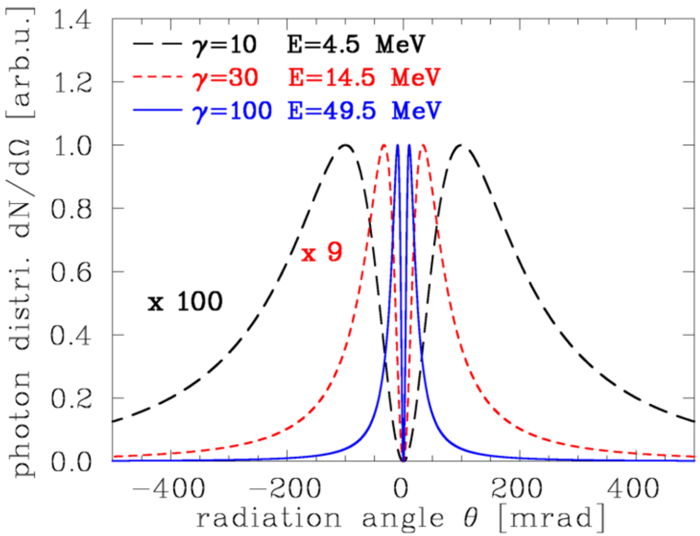

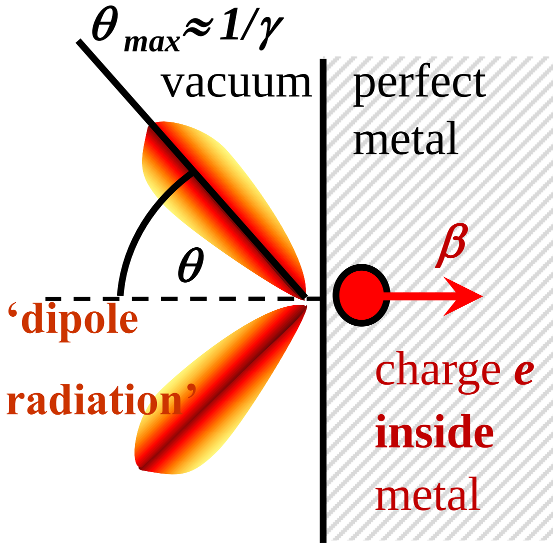

Angular distribution of radiation in optical spectrum:

- lope emission pattern depends on velocity or Lorentz factor γ
- peak at angle $\theta \approx 1/\gamma$
- emitted energy i.e. amount of photons scales with $W \propto \beta^2$
- broad wave length spectrum (i.e. no dependence on ω)

→ suited for high energy electrons

sudden change charge distribution
rearrangement of sources ⇔ radiation

Technical Realization of Optical Transition Radiation OTR

OTR is emitted by charged particle passage through a material boundary.

Photon distribution:

within a solid angle $d\Omega$ and

Wavelength interval λ_{begin} to λ_{end}

$$\frac{dN_{photon}}{d\Omega} = N_{beam} \cdot \frac{2e^2\beta^2}{\pi c} \cdot \log\left(\frac{\lambda_{begin}}{\lambda_{end}}\right) \cdot \frac{\theta^2}{\left(\gamma^{-2}+\theta^2\right)^2}$$

- Detection: Optical 400 nm < λ < 800 nm

  using image intensified CCD

- Larger signal for relativistic beam $\gamma >> 1$
- Low divergence for $\gamma >> 1 \Rightarrow$ large signal

$\Rightarrow$ **well suited for e⁻ beams**

$\Rightarrow$ **p-beam only for E_{kin} > 10 GeV $\Leftrightarrow \gamma > 10$**

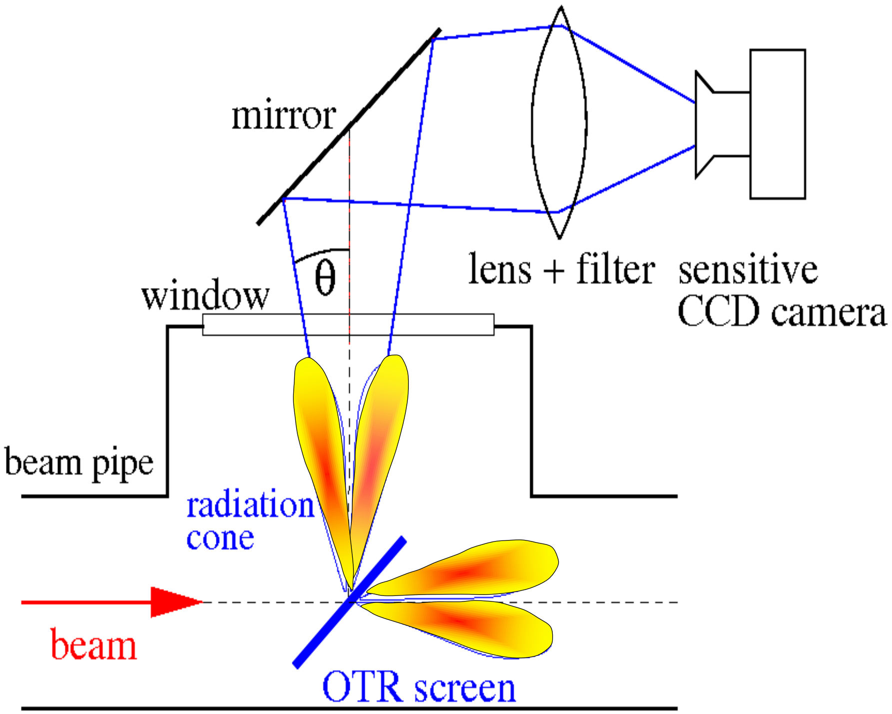

- Insertion of thin Al-foil under 45°
- Observation of low light by CCD.

Example of realization at TERATRON:

- Insertion of foil
  e.g. 5 μm Kapton coated with 0.1μm Al

Advantage: thin foil ⇒ low heating & straggling
2-dim image visible

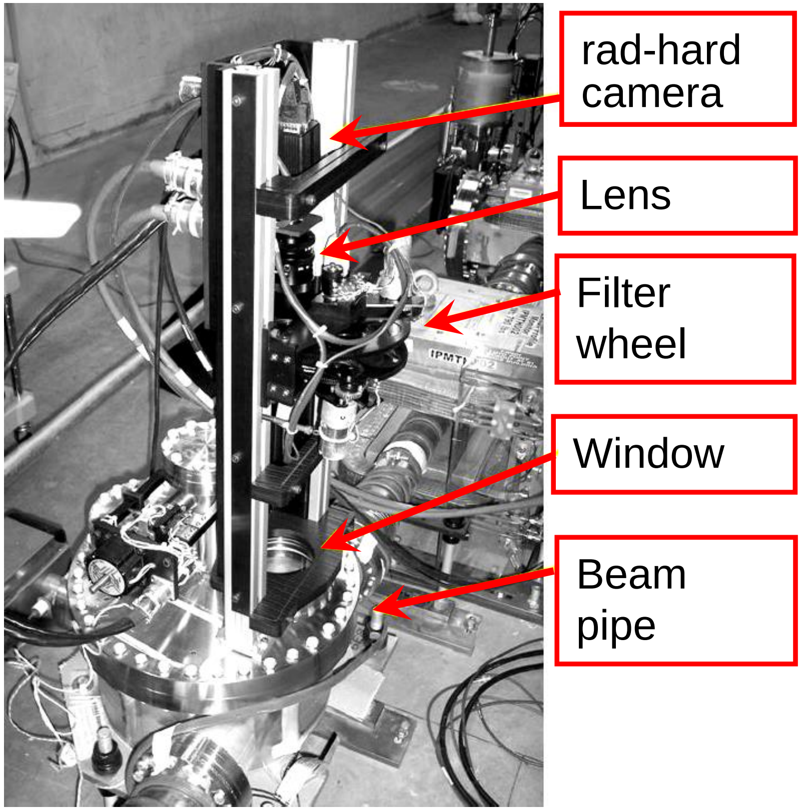

Results at FNAL-TEVATRON synchrotron with 150 GeV proton
Using fast camera: Turn-by-turn measurement

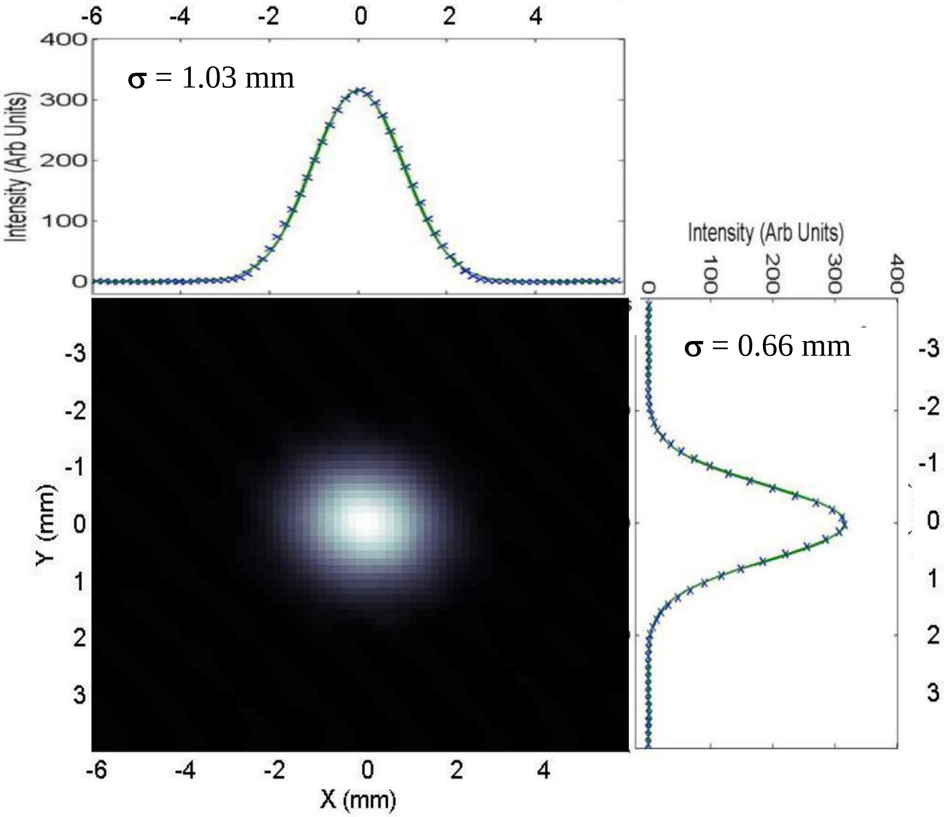

Courtesy V.E. Scarpine (FNAL) et al., BIW'06

Installation of OTR and scintillation screens on same drive :

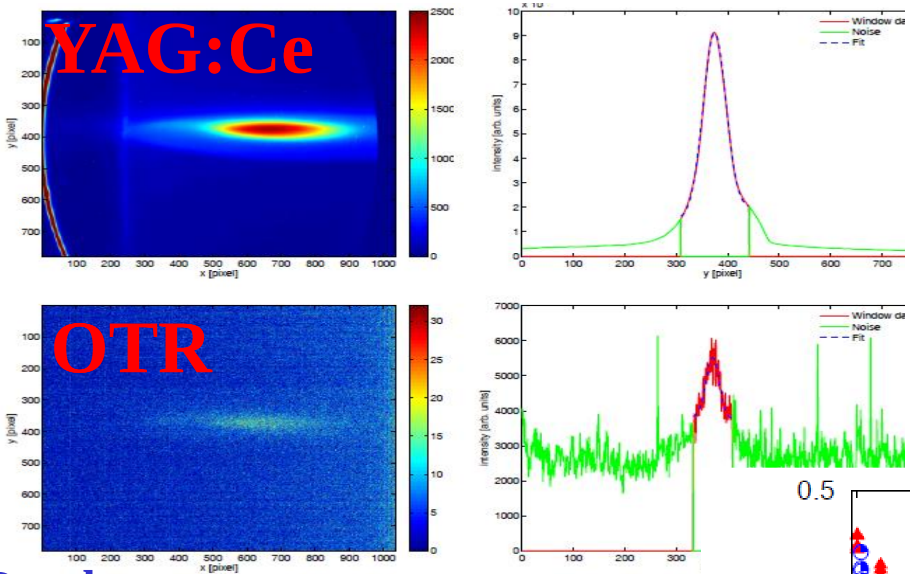

Example: ALBA LINAC 100 MeV

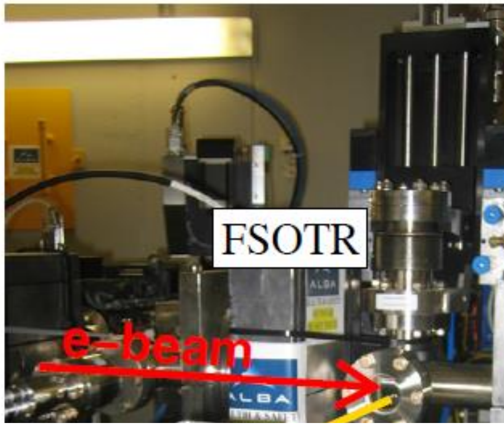

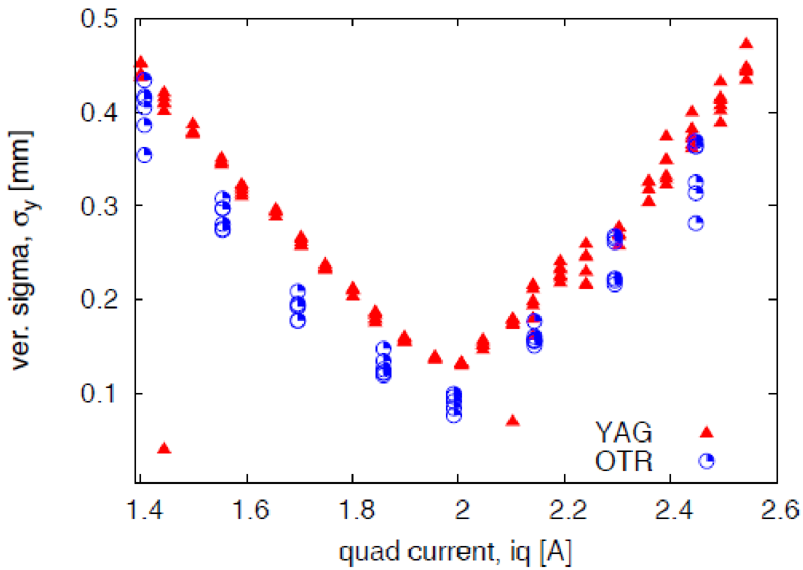

Results:

- Much more light from YAG:Ce for 100 MeV (γ=200) electrons light output $I_{YAG} \approx 10^5 I_{OTR}$
- Broader image from YAG:Ce due to finite shoulders or CCD saturation(?)

Courtesy of U. Iriso et al., DIPAC'09

Comparison between Scintillation Screens and OTR

OTR: electrodynamic process → beam intensity linear to # photons, high radiation hardness
Scint. Screen: complex atomic process → saturation possible, for some low radiation hardness

---

OTR: thin foil Al or Al on Mylar, down to 0.25 μm thickness
→ minimization of beam scattering (Al is low Z-material)
Scint. Screen: thickness ≈ 1 mm inorganic, fragile material, not radiation hard

---

OTR: low number of photons → expensive image intensified CCD
Scint. Screen: large number of photons → simple CCD sufficient

---

OTR: complex angular photon distribution → resolution limited
Scint. Screen: isotropic photon distribution → simple interpretation

---

OTR: large γ needed → e^--beam with $E_{kin} > 100$ MeV, proton-beam with $E_{kin} > 100$ GeV
Scint. Screen: for all beams

Remark: OTR **not** suited for LINAC-FEL due to **coherent** light emission (not covered here) but scintilation screens can be used.

Outline:

- Scintillation screens:
  emission of light, universal usage, limited dynamic range
- SEM-Grid: emission of electrons, workhorse, limited resolution
- Wire scanner: emission of electrons, workhorse, scanning method
- Ionization Profile Monitor:
  secondary particle detection from interaction beam-residual gas
- Optical Transition Radiation:
  crossing optical boundary, for relativistic beams only
- Synchrotron Light Monitors
  photon detection of emitted synchrotron light in optical and X-ray range
- Summary

An electron bent (i.e. accelerated) by a dipole magnet emit synchrotron light.

This light is emitted into a cone of opening $2/\gamma$ in lab-frame.
$\Rightarrow$Well suited for rel. e^-
For protons:
Only for energies E_{kin} > 100 GeV

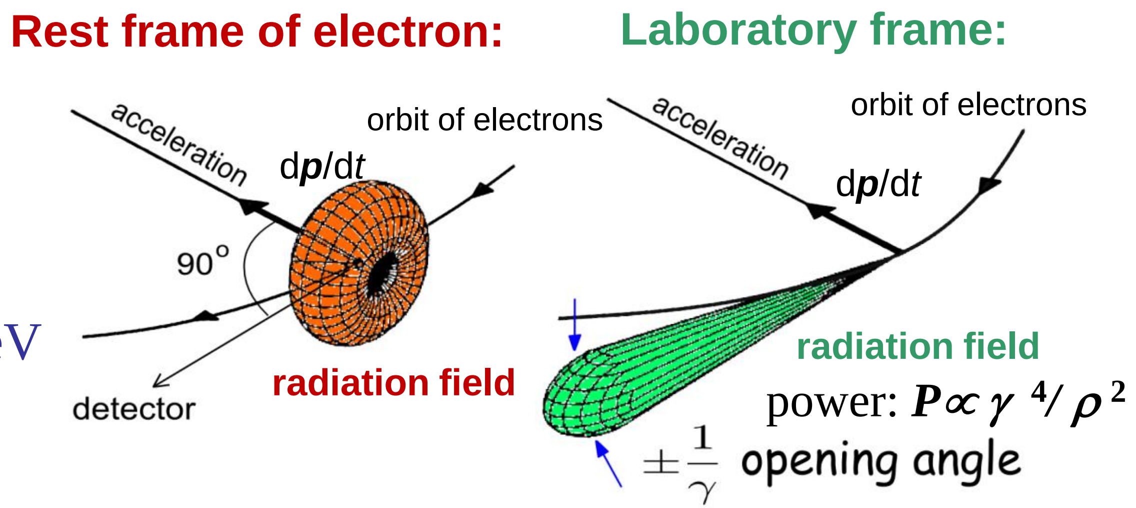

The light is focused to a intensified CCD.

Advantage:
Signal anyhow available!

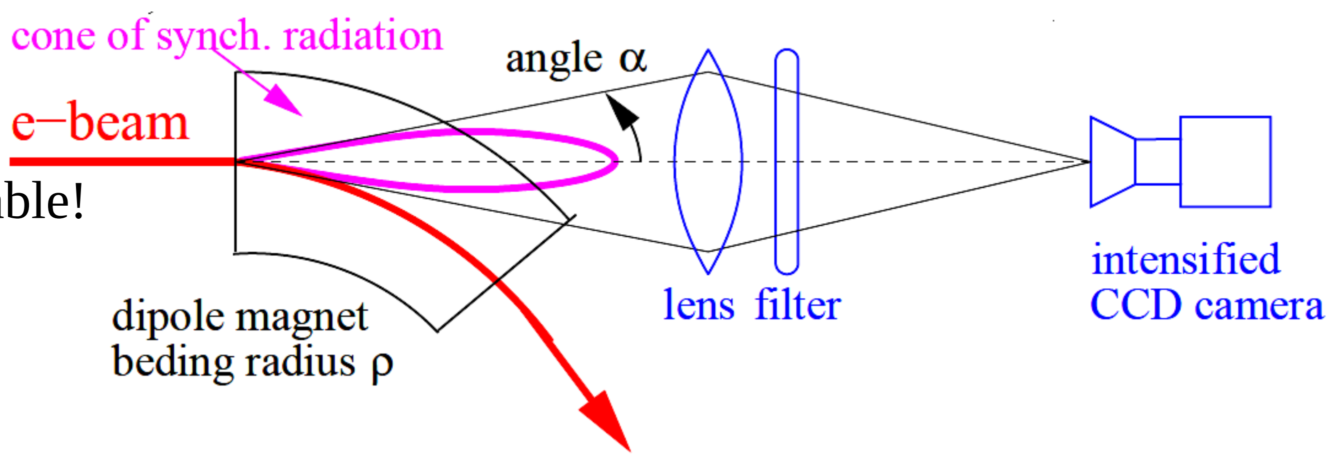

Realization of a Synchrotron Light Monitor

Extracting out of the beam's plane by a (cooled) mirror
→ Focus to a slit + wavelength filter for optical wavelength
→ Image intensified CCD camera

Example: CERN LEP-monitor with bending radius 3.1 km (blue or near UV)

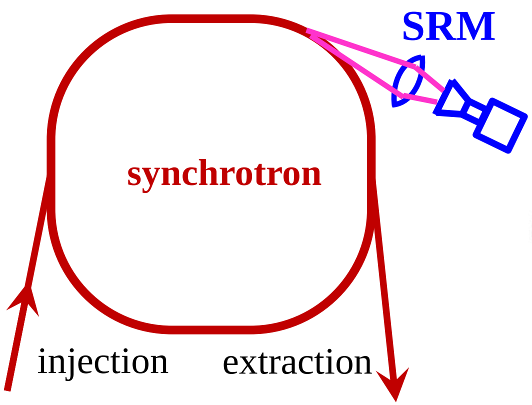

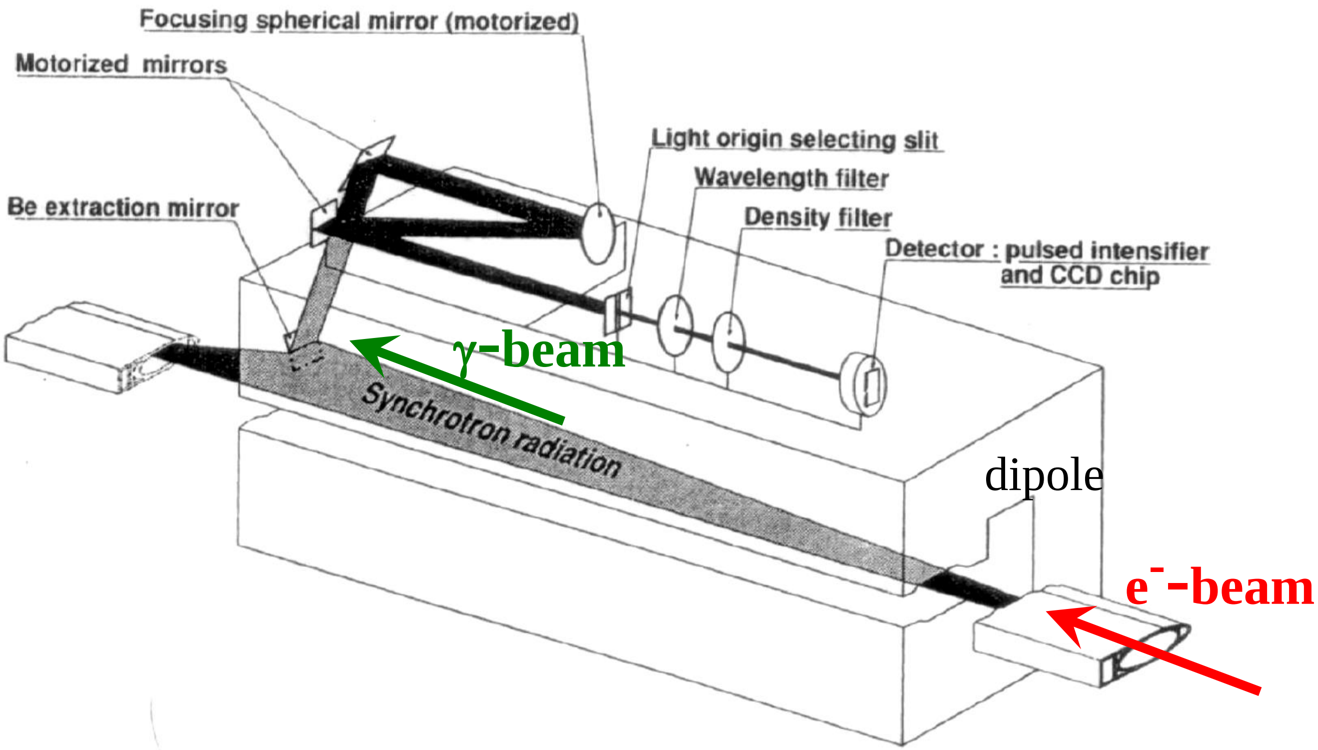

Courtesy C. Bovet (CERN) et al., PAC'91

Result from a Synchrotron Light Monitor

Example: Synchrotron radiation facility APS accumulator ring and blue wavelength:

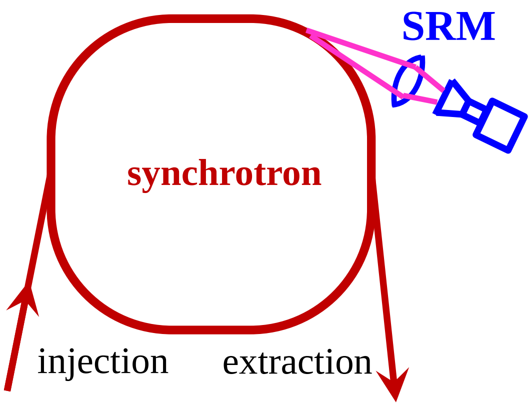

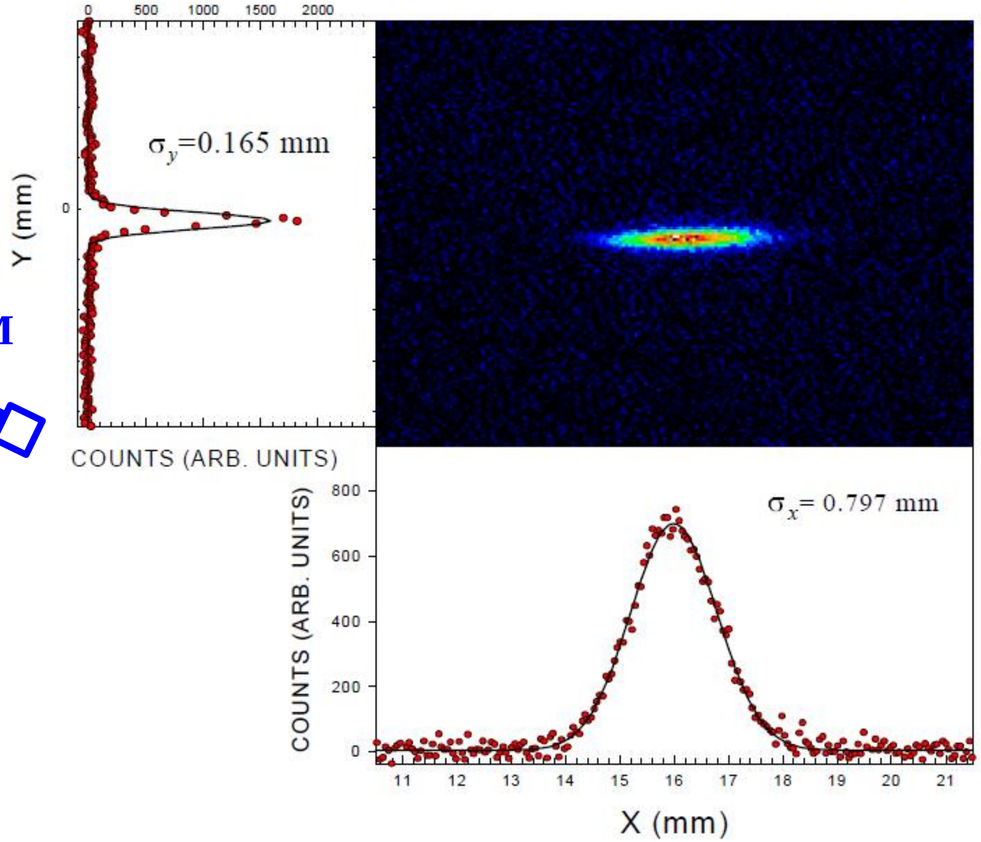

B.X. Yang (ANL) et al. PAC'97

Advantage: Direct measurement of 2-dim distribution, only mirror installed in the vacuum pipe

Realization: Optics outside of vacuum pipe

Disadvantage: Resolution limited by the diffraction due to finite apertures in the optics.

Adiabatic Damping for an Electron Beam

Example: Booster at the light source ALBA acceleration from 0.1 → 3 GeV within 130 ms

Profile measure by synchrotron light monitor:

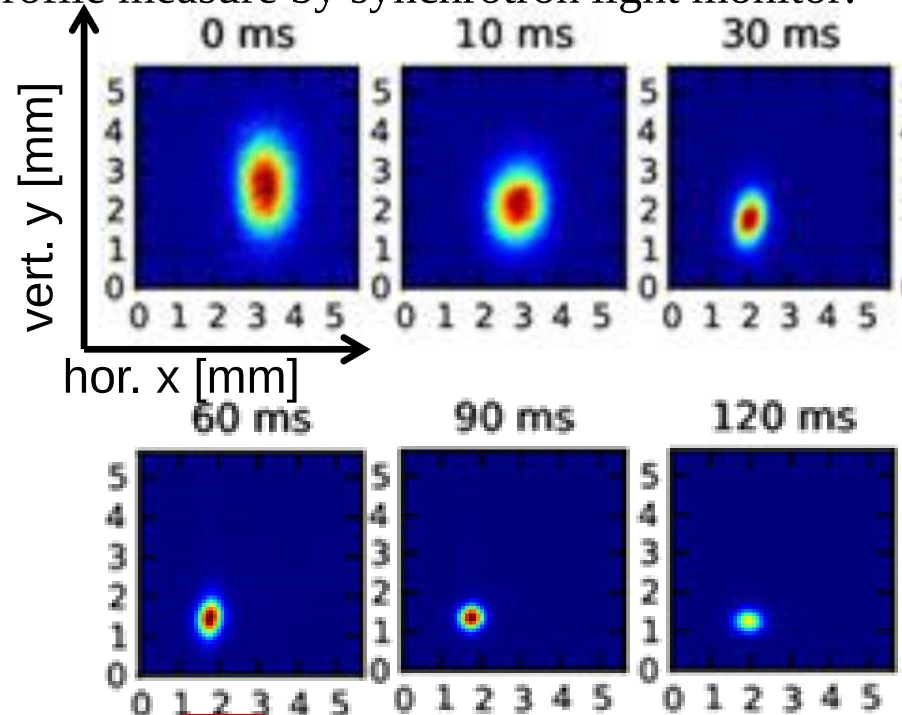

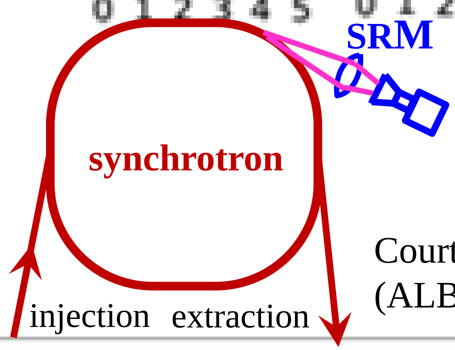

Courtesy U. Iriso & M. Pont (ALBA) et al. IPAC 2011

The beam emittance in influenced by:

- Adiabatic damping
- Longitudinal momentum contribution via dispersion $\Delta x_D(s) = D(s) \cdot \frac{\Delta p}{p}$

  total width $\Delta x_{tot}(s) = \sqrt{\varepsilon\beta(s) + D(s) \cdot \frac{\Delta p}{p}}$
- Quantum fluctuation due to light emission

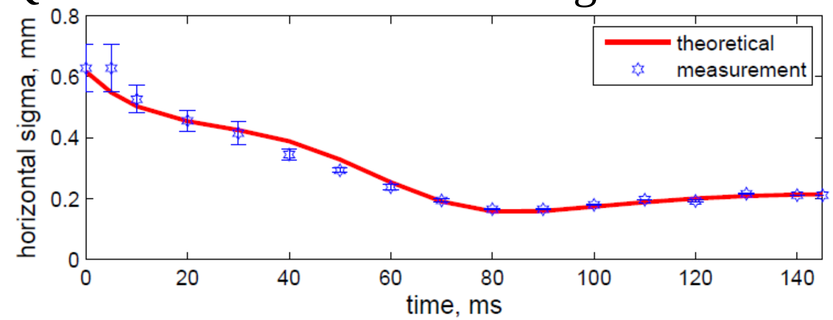

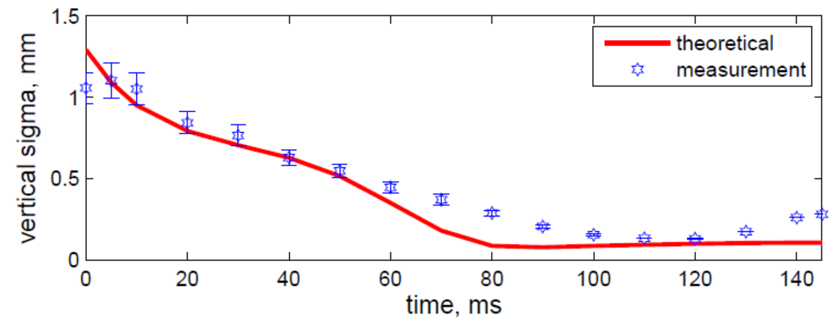

The Artist View of a Synchrotron Light Monitor

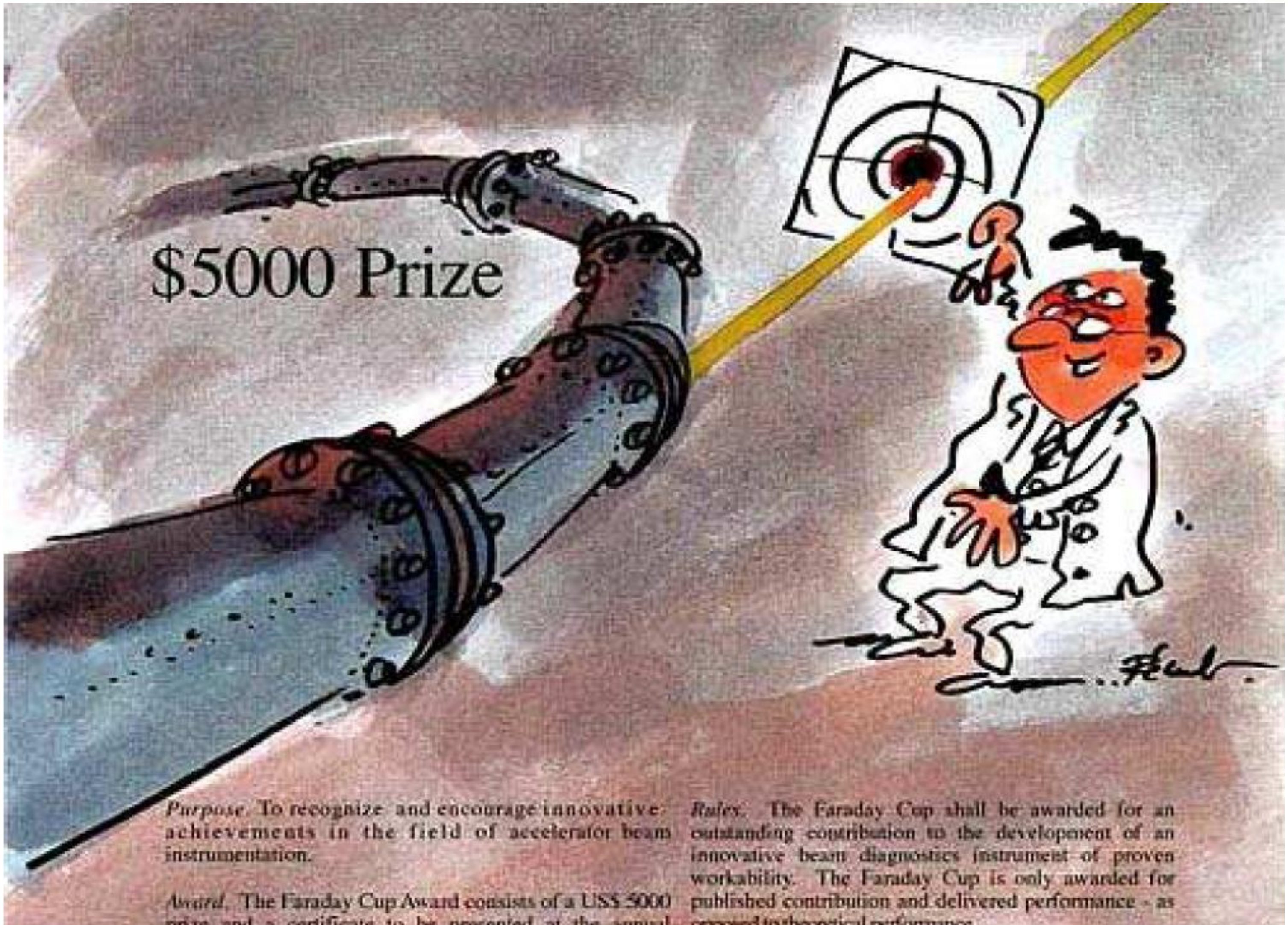

Diffraction Limit of Synchrotron Light Monitor

Limitations:
Diffraction limits the resolution due to Fraunhofer diffraction

$$\Rightarrow \sigma \cong 0.6 \cdot \left(\lambda^2 / \rho\right)^{1/3}$$

$$\approx 100\ \mu\text{m for typical case}$$

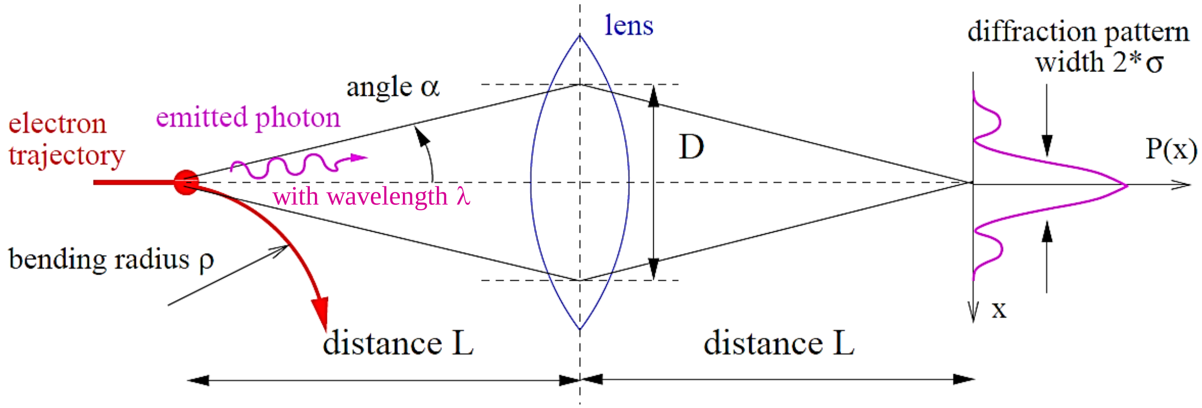

Improvements:

- ***Shorter wavelength:***

  Using X-rays and an aperture of Ø 1mm → 'X-ray pin hole camera', achievable resolution $\sigma \approx 10\ \mu$m

- ***Interference technique:***

  At optical wavelength using a double slit → interference fringes achievable resolution $\sigma \approx 1\ \mu$m.

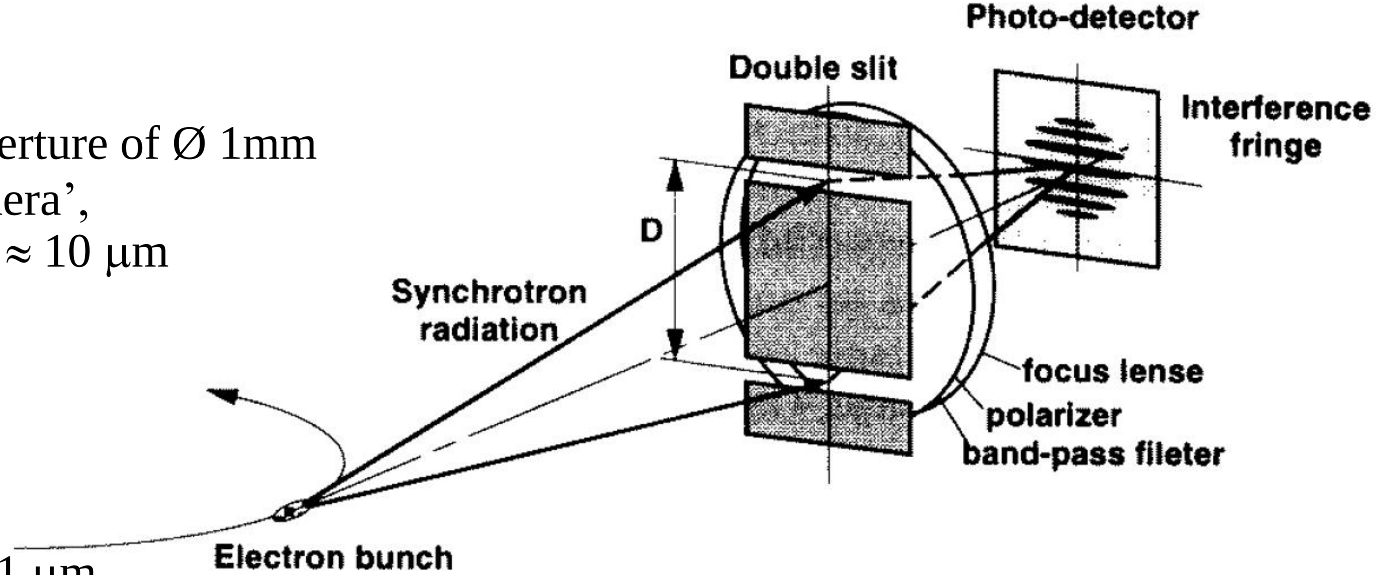

X-ray Pin-Hole Camera

The diffraction limit is $\Rightarrow \sigma \cong 0.6 \cdot \left(\lambda^2 / \rho\right)^{1/3}$ $\Rightarrow$ s***horter wavelength by X-rays***.

Example: PETRA III Courtesy K. Wittenburg, DESY

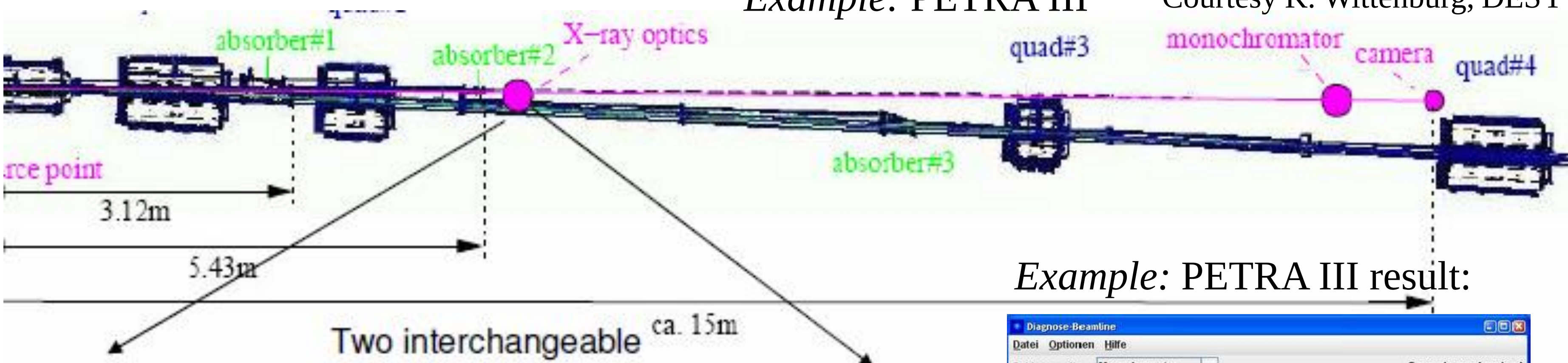

Two interchangeable X-ray optics:

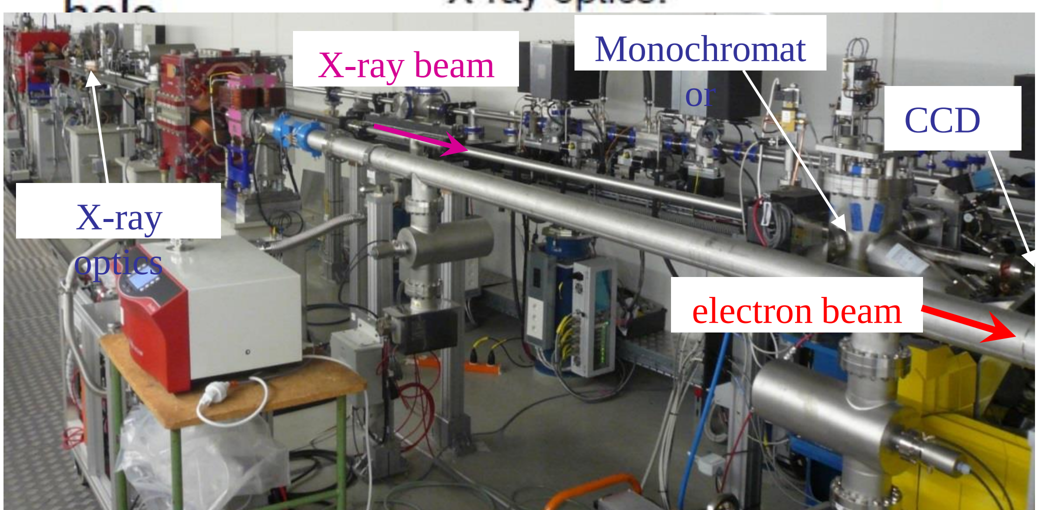

Example: PETRA III result:

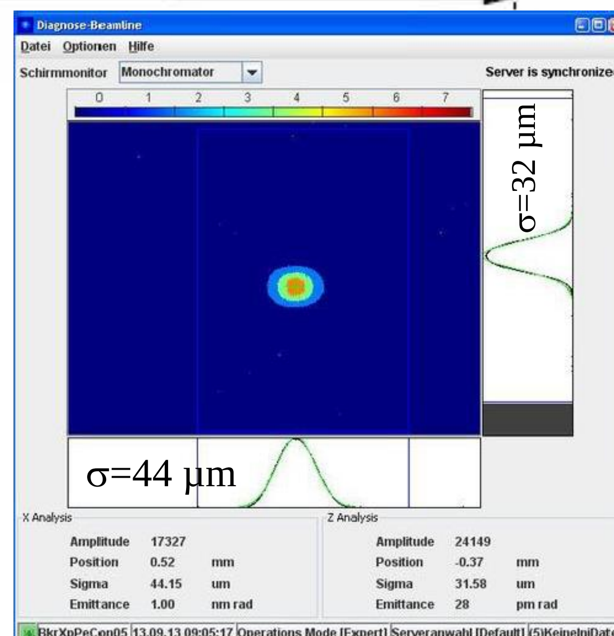

Summary for Beam Profile Measurement

Different techniques are suited for different beam parameters:

e⁻-beam: typically Ø 0.1 to 3 mm, **protons:** typically Ø 3 to 30 mm

Intercepting ↔ non-intercepting methods

Direct observation of electrodynamics processes:

- Optical synchrotron radiation monitor: non-destructive, for e⁻-beams, complex, limited res.
- X-ray synchrotron radiation monitor: non-destructive, for e⁻-beams, very complex
- OTR screen: nearly non-destructive, large relativistic γ needed, e⁻-beams mainly

Detection of secondary photons, electrons or ions:

- Scintillation screen: destructive, large signal, simple setup, all beams
- Ionization profile monitor: non-destructive, expensive, limited resolution, for protons
- xxx Residual fluorescence monitor: non-destructive, limited signal strength, for protons

Wire based electronic methods:

- SEM-grid: partly destructive, large signal and dynamic range, limited resolution
- Wire scanner: partly destructive, large signal and dynamics, high resolution, slow scan.

Measurement of transverse Emittance

The emittance characterizes the whole beam quality, assuming linear behavior as described by second order differential equation.

It is defined within the phase space as: $\varepsilon_x = \frac{1}{\pi}\int_A dx dx'$

The measurement is based on determination of:

either profile width $\boldsymbol{\sigma_x}$ and angular width $\boldsymbol{\sigma_x'}$ at one location
or $\boldsymbol{\sigma_x}$ at different locations and linear transformations.

Different devices are used at transfer lines:

- Lower energies E_{kin} < 100 MeV/u: slit-grid device, pepper-pot (suited in case of non-linear forces).
- All beams: Quadrupole variation, 'three grid' method using linear transformations (**not** well suited in the presence of non-linear forces)

Synchrotron: lattice functions results in stability criterion

⇒ beam width delivers emittance: $\varepsilon_x = \frac{1}{\beta_x(s)}\left[\sigma_x^2 - \left(D(s)\frac{\Delta p}{p}\right)\right]$ and $\varepsilon_y = \frac{\sigma_y^2}{\beta_y(s)}$

Trajectory and Characterization of many Particles

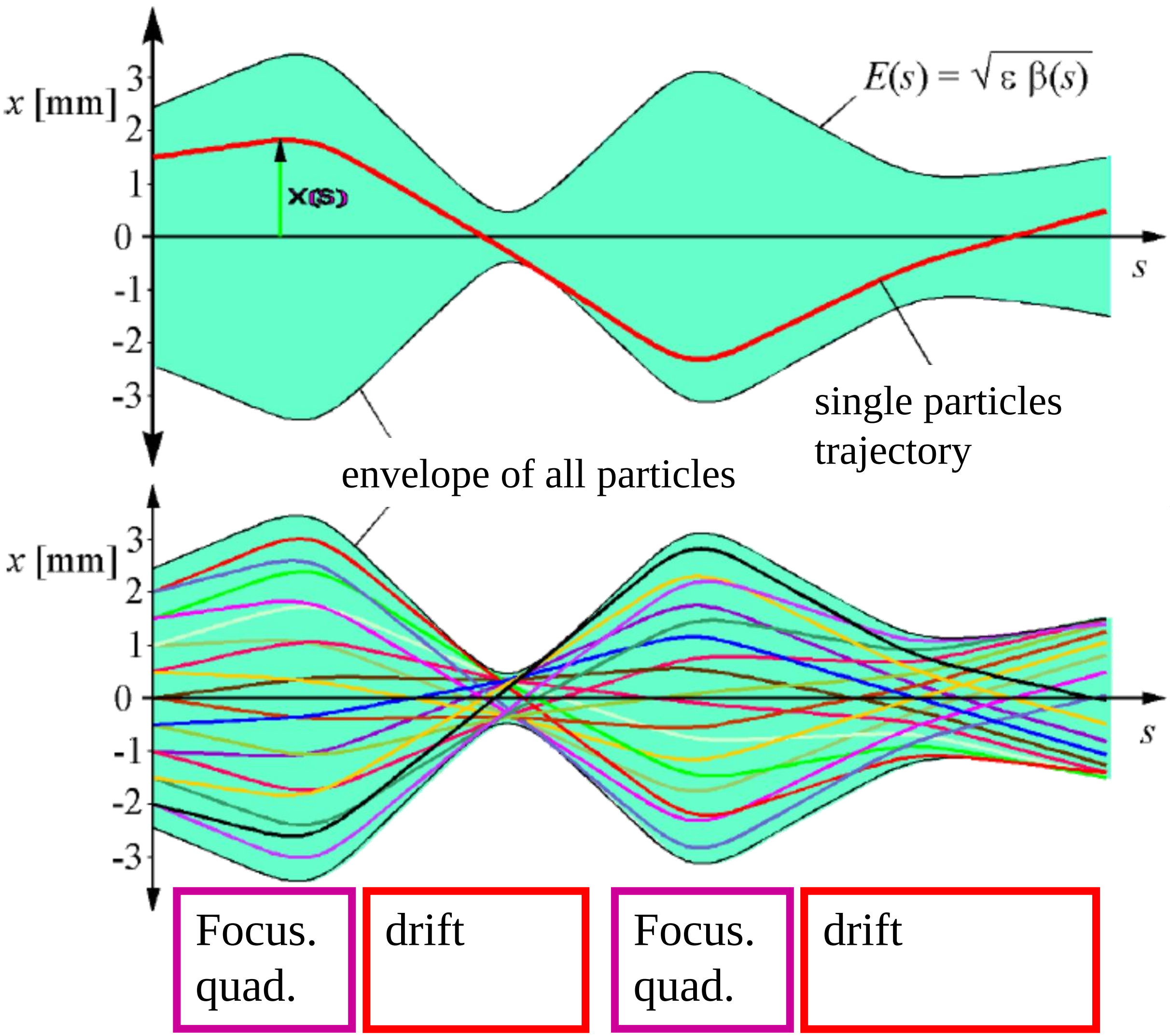

- ➢ Single particle trajectories are forming a beam
- ➢ They have a distribution of start positions and angles

⇒ Characteristic quantity is the **beam envelope**

- ➢ **Goal:**

Transformation of envelope

⇔ behavior of whole ensemble

Courtesy K.Wille

The basic vector is 6 dimensional:

$$\vec{x}(s) = \begin{pmatrix} x \\ x' \\ y \\ y' \\ l \\ \delta \end{pmatrix} = \begin{pmatrix} \text{hori. spatial deviation} \\ \text{horizontal divergence} \\ \text{vert. spatial deviation} \\ \text{vertical divergence} \\ \text{longitudinal deviation} \\ \text{momentum deviation} \end{pmatrix} = \begin{pmatrix} [\text{mm}] \\ [\text{mrad}] \\ [\text{mm}] \\ [\text{mrad}] \\ [\text{mm}] \\ [‰] \end{pmatrix}$$

The transformation of a single particle from a location s_0 to s_1 is given by the Transfer Matrix R:

$$\vec{x}(s_1) = \mathrm{R}(s) \cdot \vec{x}(s_0)$$

The transformation of a the envelope from a location s_0 to s_1 is given by the Beam Matrix σ:

$$\sigma(s_1) = \mathrm{R}(s) \cdot \sigma(s_0) \cdot \mathrm{R}^{T}(s)$$

6-dim Beam Matrix with *decoupled* hor. & vert. plane:

$$\boldsymbol{\sigma} = \begin{pmatrix} \sigma_{11} & \sigma_{12} & 0 & 0 & \sigma_{15} & \sigma_{16} \\ \sigma_{12} & \sigma_{22} & 0 & 0 & \sigma_{25} & \sigma_{26} \\ 0 & 0 & \sigma_{33} & \sigma_{34} & 0 & 0 \\ 0 & 0 & \sigma_{34} & \sigma_{44} & 0 & 0 \\ \sigma_{15} & \sigma_{25} & 0 & 0 & \sigma_{55} & \sigma_{56} \\ \sigma_{16} & \sigma_{26} & 0 & 0 & \sigma_{56} & \sigma_{66} \end{pmatrix}$$

horizontal
vertical
longitudinal
hor.-long. coupling
→ 13 values

Beam width for the three coordinates:

$$x_{rms} = \sqrt{\sigma_{11}}$$
$$y_{rms} = \sqrt{\sigma_{33}}$$
$$l_{rms} = \sqrt{\sigma_{55}}$$

Horizontal beam matrix:

$$\sigma_{11} = \langle x^2 \rangle$$
$$\sigma_{12} = \langle x\, x' \rangle$$
$$\sigma_{22} = \langle x'^2 \rangle$$

The Emittance for Gaussian and non-Gaussian Beams

The beam distribution can be non-Gaussian, e.g. at:

- beams behind ion source
- space charged dominated beams at LINAC & synchrotron
- cooled beams in storage rings

General description of emittance using terms of 2-dim distribution:

$$\varepsilon_{rms} = \sqrt{\underbrace{\langle x^2 \rangle \langle x'^2 \rangle}_{\text{Variances}} - \underbrace{\langle xx' \rangle^2}_{\text{Covariance i.e. correlation}}}$$

Variances **Covariance i.e. correlation**

It describes the value for 1 standard derivation

For <u>Gaussian</u> beams only: ε_{rms} ↔ interpreted as area containing a fraction f of ions:

$$\varepsilon(f) = -2\pi\varepsilon_{rms} \cdot \ln(1-f)$$

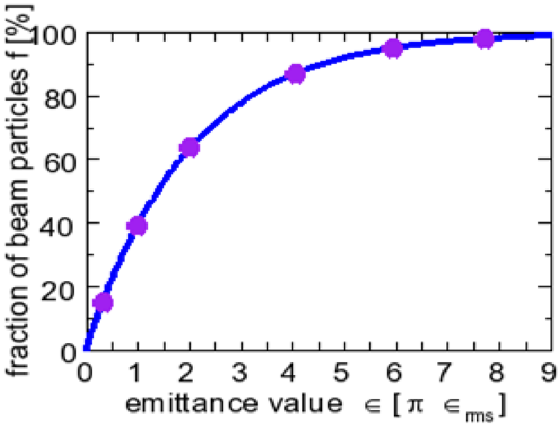

Emittance $\varepsilon(f)$	Fraction f
$1 \cdot \varepsilon_{rms}$	15 %
$\pi \cdot \varepsilon_{rms}$	39 %
$2\pi \cdot \varepsilon_{rms}$	63 %
$4\pi \cdot \varepsilon_{rms}$	86 %
$8\pi \cdot \varepsilon_{rms}$	98 %

Care:
No common definition of emittance concerning the fraction ***f***

Outline:

- ➢ Definition and some properties of transverse emittance
- ➢ Slit-Grid device: scanning method

  scanning slit → beam position & grid → angular distribution
- ➢ Quadrupole strength variation and position measurement
- ➢ Summary

Slit-Grid: Direct determination of position and angle distribution.

Used for protons with E_{kin} < 100 MeV/u ⇒ range R < 1 cm.

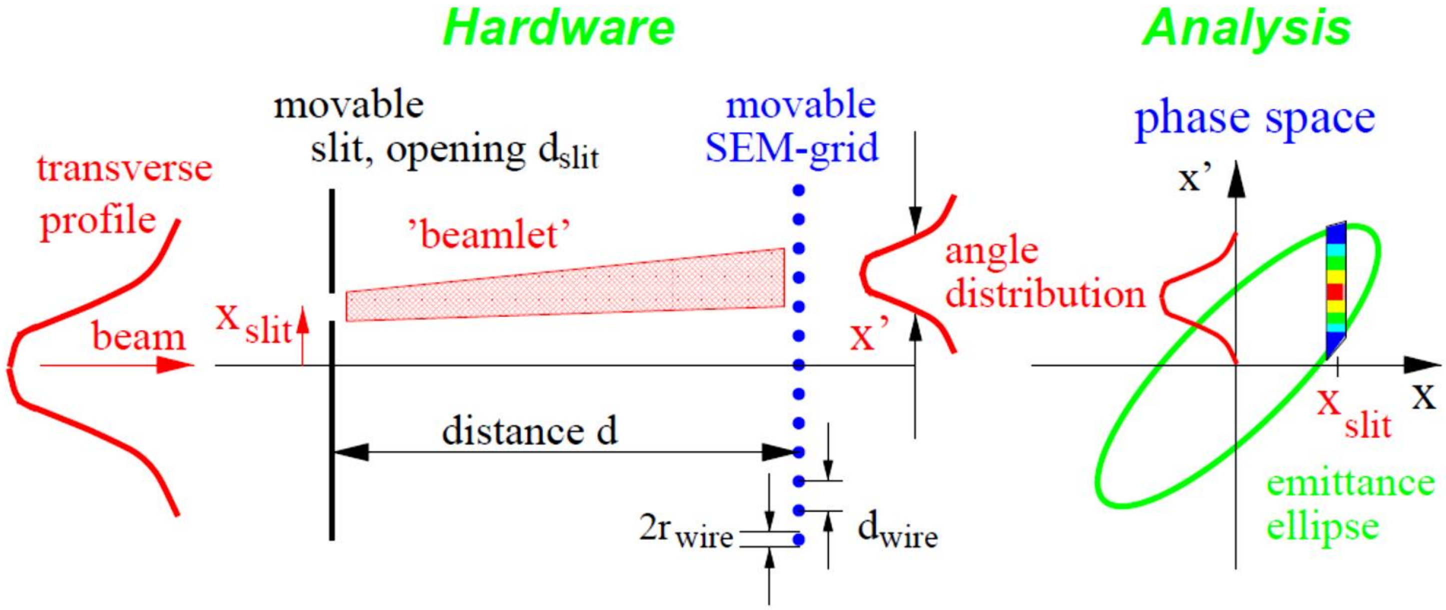

Slit: position ***P(x)*** with typical width: 0.1 to 0.5 mm

Distance: typ. 0.5 to 5 m (depending on beam energy 0. 1 ... 100 MeV)

SEM-Grid: angle distribution ***P(x')***

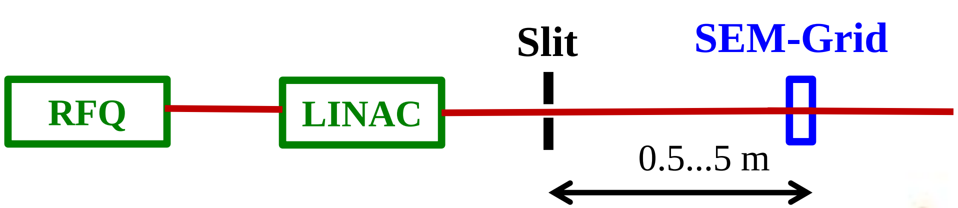

The distribution is depicted as a function of position [mm] & angle [mrad]

The distribution can be visualized by

- Mountain plot
- Contour plot

Calc. of 2nd moments $\langle x^2 \rangle$, $\langle x'^2 \rangle$ & $\langle xx' \rangle$

Emittance value ε_{rms} from

$$\varepsilon_{rms} = \sqrt{\langle x^2 \rangle \langle x'^2 \rangle - \langle xx' \rangle^2}$$

⇒ **Problems:**

- Finite **binning** results in limited resolution
- **Background** → large influence on $\langle x^2 \rangle$, $\langle x'^2 \rangle$ and $\langle xx' \rangle$

Or fit of distribution with an ellipse

⇒ **Effective emittance only**

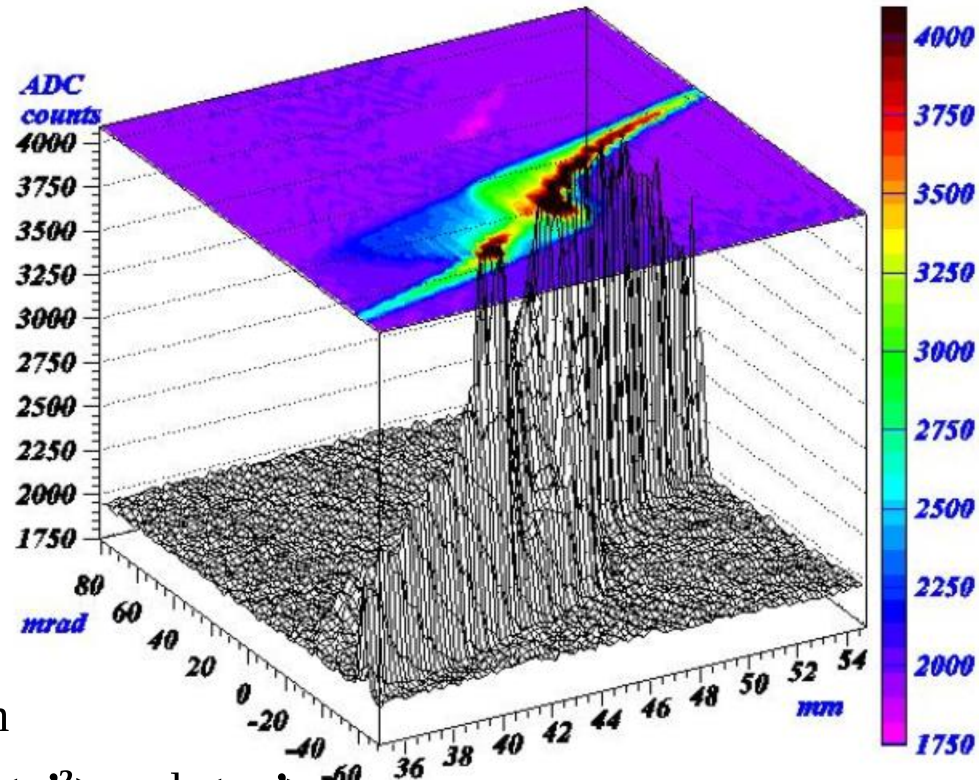

Beam: Ar^{4+}, 60 keV, 15 μA

at Spiral2 Phoenix ECR source.

P. Ausset, DIPAC 2009

Remark: Behind a ion source the beam might very non-Gaussian due to plasma density and aberration at quadrupoles

Outline:

- Definition and some properties of transverse emittance
- Slit-Grid device: scanning method

  scanning slit → beam position & grid → angular distribution
- **Quadrupole strength variation and position measurement**

  emittance from several profile measurement and beam optical calculation
- Summary

Emittance Measurement by Quadrupole Variation

From a profile determination, the emittance can be calculated via linear transformation, if a well known and constant distribution (e.g. Gaussian) is assumed.

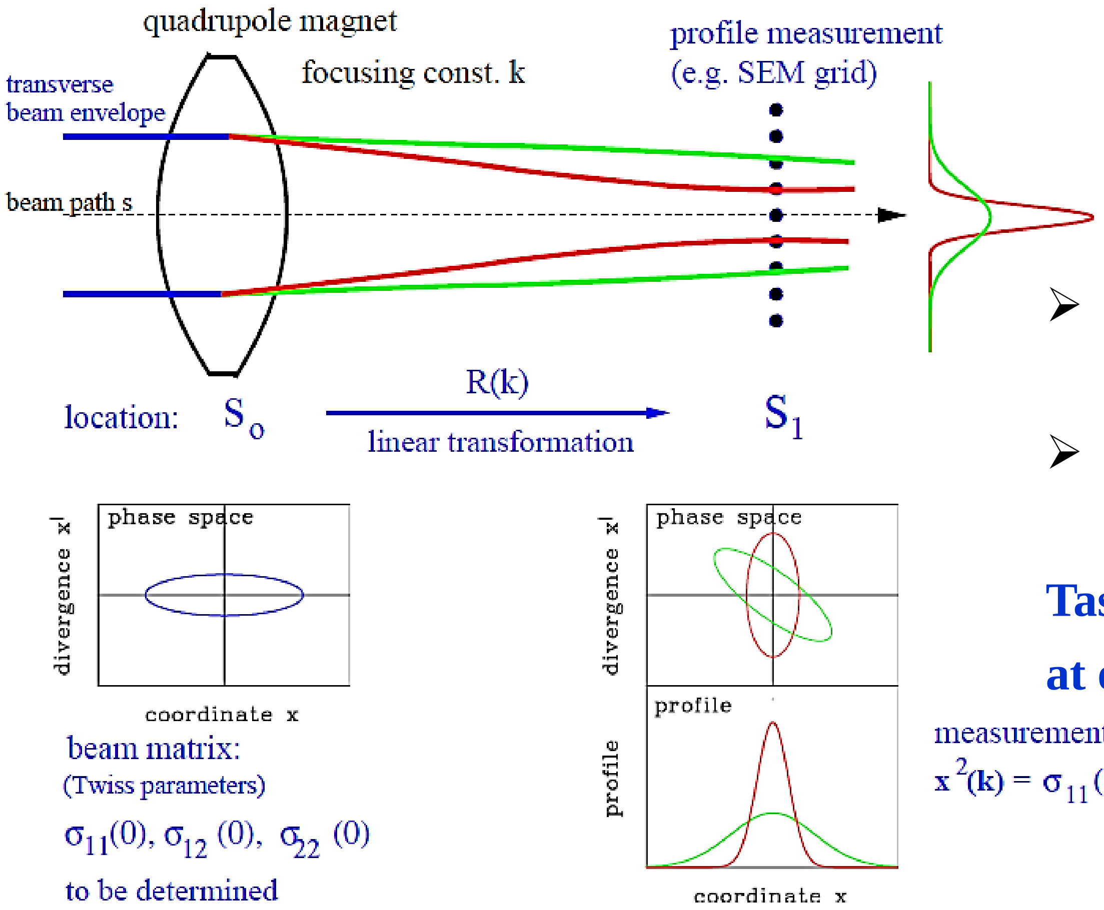

beam matrix:
(Twiss parameters)
$\sigma_{11}(0)$, $\sigma_{12}(0)$, $\sigma_{22}(0)$
to be determined

- Measurement of beam width

  $x^2_{max} = \sigma_{11}(1, k)$

  matrix **R(*k*)** describes the focusing.
- With the drift matrix the transfer is

  $\mathbf{R}(k_i) = \mathbf{R}_{drift} \cdot \mathbf{R}_{focus}(k_i)$
- Transformation of the beam matrix

  $\sigma(1,k_i) = \mathbf{R}(k_i) \cdot \sigma(0) \cdot \mathbf{R}^T(k_i)$

Task: Calculation of $\sigma(0)$

at entrance s_0 i.e. all three elements

measurement:
$x^2(k) = \sigma_{11}(1,k)$

Measurement of transverse Emittance

Using the 'thin lens approximation' i.e. the quadrupole has a focal length of ***f***:

$$\mathrm{R}_{focus}(K) = \begin{pmatrix} 1 & 0 \\ -1/f & 1 \end{pmatrix} \equiv \begin{pmatrix} 1 & 0 \\ K & 1 \end{pmatrix} \Rightarrow \mathrm{R}(L,K) = \mathrm{R}_{drift}(L)\cdot \mathrm{R}_{focus}(K) = \begin{pmatrix} 1+LK & L \\ K & 1 \end{pmatrix}$$

Measurement of the matrix-element $\sigma_{11}(1,K)$ from $\sigma(1,K) = \mathrm{R}(K)\cdot\sigma(0)\cdot\mathrm{R}^T(K)$

Example: Square of the beam width at ELETTRA 100 MeV e⁻ Linac, YAG:Ce:

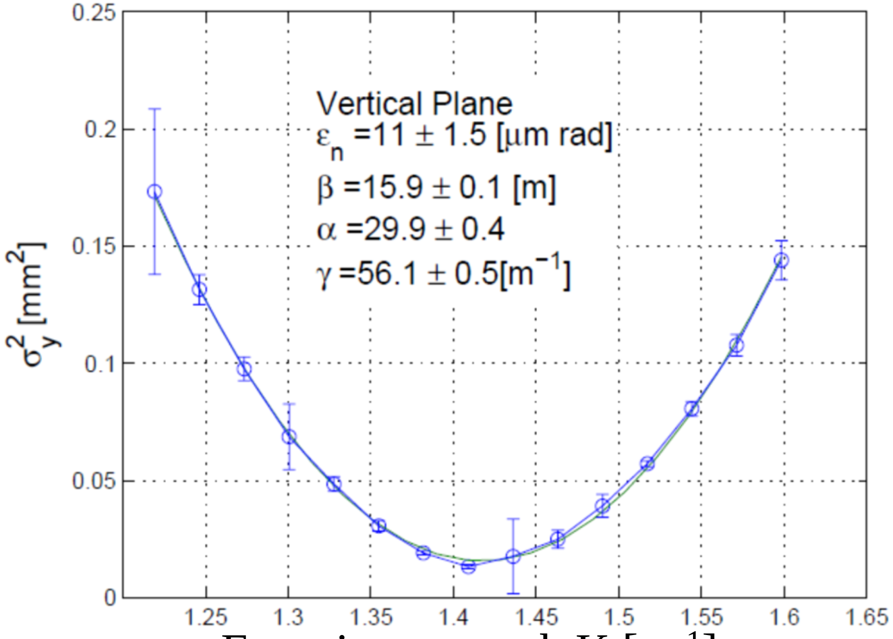

Focusing strength K [m⁻¹]

G. Penco (ELETTRA) et al., EPAC'08

For completeness: The relevant formulas

$$\sigma_{11}(1,K) = L^2\sigma_{11}(0)\cdot K^2 + 2\cdot(\ L\sigma_{11}(0) + L^2\sigma_{12}(0)\ )\cdot K + L^2\sigma_{22}(0) + \sigma_{11}(0)$$

$$\equiv a\cdot K^2 - 2ab\cdot K + ab^2 + c$$

The three matrix elements at the quadrupole:

$$\sigma_{11}(0) = \frac{a}{L^2}$$

$$\sigma_{12}(0) = -\frac{a}{L^2}\left(\frac{1}{L} + b\right)$$

$$\sigma_{22}(0) = \frac{1}{L^2}\left(ab^2 + c + \frac{2ab}{L} + \frac{a}{L^2}\right)$$

$$\varepsilon_{rms} \equiv \sqrt{\det\sigma(0)} = \sqrt{\sigma_{11}(0)\cdot\sigma_{22}(0) - \sigma_{12}^2(0)} = \sqrt{ac}\,/\,L^2$$

Summary for transverse Emittance Measurement

Emittance is the important quantity for comparison to theory.

It includes size (value of ε) and orientation in phase space (**σ_{ij}** or **α, β** and γ)

three independent values $\varepsilon_{rms} = \sqrt{\sigma_{11} \cdot \sigma_{22} - \sigma_{12}} = \sqrt{< x^2 > \cdot < x'^2 > - < xx' >^2}$

assuming no coupling between horizontal, vertical and longitudinal planes

Transfer line, low energy beams → direct measurement of x- and x′-distribution

- ***Slit-grid:*** movable slit → ***x***-profile, grid → ***x′***-profile

Transfer line, all beams → profile measurement + linear transformation:

- ***Quadrupole variation:*** one location, different setting of a quadrupole

Assumptions:
- well aligned beam, no steering
- no emittance blow-up due to space charge.

Important remark: For a synchrotron with a *stable beam storage*,

width measurement is sufficient using $x_{rms} = \sqrt{\varepsilon_{rms} \cdot \beta}$

Measurement of longitudinal parameter:

Bunch length measurement at

- **Synchrotron light sources**
- **Linear light sources**
- **Summary**

Longitudinal ↔ transverse correspondences:

- position relative to rf ↔ transverse center-of-mass
- bunch structure in time ↔ transverse profile
- momentum or energy spread ↔ transverse divergence
- longitudinal emittance ↔ transverse emittance.

Electron bunches are too short (σ_t < 300 ps) to be covered by the bandwidth of pick-ups (f < 1 GHz ⇔ t_{rise} >300 ps) for structure determination.

→ Time resolved observation of synchr. light with a streak camera: Resolution ≈ 1 ps.

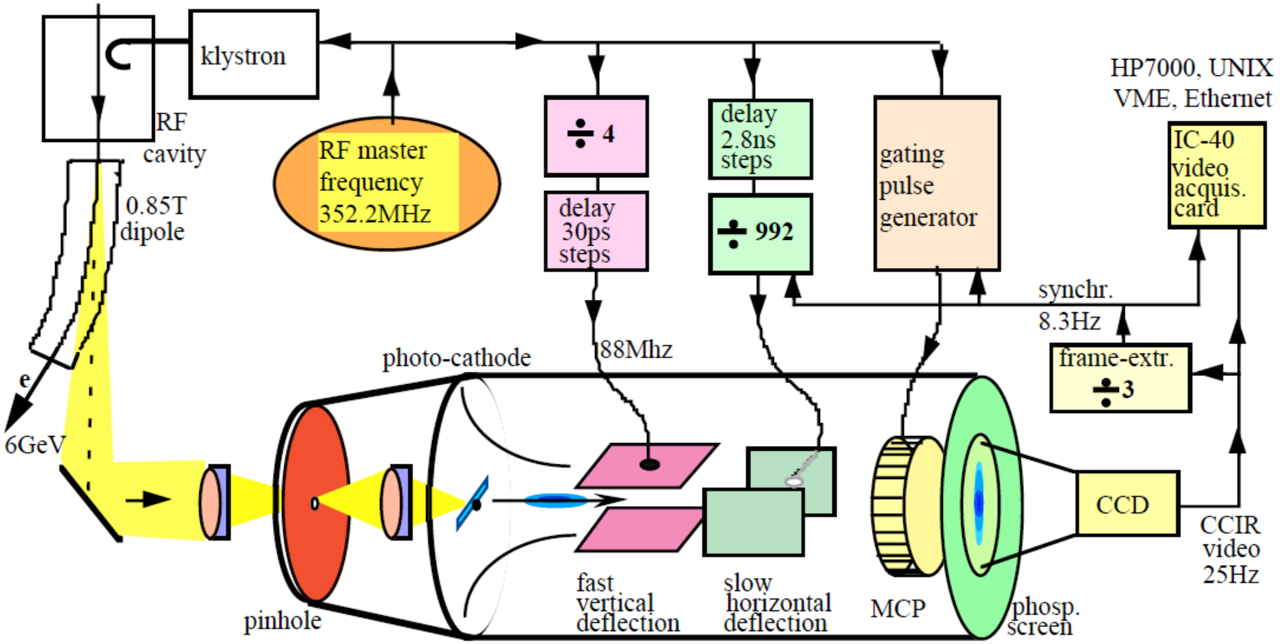

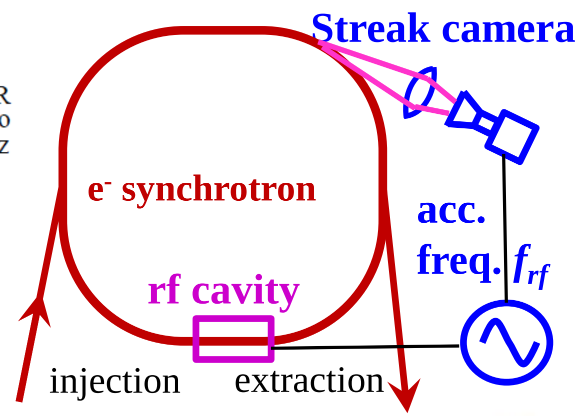

Technical Realization of Streak Camera

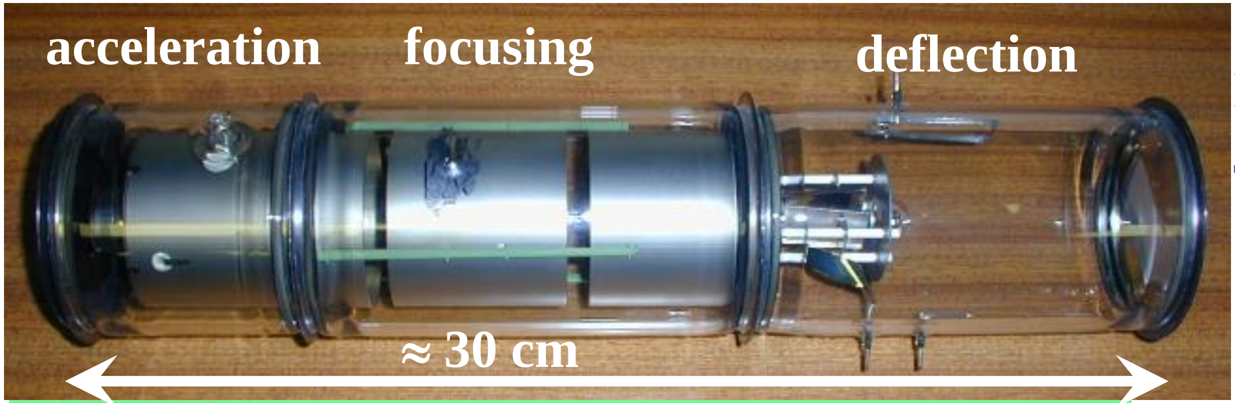

Hardware of a streak camera

Time resolution down to 0.5 ps:

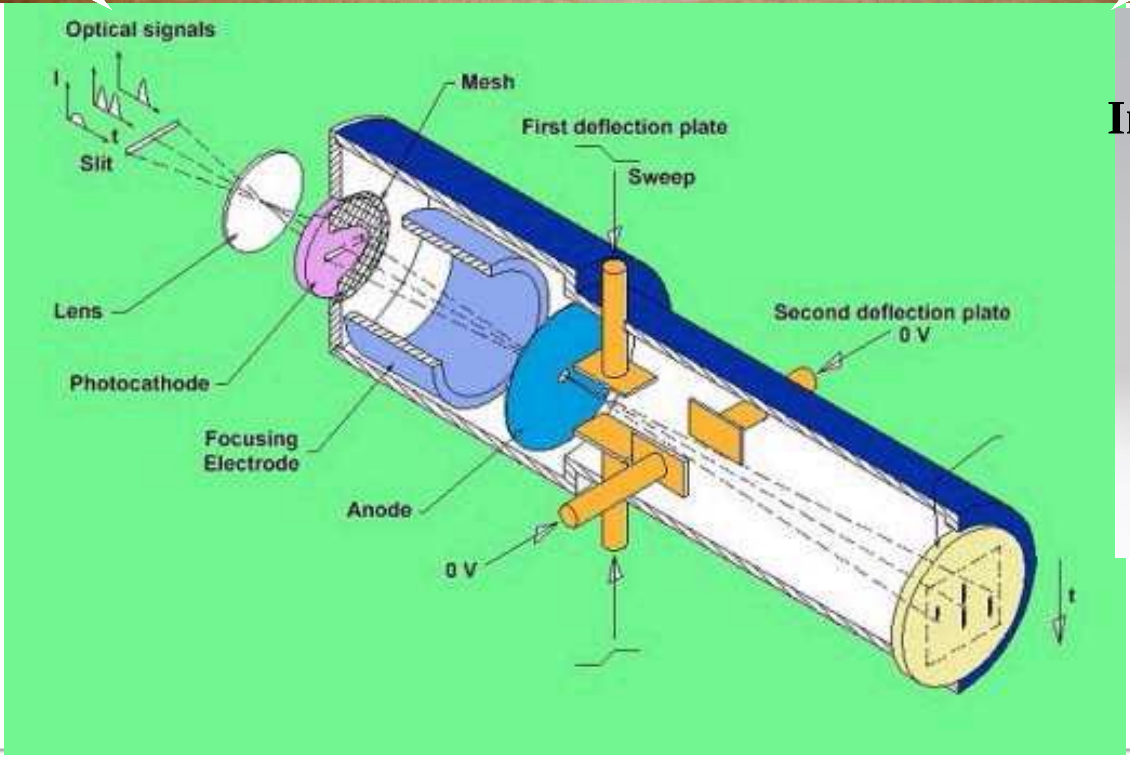

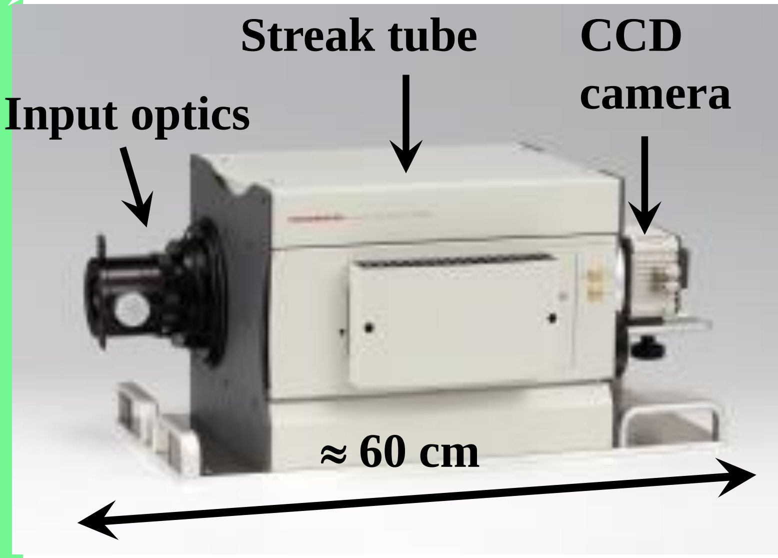

Technical Realization of Streak Camera

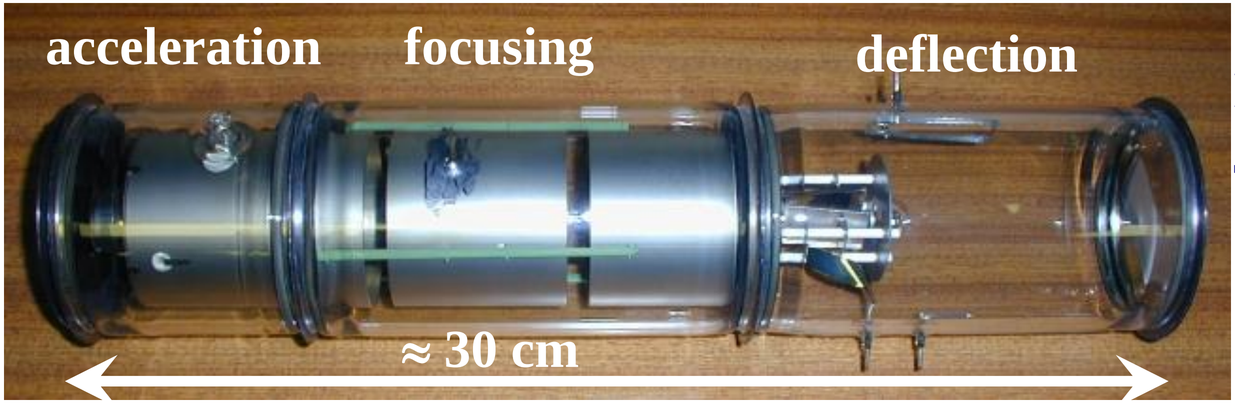

Hardware of a streak camera

Time resolution down to 0.5 ps:

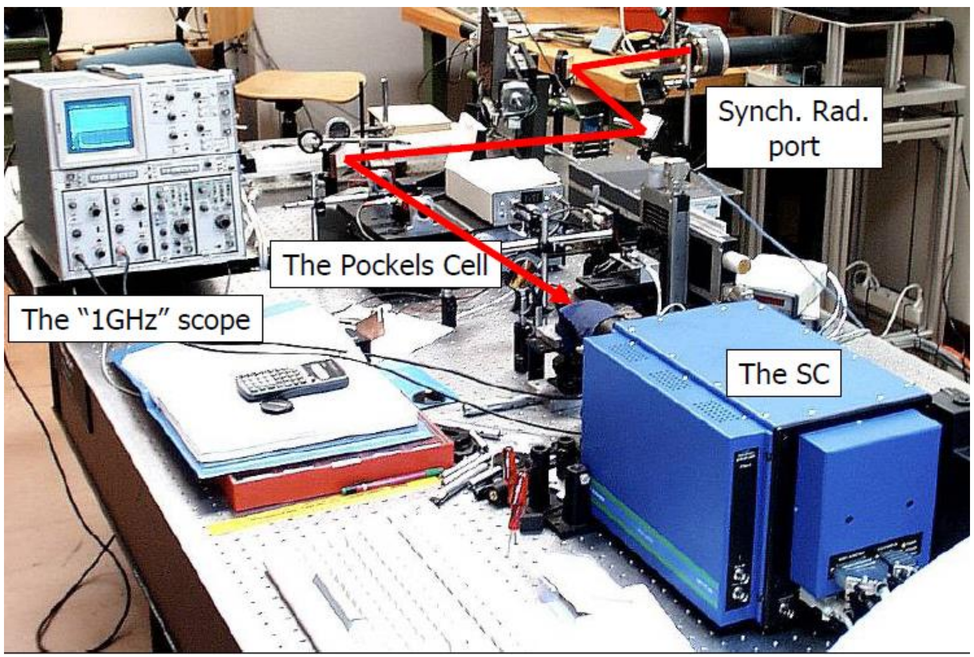

The Streak Camera setup at ELETTRA, Trieste, Italy

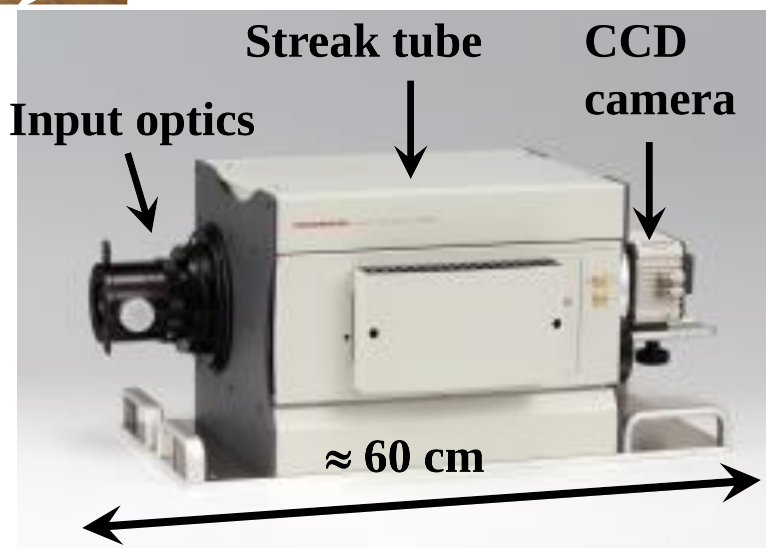

Results of Bunch Length Measurement by a Streak Camera

The streak camera delivers a fast scan in vertical direction (here 360 ps full scale) and a slower scan in horizontal direction (24 μs).

Example: Bunch length at the synchrotron light source SOLEIL for U_{rf} = 2 MV
for slow direction 24 μs and scaling for fast scan 360 ps: measure σ_t = 35 ps.

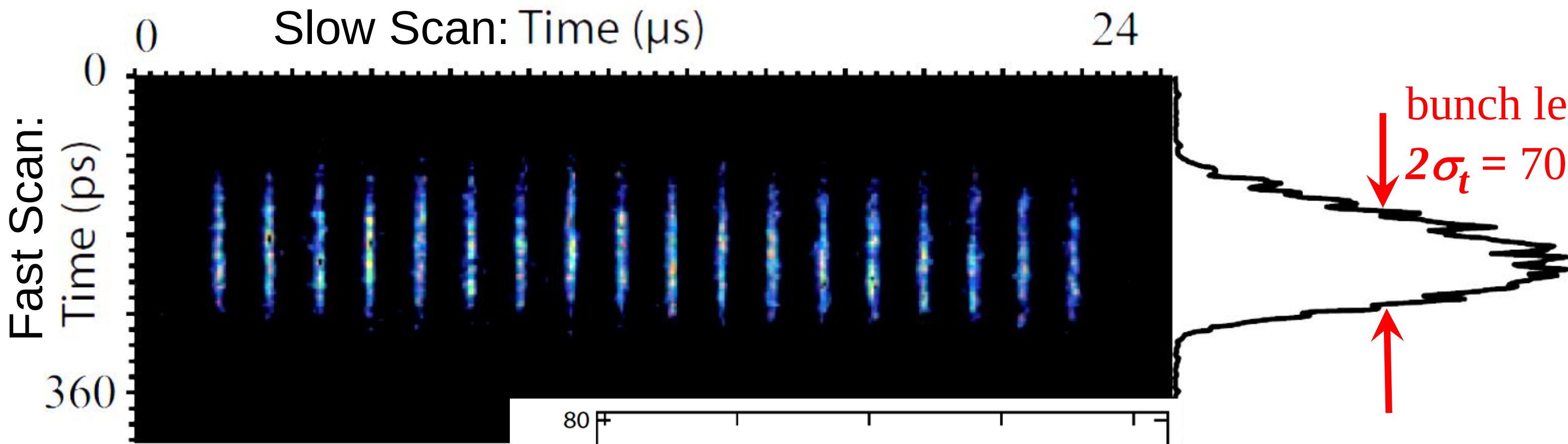

Short bunches are desired by the users

Example: Bunch length σ_t as a function of stored current (i.e. space charge de-focusing) at SOLEIL

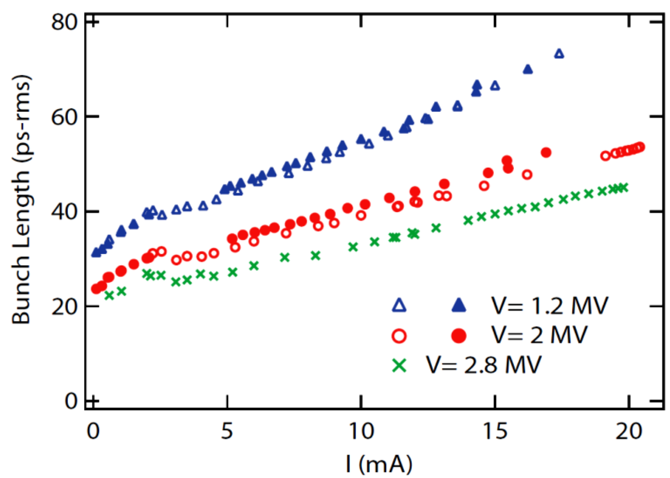

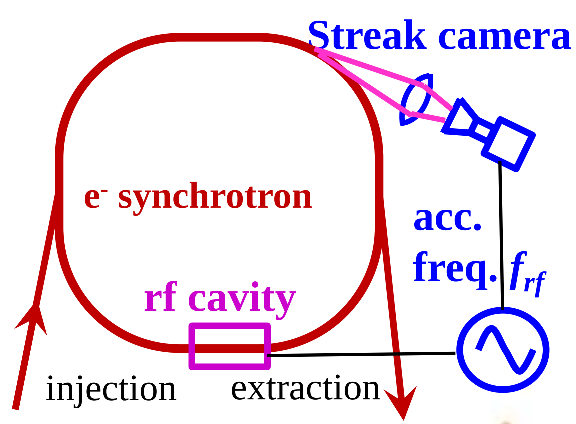

Courtesy of M. Labat et al., DIPAC'07

The Artist View of a Streak Camera

4th Generation Light Sources: LINAC based, single pass with large energy loss

$E_{electron} \approx 1 \ldots 18$ GeV, **coherent** light from undulator, $E_\gamma < 1000$ keV, temporally short pulse

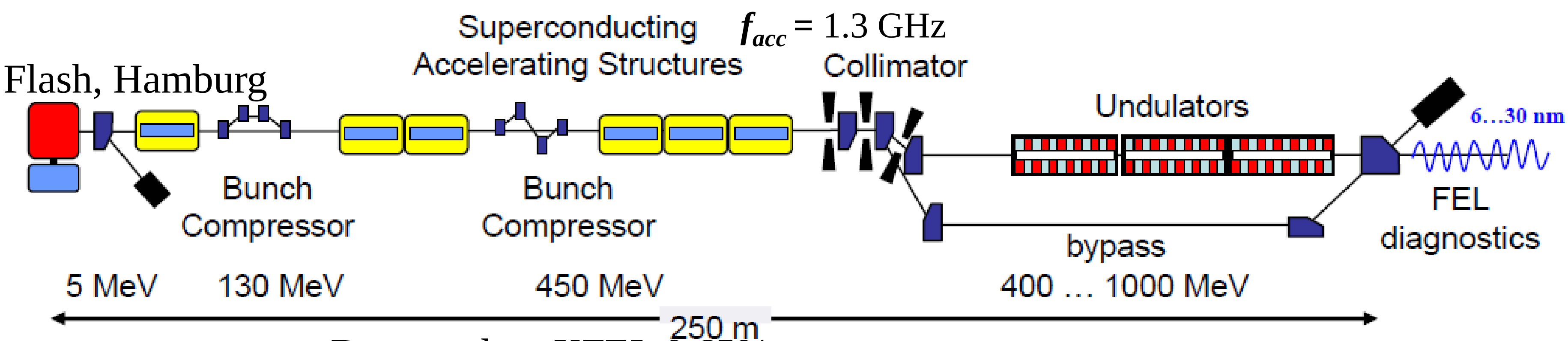

Duty cycle ~ XFEL 0.65%

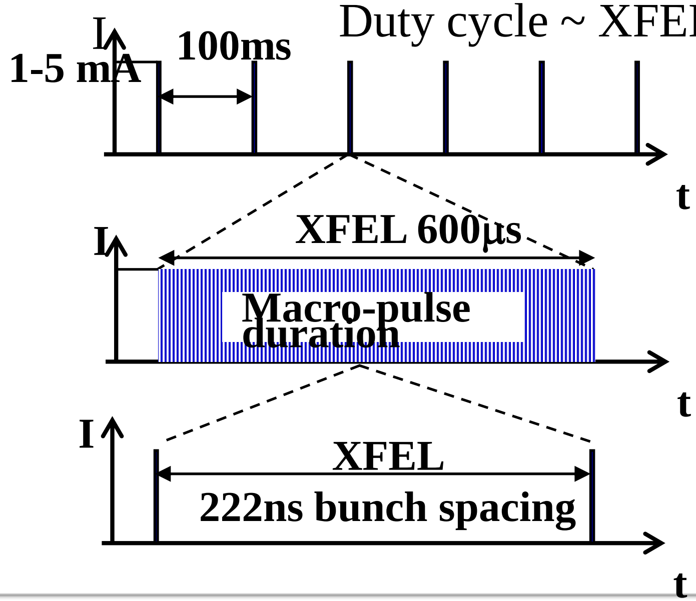

Goal: Short bunches with **high** number of particles

→ short, intense laser pulses for electron generation

Requirement: Position stability ⇒ resolution < 1 µm

Single bunch duration < 1 ps

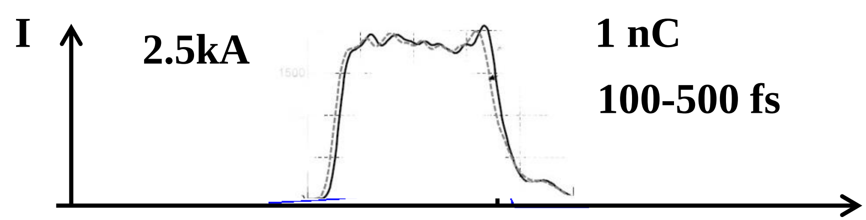

Bunch length measurement by electro-optical Method

For Free Electron Lasers → bunch length below 1 ps is achieved

→ below resolution of streak camera

→ short laser pulses with $t \approx$ **10 fs** and electro-optical modulator

Electro optical modulator: birefringent, rotation angle depends on external electric field

Relativistic electron bunches: transverse field $E_{\perp, lab} = \gamma E_{\perp, rest}$ carries the time information

Scanning of delay between bunch and laser → time profile after several pulses.

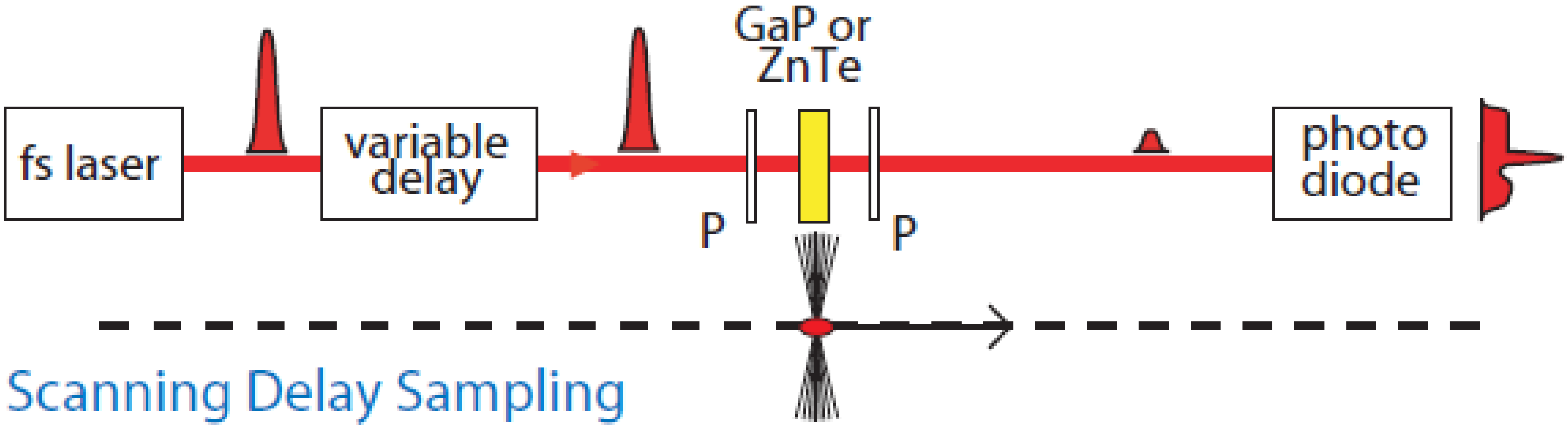

From S.P.Jamison et al., EPAC 2006

Setup of a scanning EOS method

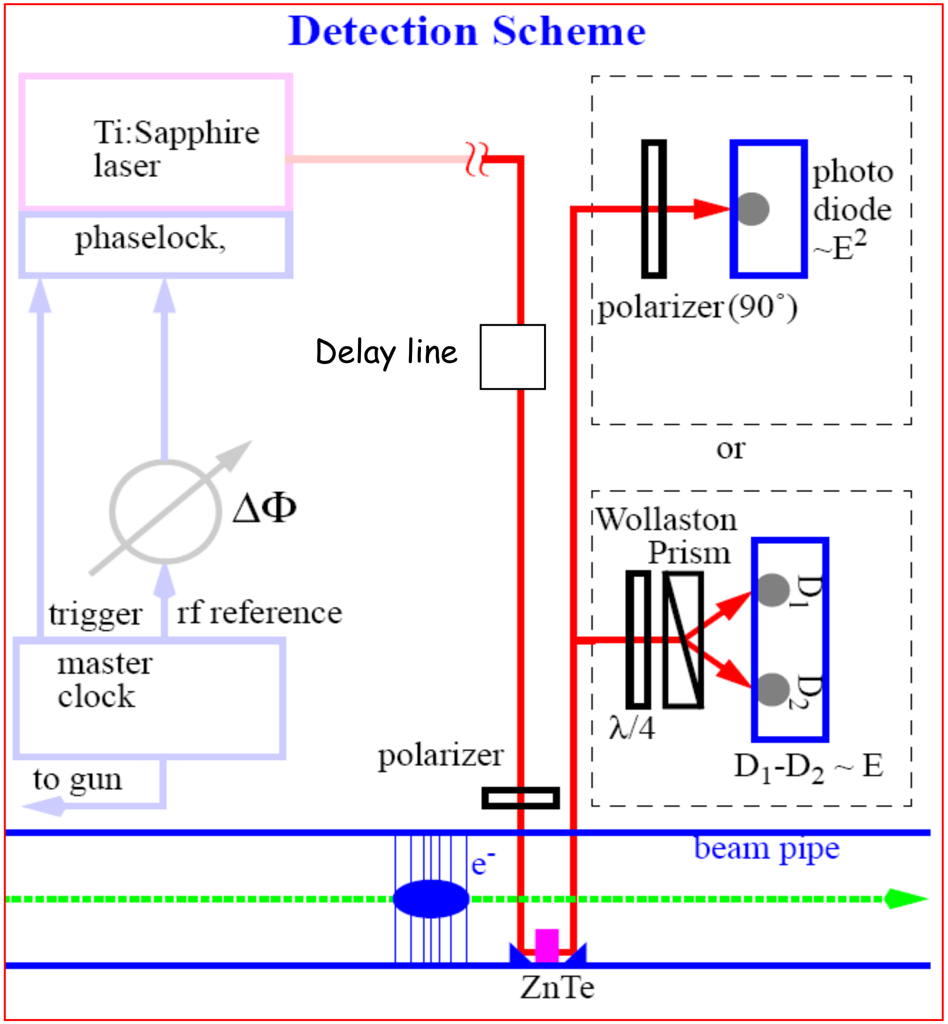

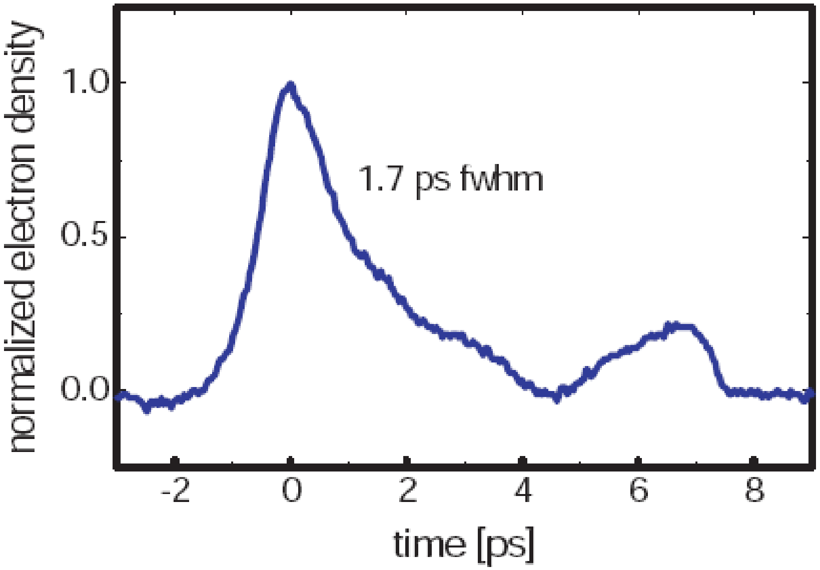

Using 12fs pulses from $Ti{:}Al_2O_3$ laser at 800nm and ZnTe crystal 0.5mm thick with a e^- - beam 46MeV of 200pC

X. Yan *et al*, PRL 85, 3404 (2000)

Hardware of a compact EOS Scanning Setup

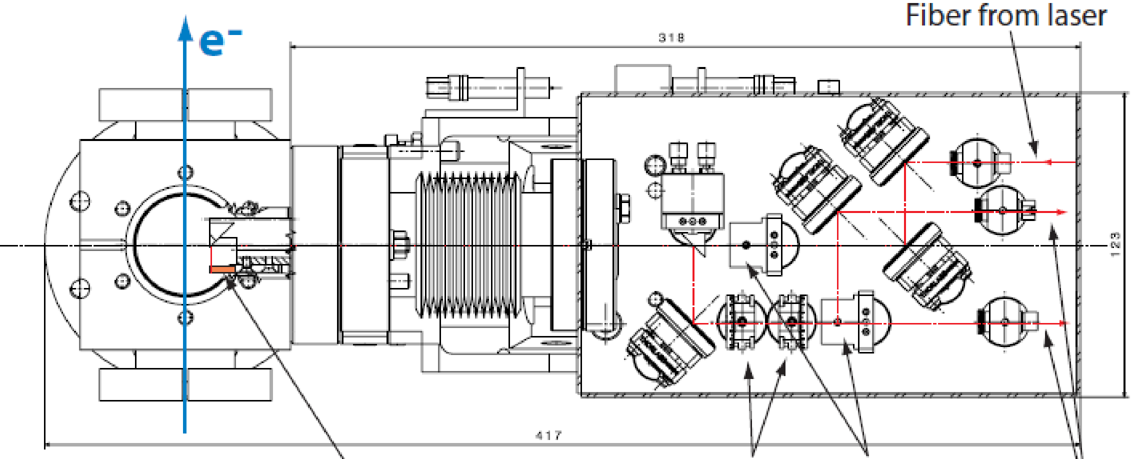

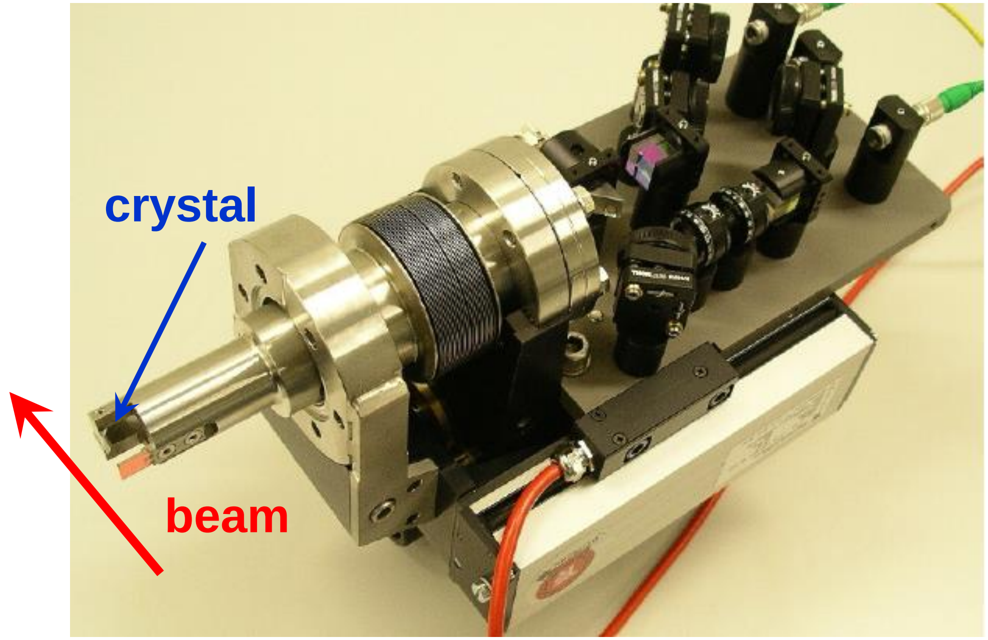

Example: Bunch length at FLASH

(1 ps bunch duration = 300 μm length)

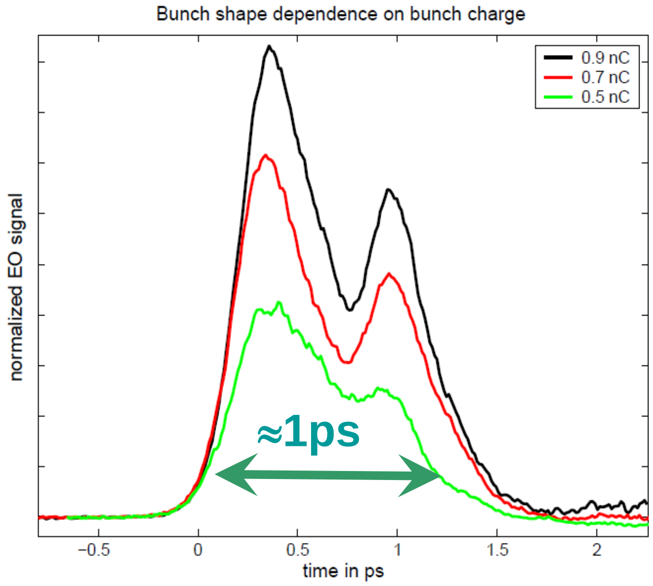

B. Steffen (PSI) et al, DIPAC 2009

B. Steffen et al., FEL Conf. 2005

Summary of longitudinal Measurements

Devices for bunch length at light sources:

Streak cameras:

- Time resolved monitoring of synchrotron radiation
  → for relativistic e^--beams, $t_{bunch} < 1$ ns, injection matching
  reason: too short bunches for rf electronics.

Laser scanning:

- Electro-optical modulation of short laser pulse
  → very high time resolution down to some fs

Diagnostics is the ’sensory organ’ for the beam.

It required for operation and development of accelerators

Several categories of demands leads to different installations:

- Quick, non-destructive measurements leading to a single number or simple plots
- Complex instrumentation used for hard malfunction and accelerator development
- Automated measurement and control of beam parameters i.e. feedback

A clear interpretation of the results is a important design criterion.

General comments:

- Quite different technologies are used, based on various physics processes
- Accelerator development goes parallel to diagnostics development

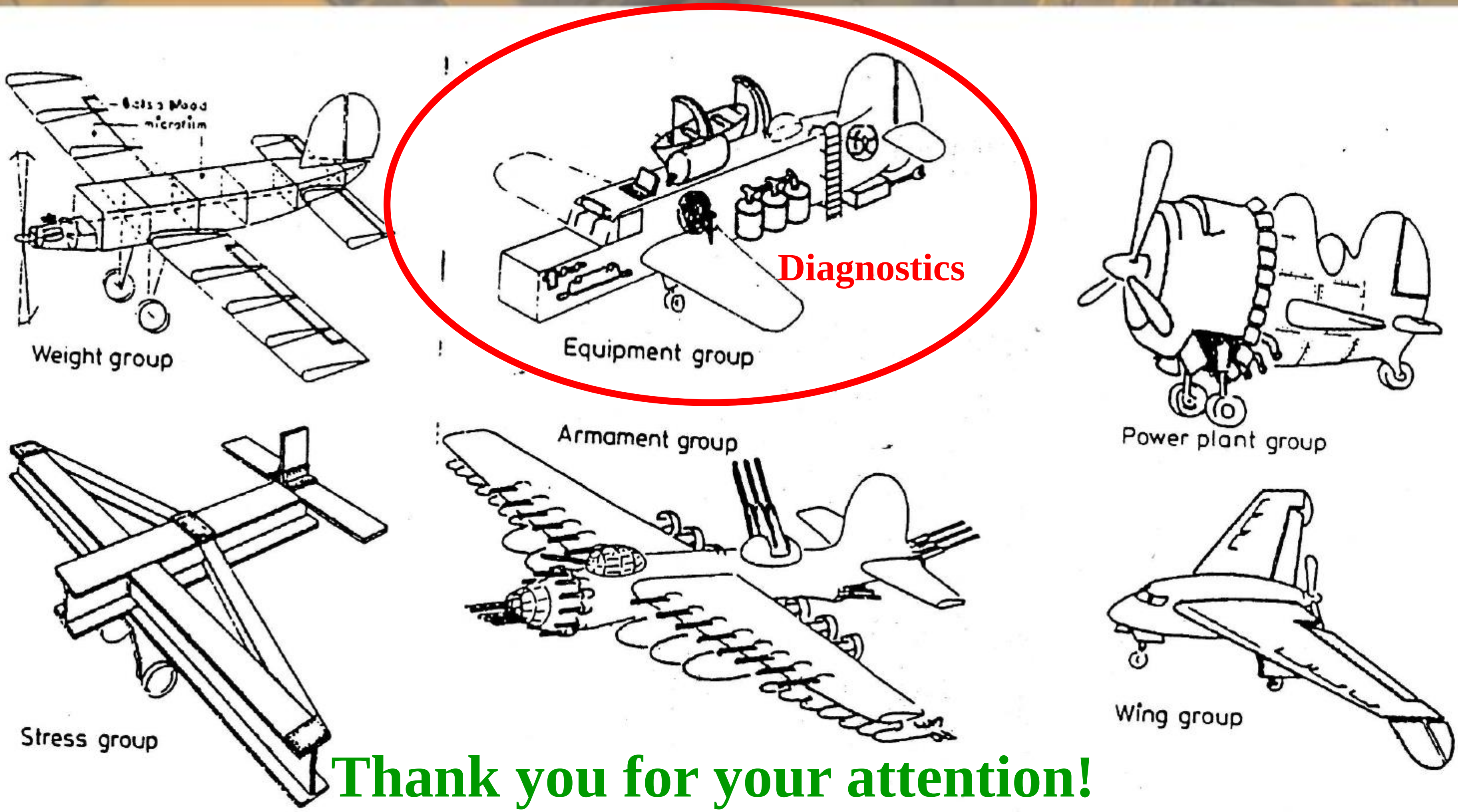

Thank you for your attention!

For a successful construction and operation of an accelerator,
the understand and right balance of all disciplines is required!

Backup slides

Example: Light Output from various Screens

Example: Beam images for various scintillators irradiated by Uranium at ≈ 300 MeV/u at GSI

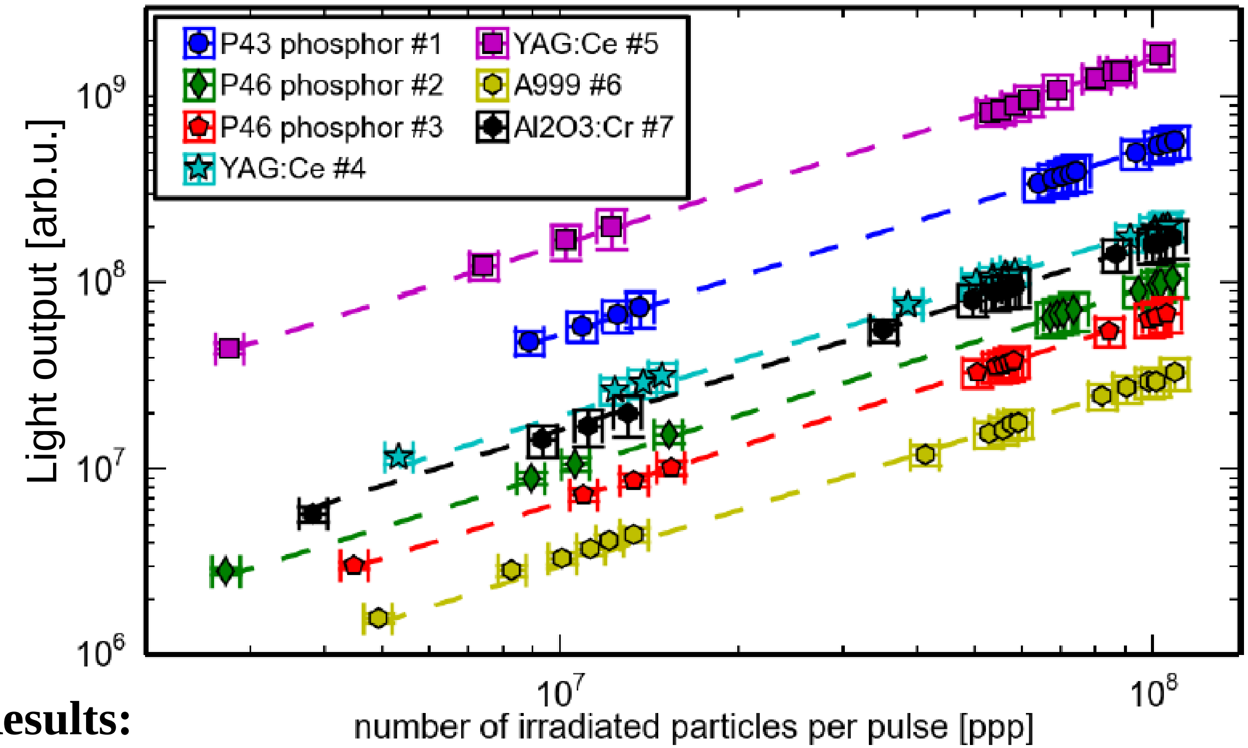

Courtesy P. Forck et al., IPAC'14, A. Lieberwirth et al., NIM B 2015

Results:

- Several orders of magnitude different light output
- ⇒ material matched to beam intensity must be chosen
- Well suited: powder phosphor screens P43 and P46
- → cheap, can be sedimented on large substrates of nearly any shape
- Light output linear with respect to particles per pulse

Influence of the residual gas ion trajectory by :

- External electric field $\boldsymbol{E_{ex}}$
- Electric field of the beam's space charge $\boldsymbol{E_{space}}$

e.g. Gaussian density distribution for round beam: $E_{space}(r) = \frac{1}{2\pi\varepsilon_0} \cdot \frac{qeN}{l} \cdot \frac{1}{r} \cdot \left[1 - \exp\left(-\frac{r^2}{2\sigma^2}\right)\right]$

Estimation of correction: $\sigma^2_{corr} \approx \frac{e^2 \ln 2}{4\pi\varepsilon_0 \sqrt{m_p c^2}} \cdot \frac{qN}{l} \cdot d_{gap} \cdot \sqrt{\frac{1}{eU_{ex}}} \propto N \cdot d_{gap} \cdot \sqrt{\frac{1}{U_{ex}}}$

With the measured beam width is given by convolution: $\sigma^2_{meas} = \sigma^2_{true} + \sigma^2_{corr}$

Example: U^{73+}, 10^9 particles per 3 m bunch length, cooled beam with $\boldsymbol{\sigma_{true}}$ = 1 mm FWHM.

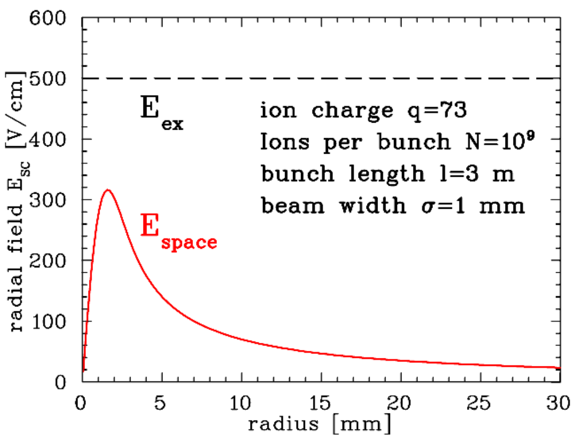

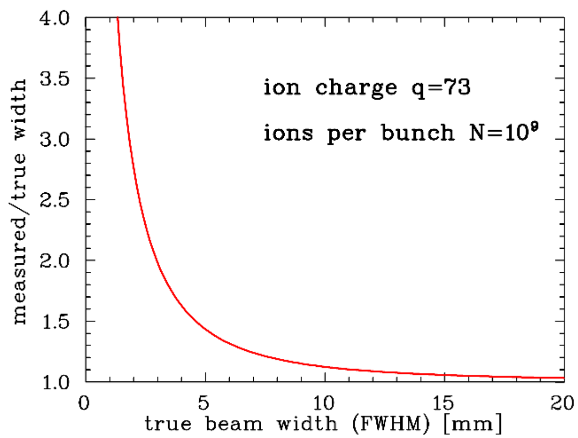

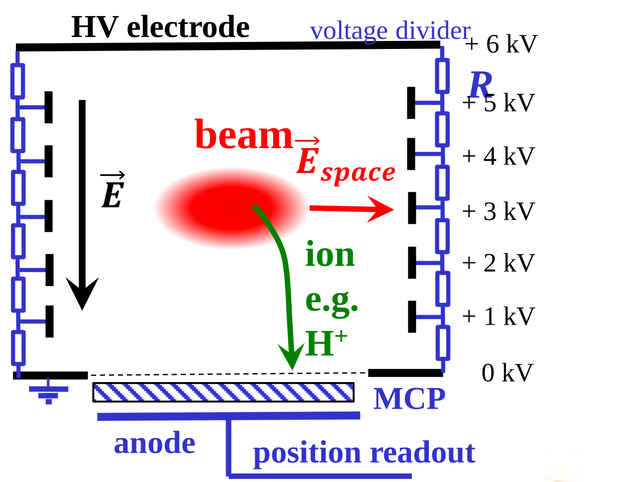

Alternative: e⁻ detection in an external magnetic field

$\rightarrow$ cyclotron radius $r_c = \sqrt{2m_e E_{kin,\perp}} / eB \Rightarrow r_c < 0.1\,\text{mm for } B = 0.1\,\text{T}$

E_{kin}, given by atomic physics, 0.1 mm is internal resolution of MCP.

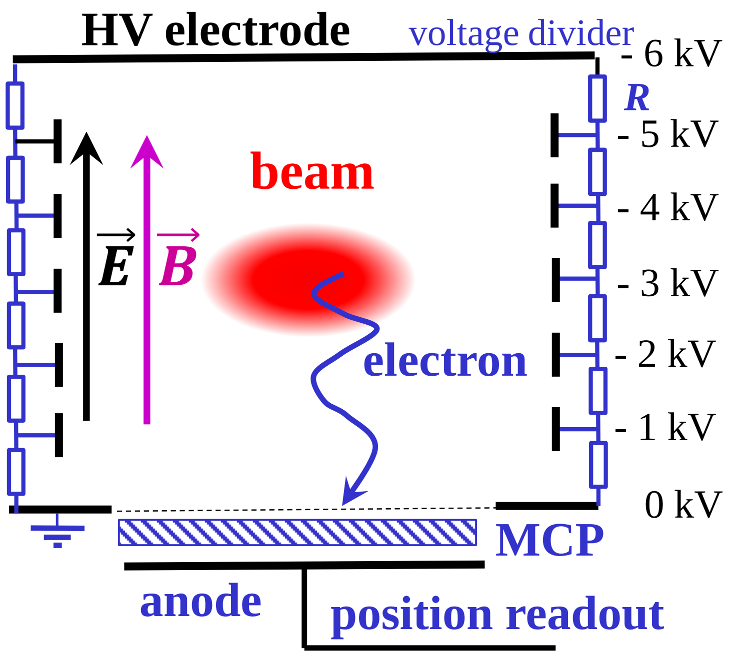

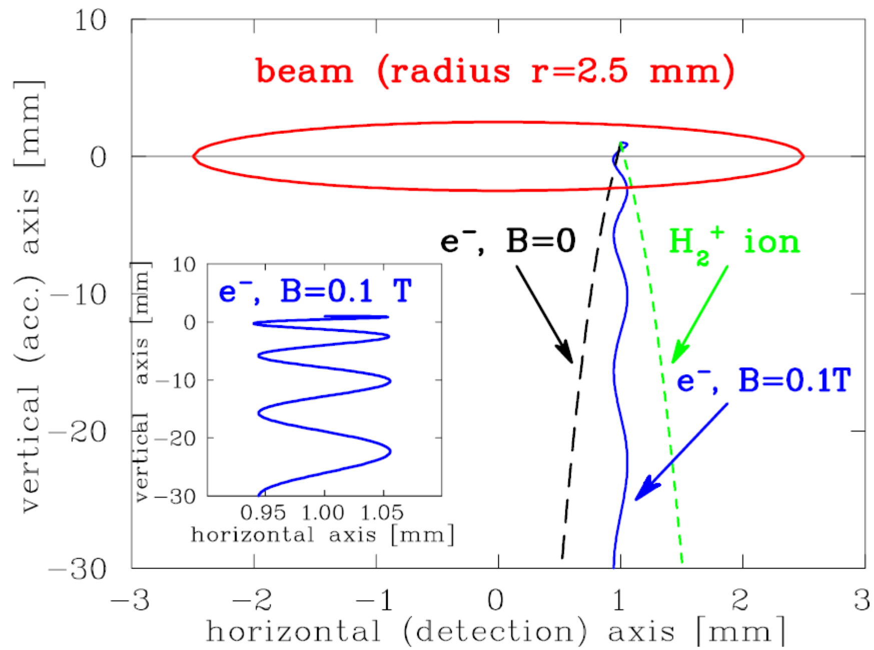

Time-of-flight: ≈1 ns $\rightarrow$ 2 or 3 cycles.

B-field: By dipole magnets with large aperture $\rightarrow$ IPM is expensive device.

IPM: Magnet Design

Magnetic field for electron guidance:

Maximum image distortion:

5% of beam width ⇒ $\Delta B/B < 1\ \%$

Challenges:

- High ***B***-field homogeneity of 1 %
- Clearance up to 500 mm
- Correctors required to compensate beam steering
- Insertion length 2.5 m incl. correctors

For MCP wire-array readout lower clearance required

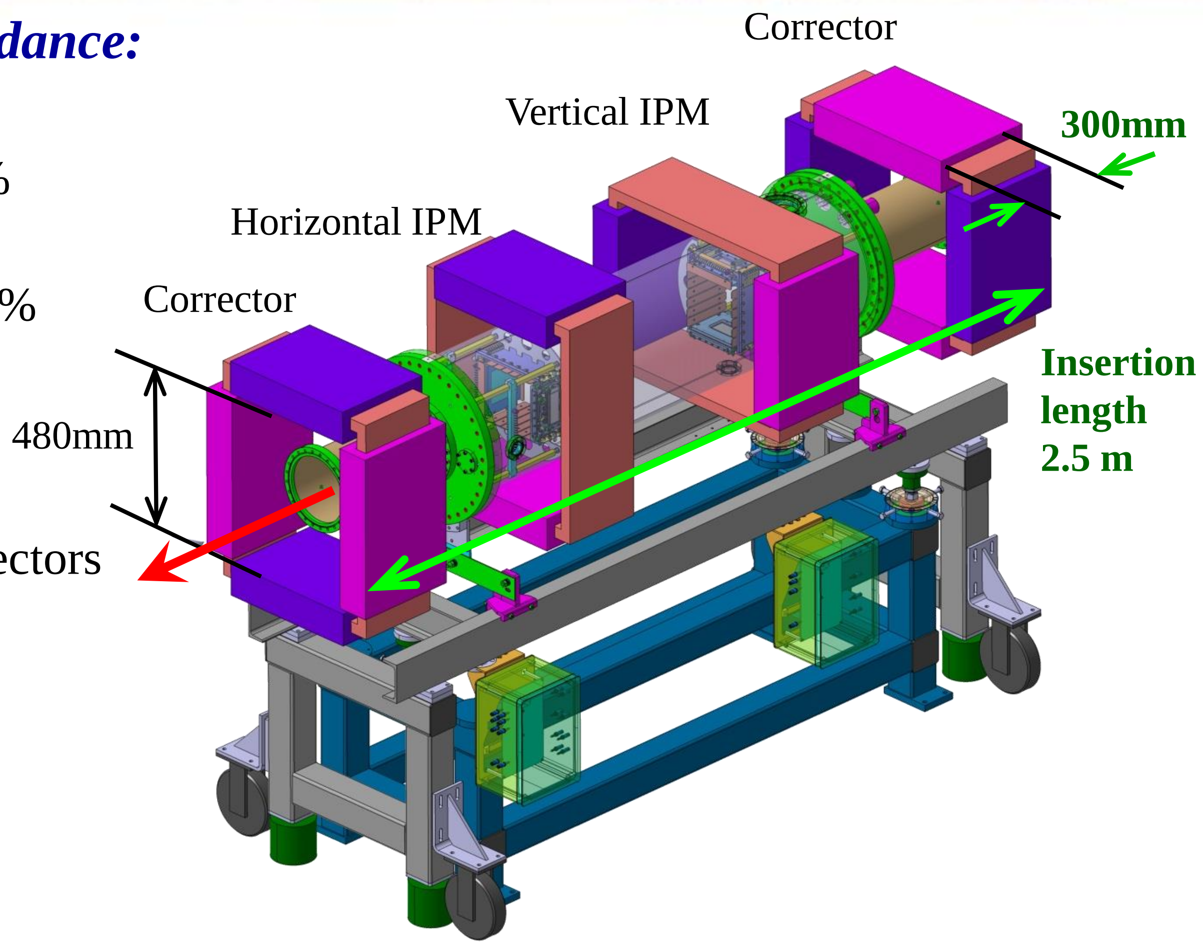

Emittance Enlargement by Injection Mis-steering

Emittance conservation requires precise injection matching

Wrong angle of injected beam:

- injection into outer phase space → large β-amplitude i.e. large beam
- might result in 'hollow' beam
- filling of acceptance i.e. loss of particles

⇒ Hadron beams: larger emittance after acceleration

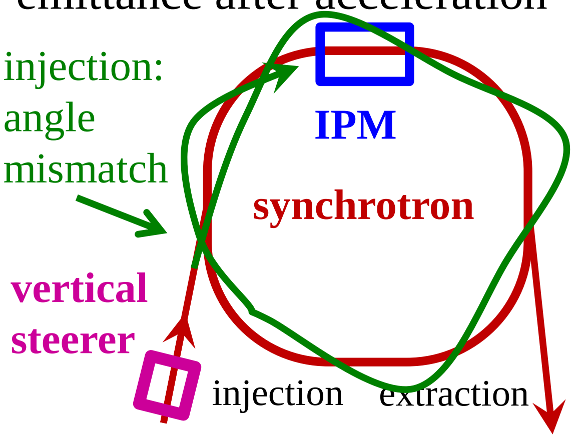

Example: Variation of vertical injection angle by magnetic steerer
Beam: C^{6+} at 6.7 MeV/u acc. to 600 MeV/u, up to $6\cdot10^9$ ions per fill with multi-turn injection, IPM integration 0.5 ms i.e. ≈ 100 turns

Vertical profile **at** injection:

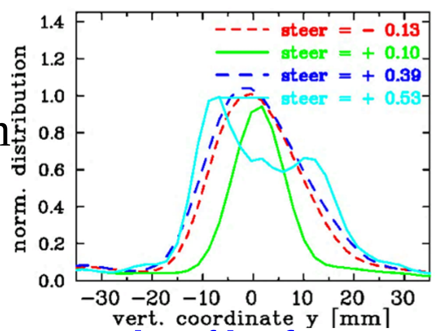

Vertical profile **after** acc.:

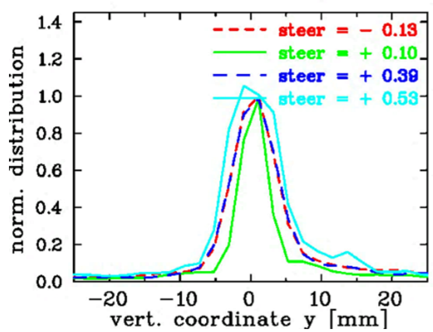

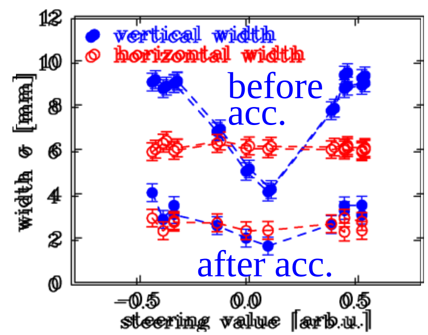

Horizontal profile **at** injection:

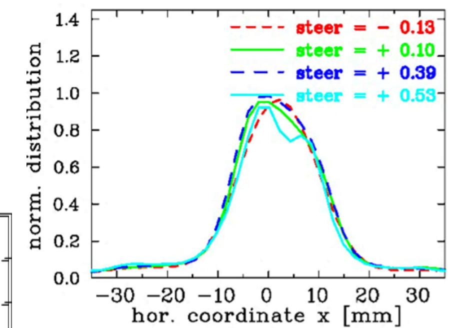

Horizontal profile **after** acc.:

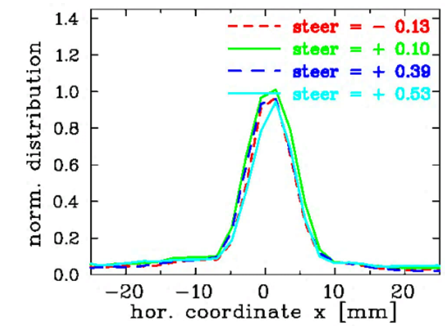

Schematic simulation:
Courtesy M. Syphers

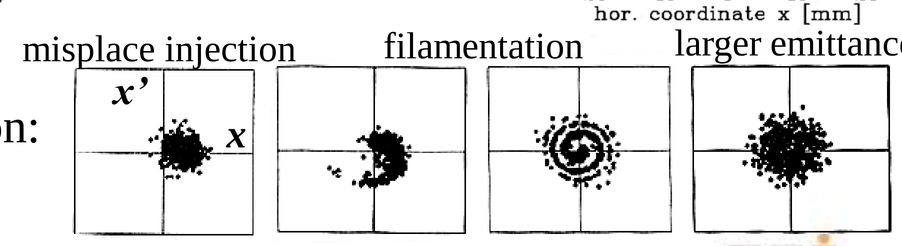

Beam Induced Fluorescence for intense Profiles

Large beam power → Non-intercepting method:
⇒ **B**eam **I**nduced **F**luorescence BIF
N_2 + Ion → $(N_2^{+})^{*}$+ Ion → N_2^{+} + γ + Ion
With single photon detection scheme
390 nm< λ< 470 nm
⇒ non-destructive, compact installation.

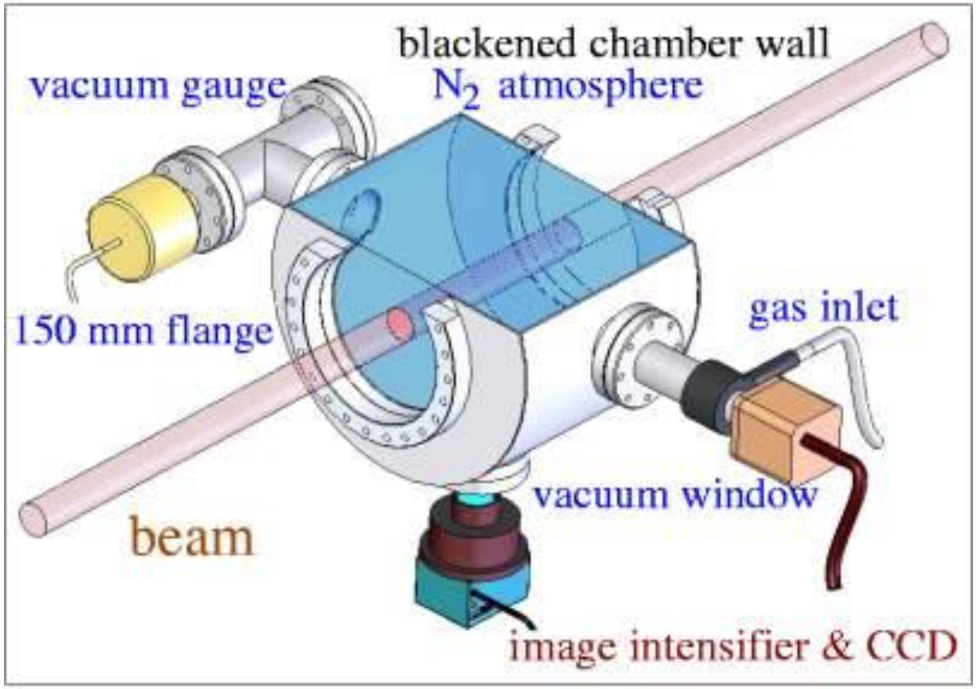

Installation of hor&vert. BIF Monitor:

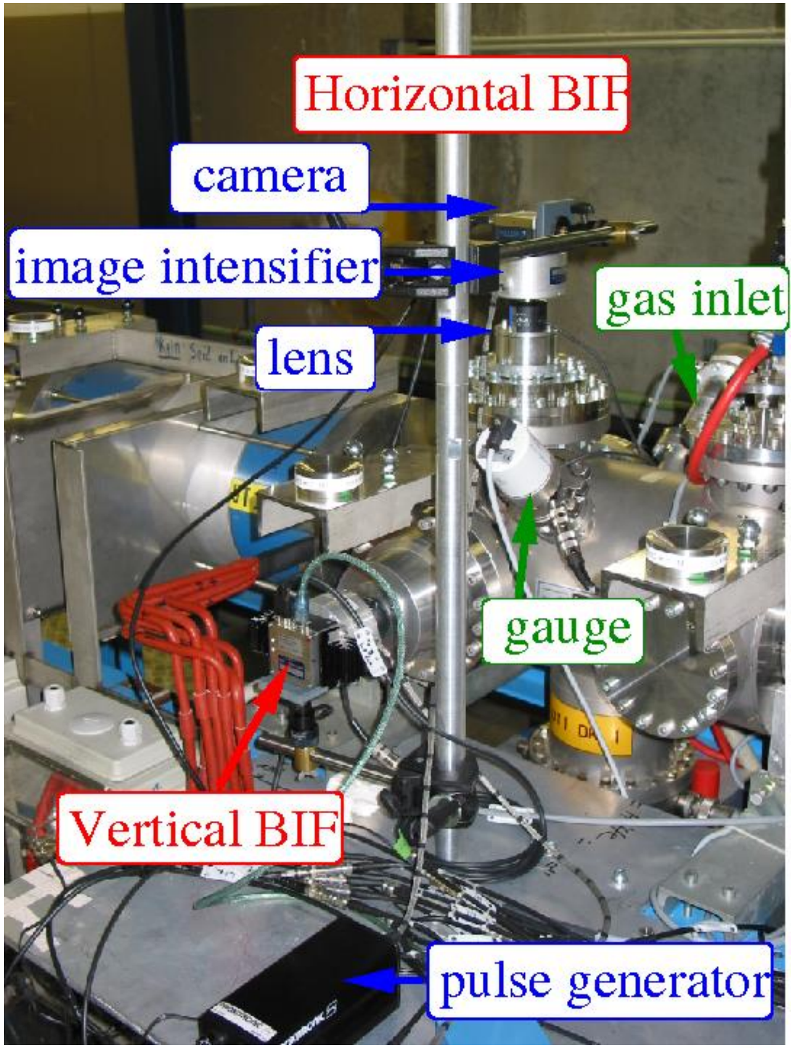

Beam Induced Fluorescence Monitor BIF: Image Intensifier

Scheme of Image intensifier:

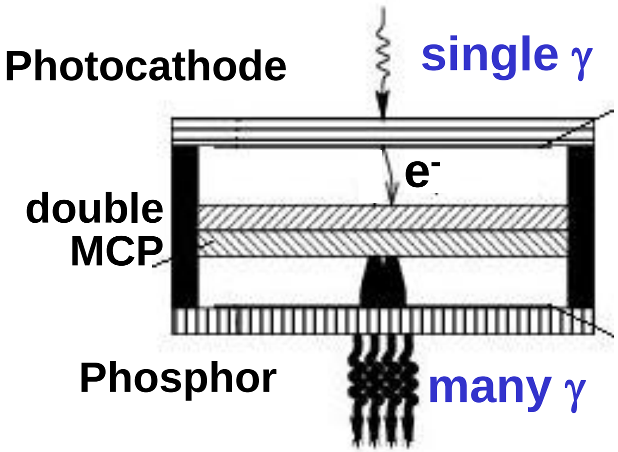

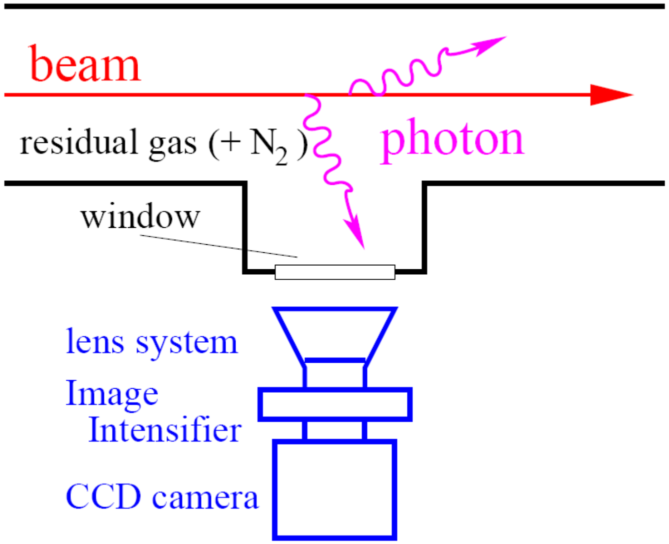

Image intensifier:

- ➢ Photo cathode → creation of photo-e⁻
- ➢ Accelerated toward MCP for amplification
- ➢ Detection of ampl. e⁻ by phosphor screen
- ➢ Image recorded by CCD

⇒ Low light amplification
(commercially used for night vision devices)

A BIF monitor consists of only:

- ➢ optics outside beam pipe
- ➢ image intensifier + camera
- ➢ gas-inlet for pressure increase

⇒ nearly no installation inside vacuum.
only LEDs for calibration

⇒ cheaper than IPM, but lower signal.

Beam Induced Fluorescence Monitor BIF: Image Intensifier

'Single photon counting':

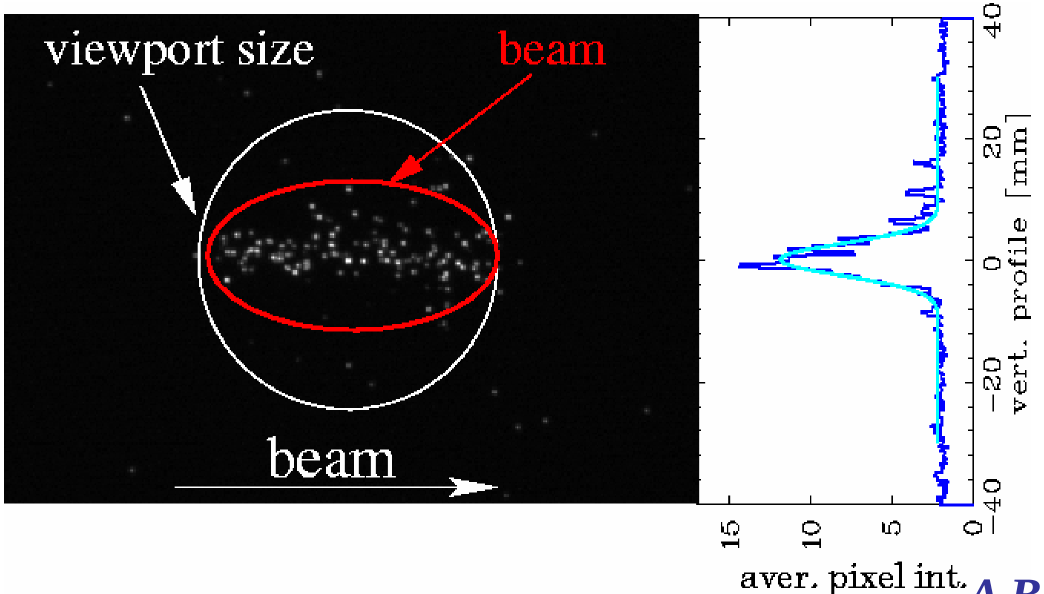

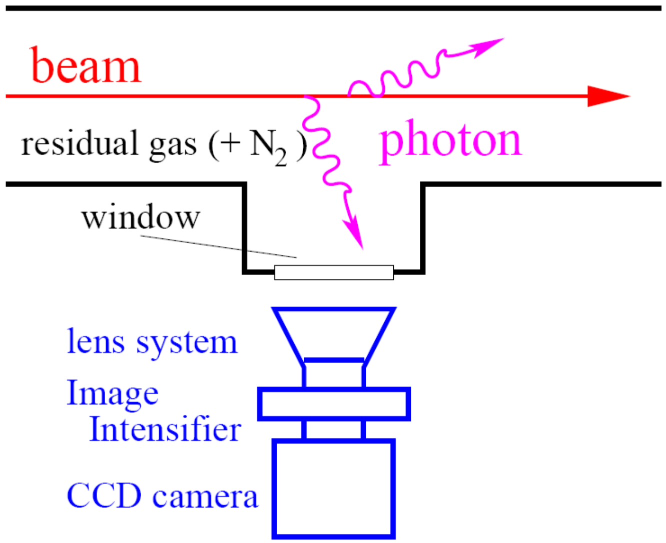

Example at GSI-LINAC:

4.7 MeV/u Ar $^{10+}$ beam

I=2.5 mA equals to 10^{11} particle

One single macro pulse of 200 μs

Vacuum pressure: p=10^{-5} mbar (N_2)

A BIF monitor consists of only:

- optics outside beam pipe
- image intensifier + camera
- gas-inlet for pressure increase

⇒ nearly no installation inside vacuum.
only LEDs for calibration

⇒ cheaper than IPM, but lower signal.

Comparison between IPM and BIF

Non-destructive methods preferred:

Beam is not influenced and diagnostics device is not destroyed!

IPM: Beam ionizes the residual gas
$\rightarrow$ measurement of all ionization products, $\boldsymbol{\Omega = 4\pi}$-geometry due to E-field

BIF: Beam ionizes and excites the residual gas
$\rightarrow$ measurement of photons emitted toward camera, solid angle $\boldsymbol{\Omega \approx 10^{-4}}$

IPM: Higher efficiency than BIF

BIF: Low detection efficiency, only $\approx 10^{-4}$ of IPM
$\Rightarrow$ longer observation time or higher pressure required

---

IPM: Complex installation inside vacuum

BIF: Nearly no installation inside vacuum

IPM: More expensive, for some beam parameters even guiding magnetic field required

BIF: More sensitive to external parameters like radiation stray light

OTR with 45^0 beam incidence and observation at 90^0 :

approximated formula for 45^0 incidence& in plane polarization:

$$\frac{d^2W}{d\theta\, d\omega} \approx \frac{2e^2\beta^2}{\pi\, c} \cdot \left(\frac{\sin\theta}{1-\beta\cos\theta} + \frac{\cos\theta}{1-\beta\sin\theta} \right)^2$$

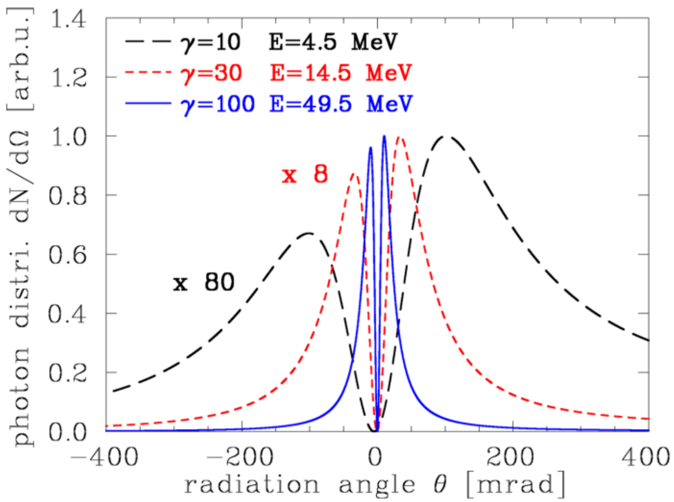

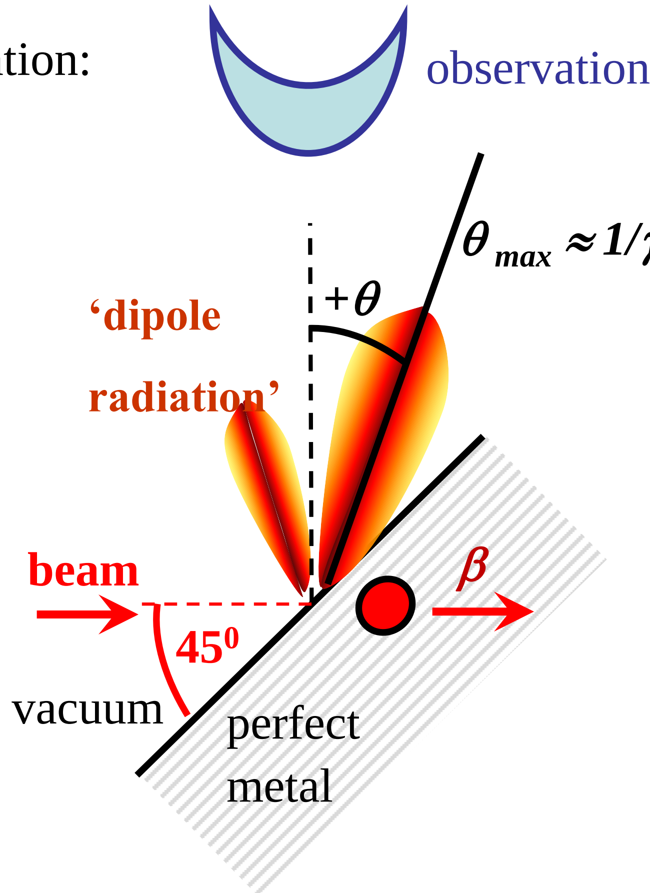

Angular distribution of radiation in optical spectrum:

- emission pattern depends on velocity
- peak at angle $\theta \approx 1/\gamma$
- emitted energy scales with $W \propto \beta^2$
- symmetric with respect to θ for $\gamma > 100$

Remark: polarization of emitted light:

- in scattering plane → parallel E-vector
- perpendicular plane → rectangular E-vector

The emittance characterizes the whole beam quality: $\varepsilon_x = \frac{1}{\pi}\int_A dx\,dx'$

Ansatz:

Beam matrix at one location: $\boldsymbol{\sigma} = \begin{pmatrix} \sigma_{11} & \sigma_{12} \\ \sigma_{12} & \sigma_{22} \end{pmatrix} = \varepsilon \cdot \begin{pmatrix} \beta & -\alpha \\ -\alpha & \gamma \end{pmatrix}$ with $\vec{x} = \begin{pmatrix} x \\ x' \end{pmatrix}$

It describes a 2-dim probability distr.

The value of emittance is:

$$\varepsilon_x = \sqrt{\det \boldsymbol{\sigma}} = \sqrt{\sigma_{11}\sigma_{22} - \sigma_{12}^2}$$

For the profile and angular measurement:

$$x_\sigma = \sqrt{\sigma_{11}} = \sqrt{\varepsilon\beta} \quad \text{and}$$

$$x'_\sigma = \sqrt{\sigma_{22}} = \sqrt{\varepsilon\gamma}$$

Geometrical interpretation:

All points $\boldsymbol{x}$ fulfilling $\boldsymbol{x}^{\mathbf{t}} \cdot \boldsymbol{\sigma}^{\mathbf{-1}} \cdot \boldsymbol{x} = \mathbf{1}$

are located on a **ellipse**

$$\sigma_{22}x^2 - 2\sigma_{12}xx' + \sigma_{11}x'^2 = \det \boldsymbol{\sigma} = \varepsilon_x^2$$